Soft Matter Theory

K. Kroy

Leipzig, 2016*

Contents

*The script is not meant to be a substitute for reading proper textbooks nor for dissemination. (See the notes for the introductory course for background information.) Comments and suggestions are highly welcome.

"Soft Matter" is one of the fastest growing fields in physics, as illustrated by the APS Council's official endorsement of the new Soft Matter Topical Group (GSOFT) in 2014 with more than four times the quorum, and by the fact that Isaac Newton's chair is now held by a soft matter theorist. It crosses traditional departmental walls and now provides a common focus and unifying perspective for many activities that formerly would have been separated into a variety of disciplines, such as mathematics, physics, biophysics, chemistry, chemical engineering, materials science. It brings together scientists, mathematicians and engineers to study materials such as colloids, micelles, biological, and granular matter, but is much less tied to certain materials, technologies, or applications than to the generic and unifying organizing principles governing them. In the widest sense, the field of soft matter comprises all applications of the principles of statistical mechanics to condensed matter that is not dominated by quantum effects.

The lecture takes a two-fold approach to this vast field. It introduces generic principles of interacting many-body physics, i.e. the "condensed matter" aspect of its title, in the first part (which could similarly also be covered in a solid-state or stat-mech class). The main theme is the emergence of the macroscopic material properties of soft materials from their interacting parts (atoms). The second part pursues a more practical approach to selected model systems, which will give a better feeling for the typical origin (low-dimensional mesostructures) and main consequences (large fluctuations and deformations) of "softness". It also introduces "activity" as a feature specific to many soft and, in particular, biological systems, giving rise to the new physical paradigm of "active soft matter". There is clearly no chance to discuss the physics of rubbers, foams, plastics, liquid crystals, pastes, gels, and living cells and tissues in all detail here, but the lecture may be helpful as a starting point for addressing some of these systems. The prevailing theoretical methodology used and developed throughout the lecture is classical field theory.

Part I
Interacting Many-Body Systems

The aim of this part is to introduce general theoretical tools that have been developed and used in many areas of physics to address interacting many-body systems on a microscopic basis.

The empty canvas

Statistical mechanics provides a microscopic foundation of the thermodynamics of many-body systems. The central paradigmatic many-body system discussed in introductory courses is an isothermal classical ideal gas. This trivial case with no interactions and no packing structure is briefly recapitulated to set the stage. Thermodynamically, the ideal gas is defined in an operational way by two equations of state: (i) the caloric equation or energy equation (in $d = 3$ space dimensions)

$$U_{\rm ig} = \frac{3}{2} N k_B T \,, \tag{1}$$

which can be measured in a calorimeter and (ii) an equation linking thermal and mechanical properties,

$$pV = N k_B T \,. \tag{2}$$

Using Eqs. (1) and (2) to express the intensive variables in terms of the extensive ones, and invoking homogeneity, the differential fundamental relation (per particle)

$$ds(u,v) = \frac{1}{T} du + \frac{p}{T} dv \tag{3}$$

in a three-dimensional thermodynamic state space spanned by U, V, and N can be integrated to yield the fundamental relation $S(U,V,N) = N s(U/N, V/N)$ and thus all thermostatic properties of the gas from these two equations of state.

In statistical mechanics, one recognizes Eq. (1) as the statement of equipartition of energy in "bits" of $k_B T/2$ among all degrees of freedom, and one could deduce Eq. (2) from it by appealing to the kinematics of free massive particles, which links the pressure $p = 2u/3$ to the kinetic energy density $u \equiv U/V$. But one can also address the fundamental relation directly via the (e.g. canonical) partition sum

$$Z \equiv \int \mathrm{d}\Gamma \, e^{-\beta H} = e^{-\beta F(T,V,N)} \qquad \mathrm{d}\Gamma \equiv \frac{\Pi_i \mathrm{d}\mathbf{q}_i \mathrm{d}\mathbf{p}_i}{N! h^{dN}} \,. \tag{4}$$

With the Hamiltonian $H_{\rm ig} = \sum_i \mathbf{p}_i^2/2m$, one easily finds the ideal-gas fundamental relation

$$Z_{\rm ig} = (V/\lambda_T^3)^N/N! \quad \Rightarrow \quad F_{\rm ig} = -k_B T \ln Z_{\rm ig} = N k_B T [\ln(\lambda_T^3 n) - 1] \tag{5}$$

The *thermal wavelength*

$$\lambda_T \equiv \frac{h}{\sqrt{2\pi m k_B T}} \tag{6}$$

appears as a natural length scale if the phase space is measured in units of a smallest action quantum $\hbar$, as appropriate for a quantum statistical description. It is essentially the de Broglie wavelength of a gas particle of mass m carrying its thermal energy bit and acts an elementary unit cell size in configuration space. The naive interpretation of V/λ_T^3 as the number of "available classical states" for each of N non-interacting particles in a volume V turns out to be inappropriate if these are indistinguishable, though. Particle permutations do not produce new states in this case, as indicated by the factor $N!$ in the denominator of Z_{ig}. Each particle can only explore the volume $v = V/N = 1/n$, before changing place with an identical particle, which does not lead to a new state. So there are only $\mathcal{W} \approx v/\lambda_T^3$ classical states per particle available, which is also apparent from the entropy[1],

$$S_{\mathrm{ig}}/(Nk_B) = 5/2 - \ln(\lambda_T^3 n) \simeq -\ln(\lambda_T^3 n)\ . \tag{7}$$

Not too surprisingly, the model therefore breaks down if one attempts to raise the density or to lower the temperature beyond the limit defined by $n\lambda_T^3 \approx 1$, which causes the condensation of an increasing fraction of particles into their quantum ground states. These particles do not scatter any more between states and therefore they carry no heat or entropy. The number of particles available to contribute to the classical gas behavior, or to any sort of thermodynamics, is thus reduced by the "sleeping" condensed fraction, and all thermodynamic quantities are diminished by a corresponding factor.

Equations (4) and (5) show how the derivation of a complete material relation (also called fundamental relation of constitutive law) from a microscopic Hamiltonian works, in principle. But in practice, the integral cannot be computed beyond the realm of a few toy models. In fact, most of this chapter serves to introduce more practical approaches to interacting many-body systems, circumventing the task of doing such a monstrous integral.

1 Pair interactions and pair correlations

Pair interactions

In the real world, potential interactions between atoms and molecules can rarely be neglected. It is through direct interactions that we usually notice the existence of these particles, in the first place. And the physical properties of real gases and plasmas as well as of condensed phases and the transitions between them are primarily the result of strong mutual interactions. The reason that the model

[1] Here, $\simeq$ means "up to arbitrary gauge constants".

of an ideal (interaction-free) gas is useful at all, and in fact highly successful, is due to the fact that many elementary excitations in condensed matter may, to a good approximation, *effectively* be described as dilute gases of quasi-particles. In their quantized version, they govern the low-temperature physics of hard matter as so-called "phonons", "magnons", "electrons", "holes", etc. Strong interactions govern the phase transitions that bring atoms into a condensed state, in the first place, as well as its packing structure and energetics, and, last but not least, the often complex and composite (hybrid) nature of the elementary excitations.

As a rule of thumb, quantum effects come into play, when "statistical interactions" arising from the exchange statistics of indistinguishable particles become important, as discussed above for the ideal gas. To extend the argument to interacting particles, one compares the range λ_T and strength k_BT of the statistical interactions, as betrayed by the chemical potential $\mu \simeq -TS_{\mathrm{ig}}/N$ of the non-interacting gas, with the direct interactions. A common feature of all direct interactions between atoms and molecules is their strong hard-core repulsion at particle distances on the order of a few Bohr radii $a_B = \hbar^2/m_e e^2$, requiring

$$\lambda_T/a_B \gg 1 \qquad \Rightarrow \qquad k_BT \ll (e^2/a_B)\, m_e/m \simeq \mathrm{m\,eV} \tag{8}$$

for noticeable quantum effects. This argument demands temperatures substantially below room temperature ($k_BT \approx 25$ meV), where, however, the strength of the statistical interactions diminishes. Namely, as entropic interactions, which deprive the particles of the phase space to roam around with their thermal momentum, they are themselves merely of strength k_BT. Condensing atoms with hard-core repulsions by their exchange interactions (which produces superfluids and Bose–Einstein condensates) is therefore a very tricky task and only achieved at very low temperatures. And the energetics and packing structure of condensed atoms and molecules is therefore, in contrast to electronic excitations in solids, usually completely dominated by "direct" potential interactions — which themselves arise from a combination of the wave-like nature of matter (uncertainty relation), exchange effects (Pauli principle), and Coulomb interactions.

The most convenient starting point for studying the effects due to such *direct interactions* are situations where pair interactions $\mathcal{V}(\{\mathbf{r}_j\}) = \sum_{i<j} \nu(\mathbf{r}_i - \mathbf{r}_j)$ dominate, corresponding to the Hamiltonian

$$H = \sum_i \frac{\mathbf{p}_i^2}{2m} + \sum_{i<j} \nu(\mathbf{r}_i - \mathbf{r}_j)\,. \tag{9}$$

A useful example is provided by the Hamiltonian for a fluid of hard spheres, for which the pair interaction potential is given by

$$\nu(r) = \begin{cases} \infty & r < \sigma \\ 0 & r > \sigma\,. \end{cases} \tag{10}$$

This model idealizes the most salient feature of all atomic, molecular and most colloidal interactions, a strong hard-core repulsion at short center-of-mass distances, which plays the major role in determining the characteristic packing structure of most simple fluids and crystals. This is why the hard sphere fluid may justly be called a paradigm of condensed matter.

Attractive interactions are often less pronounced than the hard-core repulsion and can be taken into account perturbatively once the hard sphere fluid is under control. A practical way of adding attractive interactions to the hard-sphere potential is to add more hard spheres (or small polymer coils, etc.). To see this, start with a pair of "tagged" hard spheres of diameter $\sigma_>$. Adding a solvent of other (usually smaller and possibly not visible) particles then induces an attraction between them. The crucial point is that the solvent particles behave like hard spheres of diameter $\sigma_<$ when interacting with the tagged spheres, i.e. their centers of mass cannot enter the spherical depletion zone of diameter $\sigma_d \equiv \sigma_> + \sigma_<$ around the tagged particles. The attraction can then alternatively be thought to arise either from the pressure imbalance associated with the particle depletion in a narrow gap between the tagged spheres or from the entropy gain associated with the free-volume gain for the small particles if the depletion zones around the tagged spheres overlap. In the limit where the interactions of the bath particles among themselves can be neglected, the bath may be idealized as an ideal gas. The induced attraction potential is then simply given by the ideal-gas osmotic pressure $n_< k_B T$ due to the bath particles times the overlap volume V_x of the depletion zones, and known as the Asakura–Oosawa potential

$$\nu_{\rm AO}(r) = n_< k_B T V_x = n_< k_B T \sigma_d^3 \frac{\pi}{6}\left[1 - \frac{3}{2}\frac{r}{\sigma_d} + \frac{r^3}{2\sigma_d^3}\right] \qquad (\sigma_> < r < \sigma_d)\,. \quad (11)$$

Despite the appearance, the so-called depletion attractions between two spheres are generally[2] not pair-wise additive, even on this simple level, although they arise from purely pairwise interactions between the individual hard spheres. In other words, Eq. (9) with Eq. (10) is a perfect model for a suspension of hard spheres, whereas the use of $\nu_{\rm AO}(r)$ in Eq. (9) would not generally represent a valid description of a hard-sphere suspension in a bath of other particle. This exemplifies two important points: *i)* that, even without invoking quantum mechanics, there are many situations, where a pair Hamiltonian as in Eq. (9) may be too simple to describe the interactions; and *ii)* that complex many-body interactions may always (and generally will) arise from elementary pair interactions upon coarse-graining.

Pair correlations: the radial distribution function

A convenient and powerful tool to characterize the packing structure of condensed matter are correlation functions. As a rule, the most salient features

[2]Consider a third tagged sphere that approaches the first two (exercises).

of homogeneous materials are contained in the pair correlation functions of the atoms. Higher-order correlations usually contain essential additional information (in particular if the Hamiltonian is not restricted to pair-interactions), but they are certainly more difficult to measure and to calculate. For example, dense hard spheres exhibit a dramatic slowing down of their dynamics, called a glass transition, without any obvious sign in their pair correlations. Similarly, complex ring-like bridges involving subtle correlations between many particles are responsible for the jamming of granular flows, as may be observed in a poorly designed hourglass. Yet, for most practical purposes, a framework based on pair-correlations is still the most common and most practical way forward.

In the following, the grand canonical formulation is applied and for the microscopic particle concentration the abbreviation

$$\hat{n}(\mathbf{r}) \equiv \sum_i \delta(\mathbf{r} - \mathbf{r}_i) \tag{12}$$

is introduced. The position-dependent "1-body" or "1-point" density

$$n(\mathbf{r}) = \langle \hat{n}(\mathbf{r}) \rangle = \langle \sum_i \delta(\mathbf{r} - \mathbf{r}_i) \rangle = \langle N \delta(\mathbf{r} - \mathbf{r}_1) \rangle \tag{13}$$

simply contains the information how many particles are found on average in a certain region of configuration space. The 2-point density or *pair correlation function* shall here be defined as $\langle \hat{n}(\mathbf{r}) \hat{n}(\mathbf{r}') \rangle$ minus the self-correlations[3],

$$n(\mathbf{r}', \mathbf{r}'') \equiv \langle \sum_{i \neq j} \delta(\mathbf{r}' - \mathbf{r}_i) \delta(\mathbf{r}'' - \mathbf{r}_j) \rangle = \langle N(N-1) \delta(\mathbf{r}' - \mathbf{r}_1) \delta(\mathbf{r}'' - \mathbf{r}_2) \rangle \; . \tag{14}$$

The pair correlation function encodes the neighbor correlations in the simplest possible form, namely in the form of a local particle density as seen from the center of mass positions of the particles themselves. There are usually still interesting pair correlations even if the system is translation invariant, in which case $n(\mathbf{r}', \mathbf{r}'')$ is solely dependent on the relative vector $\mathbf{r} = \mathbf{r}' - \mathbf{r}''$ and $n(\mathbf{r}) = n = \langle N \rangle / V$ is spatially constant. This can be exploited by setting the origin of the coordinate system at the center of an arbitrary particle and defining the dimensionless correlation function $g(\mathbf{r})$

$$\begin{aligned}
n^2 g(\mathbf{r}) &\equiv \frac{1}{V} \int \mathrm{d}\mathbf{r}' \, n(\mathbf{r} + \mathbf{r}', \mathbf{r}') \\
n g(\mathbf{r}) &= \frac{1}{\langle N \rangle} \int \mathrm{d}\mathbf{r}' \, n(\mathbf{r} + \mathbf{r}', \mathbf{r}') = \frac{1}{\langle N \rangle} \int \mathrm{d}\mathbf{r}' \, \langle \sum_{i \neq j} \delta(\mathbf{r} + \mathbf{r}' - \mathbf{r}_i) \delta(\mathbf{r}' - \mathbf{r}_j) \rangle \\
&= \frac{1}{\langle N \rangle} \langle \sum_{i \neq j} \delta(\mathbf{r} + \mathbf{r}_j - \mathbf{r}_i) \rangle = \frac{1}{\langle N \rangle} \langle N(N-1) \delta(\mathbf{r} + \mathbf{r}_1 - \mathbf{r}_2) \rangle \; ; \\
g(\mathbf{r}) &\overset{\mathbf{r}_{12} \equiv \mathbf{r}_2 - \mathbf{r}_1}{=\!=} \frac{V}{\langle N \rangle^2} \langle N(N-1) \delta(\mathbf{r} - \mathbf{r}_{12}) \rangle \overset{N = \text{const.}}{=\!=} V \langle \delta(\mathbf{r} - \mathbf{r}_{12}) \rangle
\end{aligned} \tag{15}$$

[3]Experts often tacitly omit the distinction between functions with/without self-correlations.

If the system is moreover isotropic, the argument of $g(\mathbf{r})$ is actually the distance $r \equiv |\mathbf{r}|$, and one speaks of the *radial distribution function* $g(r)$. It gives the probability density $4\pi r^2 g(r)/V$ to find a particle at distance r from an arbitrarily chosen test particle. For a statistically homogeneous and isotropic system the full information about the packing structure, as far as pairs of particles are concerned (i.e. excluding the information, with which probability three or more particles are found in a certain correlated state), is thus encoded in a single scalar function of a scalar variable. For hard core particles $g(r \to 0) = 0$ (remember that the self-correlations, which would contribute a $\delta(r)$ to $ng(r)$ were subtracted). For systems without long-range order, such as liquids and gases, the limit $g(r \to \infty) = 1$ exists, for crystals $g(r)$ will oscillate indefinitely around it. For Fourier transforming $g(\mathbf{r})$, it is customary to subtract the 1, which would otherwise always produce a δ-function corresponding to the forward scattering[4] of a homogeneous material. The resulting function, which only retains the non-trivial pair correlations or "pair fluctuations", is often denoted by

$$h(\mathbf{r}) \equiv g(\mathbf{r}) - 1 = \left[\langle \hat{n}(\mathbf{r})\hat{n}(0)\rangle - \langle \hat{n}(0)\rangle^2\right]/n^2 \; . \tag{16}$$

(If not formulated on a lattice, the last expression should be understood as a mere notational convention; the self correlations are understood to drop out.)

Pair correlations: the structure factor

It should be familiar from elementary optics that the Fraunhofer interference patterns resulting from scattering in optically dilute (i.e. essentially transparent) media correspond to a Fourier transform of the pattern of point scatterers. The relevant non-technical information about the (relative) scattering intensity with scattering vector $\mathbf{q}$ is contained in the *structure factor*

$$\begin{aligned}
S_{\mathbf{q}} \equiv & \frac{1}{\langle N\rangle}\langle \sum_{ij} \exp[-i\mathbf{q}\cdot(\mathbf{r}_i - \mathbf{r}_j)]\rangle \\
= & \frac{1}{\langle N\rangle}\int \mathrm{d}\mathbf{r}'\mathrm{d}\mathbf{r}''\, \exp[-i\mathbf{q}\cdot(\mathbf{r}' - \mathbf{r}'')]\langle \sum_{ij} \delta(\mathbf{r}' - \mathbf{r}_i)\delta(\mathbf{r}'' - \mathbf{r}_j)\rangle \\
= & \frac{1}{\langle N\rangle}\int \mathrm{d}\mathbf{r}'\mathrm{d}\mathbf{r}''\, \exp[-i\mathbf{q}\cdot(\mathbf{r}' - \mathbf{r}'')]\langle \hat{n}(\mathbf{r}')\hat{n}(\mathbf{r}'')\rangle \\
= & 1 + \frac{1}{\langle N\rangle}\int \mathrm{d}\mathbf{r}'\mathrm{d}\mathbf{r}''\, \exp[-i\mathbf{q}\cdot(\mathbf{r}' - \mathbf{r}'')] n(\mathbf{r}', \mathbf{r}'') \\
= & 1 + n\int \mathrm{d}\mathbf{r}\, \exp(-i\mathbf{q}\cdot\mathbf{r}) g(\mathbf{r}) \\
= & 1 + (2\pi)^d n\delta(\mathbf{q}) + n\int \mathrm{d}\mathbf{r}\, \exp(-i\mathbf{q}\cdot\mathbf{r}) h(\mathbf{r}) \; .
\end{aligned} \tag{17}$$

[4] As an experimentalist setting up a scattering experiment you would also better like to subtract this contribution by a beam stop to save your detector.

The leading 1 corresponds to the incoherent scattering from $\langle N\rangle$ independent particles and results from the self-correlations in the density auto-correlation $\langle\hat{n}(\mathbf{r})\hat{n}(\mathbf{r}')\rangle$. The remaining terms are due to interference and encode correlations. The δ-function amounts to the forward scattering from the homogeneous contribution contained in $g(r)$ and subtracted in $h(r)$. It is quite often tacitly omitted, which makes the limit $q \to 0$ of the structure factor continuous, in agreement with the experimental procedure in small (non-zero) angle scattering. The information encoded in this limit is the integral over the fluctuations $h(r)$, hence according to Eqs. (15), (16) and using a result from introductory statistical mechanics relating number fluctuations to the compressibility (see exercises), we have

$$S_{\mathbf{q}\to\mathbf{0}} \sim 1 + n\int \mathrm{d}\mathbf{r}\, h(\mathbf{r}) = 1 + \frac{\langle N(N-1)\rangle - \langle N\rangle^2}{\langle N\rangle} = nk_BT\kappa_T \qquad (18)$$

This so-called *compressibility sum rule* relates an equation of state (for the pressure) to the structural fluctuations encoded in $S_{\mathbf{q}}$. It also provides a reverse perspective at the relation between fluctuations and response. While the fluctuations are usually understood to increase in magnitude as a consequence of a decrease of the response coefficient that determines the restoring forces, Eq. (18), in return, expresses the value of a response coefficient by an integral over the fluctuations. It thereby clearly displays the connection between a diverging correlation length, which entails a (spatially) slow decay of the fluctuations encoded in $h(r)$, and a divergence of response coefficients at a critical point.

In summary, the pair distribution completely determines one of the most important experimental observables of the packing structure of a material, namely the (static) structure factor. Its spatial integral moreover also determines the materials' mechanical strength (its compression modulus) via a sum rule, which provides a special case of the general fluctuation-response theorem, one of the major predictions by statistical mechanics that repeatedly reappears in various generalizations throughout the lecture.

2 Packing structure and material behavior

Exploiting the simplifications ensuing from the limitation to pair interactions, the relation (18) between packing structure and material behavior can be taken somewhat further, to express the two constitutive equations (or equations of state) of an interacting gas in terms of the pair distribution function $g(\mathbf{r})$.

The caloric equation of state or *energy equation*, Eq. (1) is readily generalized,

$$U = \langle H\rangle = 3\langle N\rangle k_BT/2 + \langle\mathcal{V}\rangle\ . \qquad (19)$$

Noting that all $N(N-1)/2$ particle pairs give the same contribution to the last term, it may be rewritten as

$$\langle\mathcal{V}\rangle = \langle N(N-1)\nu(\mathbf{r}_{12})\rangle/2\ . \qquad (20)$$

Now, introducing a $\mathbf{1}$ in the form $\int \mathrm{d}\mathbf{r}\, \delta(\mathbf{r}-\mathbf{r}_{12})$, just as in the above calculation for the structure factor, and using Eq. (15), this may immediately be rephrased in the form

$$U = \langle H \rangle = \frac{3}{2}\langle N \rangle k_B T \left[1 + \frac{n}{3} \int \mathrm{d}\mathbf{r}\, g(\mathbf{r}) \beta \nu(\mathbf{r}) \right] . \tag{21}$$

Similarly, the thermal (mechanical) equation of state may be extended and related to the radial distribution,

$$\beta p = -\beta \partial_V F|_T = \partial_V \ln\bigl(Z_{\mathrm{ig}} Q\bigr) = n + Q^{-1} \partial_V Q \, . \tag{22}$$

The normalized configuration integral Q is defined via $Z \equiv Z_{\mathrm{ig}} Q$, hence (in the canonical ensemble)

$$Q = \int \frac{\mathrm{d}^N \mathbf{r}}{V^N}\, e^{-\beta \mathcal{V}(\{\mathbf{r}_j\})} \, , \tag{23}$$

with the short-hand notation $\mathrm{d}^N\mathbf{r}$ for the real-space measure in Eq. (4). Due to the normalization the only volume dependence in Q is due to $\nu(\mathbf{r}_{ij})$, i.e. $\partial_V \nu(\mathbf{r}_{ij}) = \nabla\nu(\mathbf{r}_{ij}) \partial_V \mathbf{r}_{ij}$. Exploiting homogeneity, $\mathbf{r}_{ij} = V^{1/3} \xi_{ij}$, one finds $\partial_V \mathbf{r}_{ij} = \mathbf{r}_{ij}/3V$ and, with Eq. (20) (N's inside averages allow for a grand canonical interpretation),

$$\partial_V Q = -\int \frac{\mathrm{d}^N \mathbf{r}}{V^N}\, \frac{N(N-1)}{2} \left[\frac{\beta\, \mathbf{r}_{12}}{3V} \cdot \nabla \nu(\mathbf{r}_{12}) \right] e^{-\beta \mathcal{V}(\{\mathbf{r}_j\})} \tag{24}$$

$$Q^{-1} \partial_V Q = -\frac{1}{6 k_B T V} \int \mathrm{d}\mathbf{r}\, \langle N(N-1) \delta(\mathbf{r}-\mathbf{r}_{12}) \rangle \mathbf{r} \cdot \nabla \nu(\mathbf{r}) \tag{25}$$

Using again Eq. (15) to rewrite the average over the $\delta-$function in terms of $g(\mathbf{r})$, the correction to the thermo-mechanical constitutive equation of the ideal gas resulting from the potential interactions is thus given by the average of the virial (weighted by the pair distribution), hence the name *virial equation of state*

$$p = n k_B T \left[1 - \frac{n}{6 k_B T} \int \mathrm{d}\mathbf{r}\, g(\mathbf{r}) \mathbf{r} \cdot \nabla \nu(\mathbf{r}) \right] . \tag{26}$$

Equations (18), (21) and (26) show how *thermodynamics follows from packing structure*[5]. They reduce the task of deriving the thermodynamic equations of state to integrations over the spatial density fluctuations. In other words, the thermodynamics of a homogeneous isotropic fluid with pair interactions has entirely been expressed in terms of a two-point correlation function $g(\mathbf{r})$. To make any practical use of this formal result, one has to find $g(\mathbf{r})$ in a continuous parameter region, which is indeed the central task of so-called *liquid state theories*. In particular, a very educated guess about the general form of $g(\mathbf{r})$ or at least of

[5]Three constitutive equations cannot be independent, of course, and errors of approximate liquid-state theories are sometimes estimated (or reduced) by comparing (or superimposing) the predictions obtained from Eq. (26) and Eq. (18), respectively.

$\nu(\mathbf{r})$ is indispensable to apply the result in reverse, namely to infer aspects of the microscopic packing structure and interaction potential from macroscopic thermodynamic measurements. Historically, we owe much of our knowledge about molecular interactions to this connection, and thanks to recent developments in microscopy, it might become a fruitful path to explore more, in the future.

Dilute systems and the second virial coefficient

It is intuitively obvious that encounters between particles in a dilute gas are rare. Then, multiple collisions are probably very weakly correlated and exponentially rare.[6] Hence, to extract the dominant thermodynamic effect of the interactions it suffices to calculate it for any pair of particles. But this amounts to knowing the radial distribution of one of the interacting particles in the field created by the other, which may be located at the origin of the coordinate system for a homogeneous system. Given the interpretation of $g(\mathbf{r})$ as a real space probability distribution for finding partners, this problem is of course equivalent to the derivation of the barometer equation, with the known result (see the exercises)

$$g(\mathbf{r}) \sim e^{-\beta\nu(\mathbf{r})} \qquad (n \to 0) \; . \tag{27}$$

The symbol $\sim$ means "asymptotically equal", i.e. an exact equality in the pertinent limit. This implies that the pair fluctuation function $h(\mathbf{r}) = g(\mathbf{r}) - 1$ is asymptotically given by the so-called *Mayer function*

$$f(\mathbf{r}) \equiv e^{-\beta\nu(\mathbf{r})} - 1 \; . \tag{28}$$

Its integral is the so-called *second virial coefficient*

$$B(T) \equiv -\frac{1}{2}\int \mathrm{d}\mathbf{r}\, f(\mathbf{r}) \; . \tag{29}$$

For hard spheres, the Mayer function is the box function $f(\mathbf{r}) = -\theta(\sigma - r)$ and the second virial coefficient $B(T)$ is the excluded volume per sphere in a pair collision. For more general interactions, a positive/negative $B(T)$ is indicative of a predominantly repulsive/attractive interaction, which increases/decreases the pressure, correspondingly.

The second virial coefficient completely quantifies the leading corrections to the ideal gas limit of the constitutive equations. Namely, inserting Eq. (27) into the energy and virial equations of state, Eqs. (21), (26), respectively, one immediately deduces the equations of state of a dilute interacting gas[7]

$$\frac{U}{3Nk_BT/2} \sim 1 - \frac{2n}{3} T\partial_T B(T) \tag{30}$$

[6] The chance of finding a single particle in a volume corresponding to the interaction range σ is $n\sigma^3 \ll 1$. For two particles, as required for pair interactions, it is $\propto n^2\sigma^6$, and so on.

[7] Use $\beta\nu e^{-\beta\nu} = -\beta\partial_\beta f = T\partial_T f$, and the definitions of $f(\mathbf{r})$ and $B(T)$.

and

$$\frac{p}{nk_BT} \sim 1 + \frac{n}{6}\int \mathrm{d}\mathbf{r}\, \mathbf{r}\cdot\nabla f(\mathbf{r}) = 1 + nB(T)\ . \tag{31}$$

The Mayer function vanishes at large arguments for fast-decaying interactions, thanks to the subtracted 1. This renders the occurring integrals finite. One may expect this property to carry over to $h(\mathbf{r})$, even at higher densities, which is indeed borne out by many observations and calculations. An exception occurs near critical points, where the correlation length diverges, so that $h(\mathbf{r})$ becomes long-ranged. A more formal derivation and an extension of the above idea to higher orders in the density is given by the Mayer cluster expansion. Calculations beyond the leading orders are laborious, though, and the whole expansion will break down at the first really interesting occasion (e.g. a phase transition, or long-ranged interactions, which jeopardize the otherwise plausible fast convergence of the series), which is why it is omitted, here.

In summary, for dilute systems, the corrections to the thermodynamics of an ideal gas are completely contained in $B(T)$, which is a two-body configuration integral. Assuming the general functional form of the interaction potential to be given — e.g. Lennard–Jones, (sticky) hard sphere, etc. — measurements of $B(T)$ can be used (and have excessively been used) to determine the potential parameters for atoms, simple molecules, colloidal particles or globular proteins. Dilute interacting gases are not more complex than ideal gases in an external field, i.e., they boil down to the barometer equation.

Potential of mean force

Motivated by Eq. (27), one writes also the pair distribution $g(\mathbf{r})$ of a dense fluid in the form

$$g(\mathbf{r}) = e^{-\beta w(\mathbf{r})}\ , \tag{32}$$

which can be used to define the *potential of mean force* $w(\mathbf{r})$. With Eq. (15)

$$\nabla w(\mathbf{r}) = \frac{V}{\beta g(\mathbf{r})}\langle\nabla_{\mathbf{r}_{12}}\delta(\mathbf{r}-\mathbf{r}_{12})\rangle = \frac{V}{g(\mathbf{r})}\langle\delta(\mathbf{r}-\mathbf{r}_{12})\nabla_{\mathbf{r}_{12}}\nu(\mathbf{r}_{12})\rangle = \langle\nabla_{\mathbf{r}_{12}}\nu(\mathbf{r}_{12})\rangle_{\mathbf{r}_{12}=\mathbf{r}}$$

by partial integration, which explains the name and provides an alternative definition. From the last expression — or by analogy with the barometer formula from Eq. (32) — $w(\mathbf{r})$ is seen to be the reversible work needed to approach two infinitely distant particles of the fluid to a distance r through the "background solvent" provided by all the other particles. Splitting off the corresponding work $\nu(\mathbf{r})$ for the pair in empty space,

$$w(\mathbf{r}) = \nu(\mathbf{r}) + \Delta w(\mathbf{r})\ , \tag{33}$$

one obtains the work — or, in fact, free energy — $\Delta w(\mathbf{r})$ isothermally absorbed by the solvent during this process, i.e. the part of the reversible work solely

due to the presence of the solvent. In other words, the other particles induce an effective interaction $\Delta w(\mathbf{r})$ between a chosen pair of test particles. This is further discussed in the exercises for the example of depletion attractions induced in a fluid of purely repulsive particles.

The work in displacing a pair of hard spheres for distances $r > \sigma$ is completely due to the effective interactions $\Delta w(r)$ induced by the solvent, i.e. by the solvent of surrounding spheres. The function $\Delta w(r)$ can therefore be identified as the free energy cost for bringing two cavities of the size of the spheres from infinity to a distance r. The corresponding part of the radial distribution function $g_c(r) = e^{-\beta\Delta w(r)}$ is therefore also known as the "cavity distribution". Inserting Eq. (32) into the virial equation (26) yields a relation between the pressure and the contact value $g(\sigma)$ of $g(r)$,

$$\begin{aligned}\frac{p}{nk_BT} &= 1 - \frac{n}{6}\int \mathrm{d}\mathbf{r}\, e^{-\beta\nu(r)-\beta\Delta w(r)}\beta\nu'(r)r \\ &= 1 + \frac{2\pi n}{3}\int \mathrm{d}r\, \left(e^{-\beta\nu(r)}\right)' e^{-\beta\Delta w(r)} r^3 \\ &= 1 + \frac{2\pi n}{3}\int \mathrm{d}r\, \delta(r-\sigma) g_c(r) r^3 \\ &= 1 + \frac{2\pi}{3} n\sigma^3 g_c(\sigma) = 1 + 4\phi g(\sigma)\ .\end{aligned} \tag{34}$$

The final $g(\sigma)$ should be understood[8] as $g_c(\sigma) = g(r \to \sigma+)$, and $\phi \equiv n\pi\sigma^3/6$ denotes the *volume fraction* of the spheres. The take-home message is that the equation of state of a hard sphere fluid is determined by the contact value of the radial distribution function, i.e. by the collisions between the spheres. For concentrations $n \approx n_{\mathrm{cp}} = 1/v_{\mathrm{cp}}$ near close-packing[9], a free-volume consideration suggests that the radial distribution function must develop a pointed next-neighbor peak of width $\Delta \approx (v - v_{\mathrm{cp}})/3\sigma^2$ at $r = \sigma$. The spatial integral over the next neighbor peak,

$$4\pi n \int_\sigma^{\sigma+\Delta} \mathrm{d}r\, r^2 g(r) \approx C \qquad (n \approx n_{\mathrm{cp}}) \tag{35}$$

gives an estimate for the number of nearest neighbors or "coordination number" C. For dense fluids and close-packed crystals $C \approx 12$. A simple unsystematic guess of the hard-sphere equation of state $p(\phi)$ is thus obtained by parametrizing the next-neighbor peak for $r \gtrsim \sigma$ by some function such as $g(\sigma)e^{-(r-\sigma)/\Delta}$, plugging it into Eq. (35), and solving for $g(\sigma)$ as a function of $n = 1/v$. This produces the form $p = nk_BT[1 + c\,\phi/(1 - \phi/\phi_{\mathrm{cp}})]$ with a (poorly determined) constant c that one might wish to set to $c = 4$ in order to get Eq. (31) right.

[8] In contrast to g, g_c is smooth at $r = \sigma$, which helps to avoid ambiguities at the discontinuity.

[9] In three dimensions, closest packing is attained in a fcc/hcp-crystal with $n = n_{\mathrm{cp}} \equiv \sqrt{2}/\sigma^3$ corresponding to $\phi_{\mathrm{cp}} \approx 0.74$, as conjectured by J. Kepler, proved by K. F. Gau with respect to all crystalline packings, and, at the end of the 20$^{\mathrm{th}}$ century, by T. C. Hales in full generality.

3 Ornstein–Zernike integral equation

A central task in many-body theory is the prediction of phase transitions and the accompanying structural changes, as these provide not only the most spectacular applications but also the most significant and critical tests of the theory. The challenge then is to demonstrate how long-range correlations and divergent response coefficients emerge from a typically short-ranged interaction potential. At a critical point or at a spinodal, the pair correlation function $h(\mathbf{r}) = g(\mathbf{r}) - 1$ has to become long ranged such that its integral and, according to Eq. (18), the compressibility $S_{q\to 0}/(nk_BT)$ diverges within a narrow parameter range. A standard trick to guarantee that this subtle structure is preserved in practical calculations (which are, of course, approximate calculations) consists in introducing a new function $c(\mathbf{r})$ and its Fourier transform $c_{\mathbf{q}}$, called the *direct correlation function*, via

$$S_{\mathbf{q}} = 1 + nh_{\mathbf{q}} = \frac{1}{1 - nc_{\mathbf{q}}} \tag{36}$$

A small change in the density n then translates into singular behavior of $S_{q\to 0}$, and a finite error in $c_{\mathbf{q}}$ will only affect the precise location of the phase transition but not wreck its singular nature. This equation, and its transformation into real space

$$h(\mathbf{r}) = c(\mathbf{r}) + n \int d\mathbf{r}'\, c(\mathbf{r} - \mathbf{r}')h(\mathbf{r}')\,, \tag{37}$$

are called *Ornstein–Zernike* (integral) equations (OZE). A formal justification of the pertinence of this structure and the interpretation of $c(\mathbf{r})$ are postponed to the next section, while the remainder of this section first attempts to provide an intuitive physical interpretation.

By expanding the denominator in Eq. (36) or iterating Eq. (37), respectively, one immediately sees that the OZE decomposes the correlations in $h(\mathbf{r})$ into chains of "direct correlations" as expressed by $c(\mathbf{r})$ (each $*$ stands for a convolution integral in real space or multiplication in Fourier space, respectively)

$$h = c + nc * c + n^2 c * c * c + \dots\ . \tag{38}$$

Indeed, the intuition of long-range correlations in $g(\mathbf{r})$ building up as chains of short-range correlations in $c(\mathbf{r})$ is an important guide in applications of the OZE. For long-ranged interactions, such as a Coulomb potential, the trick also works backwards and helps to explain how a long-ranged pair interaction gets screened by the presence of other charges.

There are essentially two different ways of applying Eq. (37) to a system of interest. First, as an exact self-consistency relation that has to be solved for the functions h and c, simultaneously. To this end, one has to supply closure conditions to constrain the two unknowns. Ideally, one would like to choose closures that avoid violations of any *a priori* known properties of $g(\mathbf{r})$, but there

is no general systematic way how to find an exact closure. In practice, the self-consistent solutions are therefore non-perturbative, uncontrolled approximations corresponding to partial resummations of the virial series. A popular example is the Percus–Yevick closure for hard spheres,

$$g(r<\sigma)=0 \qquad c(r>\sigma)=0\;. \tag{39}$$

While the first equation is obviously exact, the second expresses the expectation that the direct correlation function should be of similar range as the interaction potential itself. With this closure (and some effort), the OZE is analytically solvable and yields

$$c(r<\sigma)=\frac{1}{(1-\phi)^4}\left[6\phi(1+\phi/2)^2 r/\sigma-(1+2\phi)^2(1+\phi\, r^3/2\sigma^3)\right]\;. \tag{40}$$

From this one gets pretty accurate approximations (see the yellow curve in Fig. 1) to the numerically exact $g(r)$ and S_q, which are known from Monte Carlo simulations (not shown). After integration, it yields approximate expression for the equation of state and the free energy, similar to the phenomenologically very successful Carnahan–Starling relation

$$\frac{p}{nk_BT}\approx 1+\phi\frac{4-2\phi}{(1-\phi)^3}\;, \qquad \frac{F}{Nk_BT}\approx\frac{F_{\rm ig}}{Nk_BT}+\phi\frac{4-3\phi}{(1-\phi)^2}\;. \tag{41}$$

These expressions can be understood as results of mixing the slightly different predictions for the pressure obtained by inserting Eq. (40) into Eqs. (18) and (26), and also of a heuristic approach called "scaled particle theory", or of a Borel resummation of the leading terms of the virial expansion, respectively. Reality is more complex. There is a fluid-crystal phase coexistence with $p(n)=$ constant for $0.49\lesssim\phi\lesssim 0.55$, which is overlooked by all these approaches, and best addressed by density functional theories, as outlined further below. And at $\phi\approx 0.58$ one observes a dramatic slowdown of the dynamics attributed to a glass transition that can not quantitatively be assessed by simple free-volume arguments or by any other of the mentioned theories, but is very well described by *mode-coupling theory*[10], a dynamic theory that builds on liquid state theory.

The second reading of the OZE is as a kind of perturbation series that essentially "creates a highbrow $h(\mathbf{r})$ out of a lowbrow $c(\mathbf{r})$". This view can also provide some insight as to what might be a good closure. For example, one may start from the observation that in the low-density limit

$$n\to 0 \quad\Rightarrow\quad h(\mathbf{r})\sim c(\mathbf{r})\sim f(\mathbf{r})=e^{-\beta\nu(\mathbf{r})}-1\;. \tag{42}$$

[10] W. Gtze, Complex Dynamics of Glass-Forming Liquids: A Mode-Coupling Theory, Oxford Univ. Press, Oxford 2009.

Using this approximation for $c(\mathbf{r})$ in the OZE, one obtains the first correction to the limiting form for $h(\mathbf{r}) \sim f(\mathbf{r})$, namely

$$h(\mathbf{r}) \sim f(\mathbf{r}) + n \int \mathrm{d}\mathbf{r}'\, f(\mathbf{r}-\mathbf{r}')f(\mathbf{r}') \; . \tag{43}$$

In particular, for hard spheres, this simple procedure gives already qualitatively quite reasonable approximations for the structure factor S_q, as illustrated in Fig. 1. Using $f(r > \sigma) = 0$ and $h(r > \sigma) = e^{-\beta\Delta w(r)} - 1 \sim -\beta\Delta w(r)$ (the final expression holds asymptotically at low densities, where $\beta\Delta w \ll 1$), one moreover immediately reads off

$$\beta\Delta w(\mathbf{r}_{12}) = -n \int \mathrm{d}\mathbf{r}_3\, f(\mathbf{r}_{13})f(\mathbf{r}_{23}) + \mathcal{O}(()n^2) \; . \tag{44}$$

Inserting the hard-sphere Mayer function and doing the integral, one thus obtains the interesting prediction that the pair of test spheres experiences an effective attraction ($\Delta w < 0$), the depletion attraction, due to the unbalanced pressure exerted by the surrounding particles (see exercises). The product of the two Mayer functions indicates that to leading order $\Delta w(\mathbf{r})$ takes the effect of a single additional particle onto the pair of test particles into account. The leading order approximation therefore amounts to treating the solvent as an ideal gas except for its interactions with the two test particles, which is known as the Asakura–Oosawa approximation in colloid science. A more accurate expression for Δw that takes the interactions of the solvent particles into account, is easily obtained from Eqs. (32), (33) and the Percus–Yevick form for $g(r)$, of course. (Consider first the case that the solvent spheres are of the same type as the test spheres and contemplate how this will change the form of the depletion potential; then consider the case of smaller solvent particles.)

To summarize, by an apparently simple rewriting (expressing h or S in terms of c), one has thus gained a robust and efficient approximation scheme for the otherwise forbiddingly complicated many-body problem. Remember that the original task was to solve a ridiculously high-dimensional configuration integral for $N \simeq 10^{23}$ strongly interacting particles. The OZE involves only a single integration and the guessing of appropriate closures. With the OZE, already the simple limiting form of the direct correlation function for vanishing density (in fact, nothing but the good old barometer equation) yields interesting predictions for the pair correlations and the structure factor that moreover stay qualitatively trustworthy for finite (not too large) densities n and may even give a rough idea whereabout and how a liquid-gas phase transition might occur.

The following section establishes the above structure of pair correlations and direct correlations that are related by the OZE on a more systematic basis, the double hierarchy of correlation functions generated from a twin couple of generating functionals, namely the free energy and the grand canonical potential. This field theoretical formalism has widespread applications in physics. In particular, it is the starting point of density functional theories.

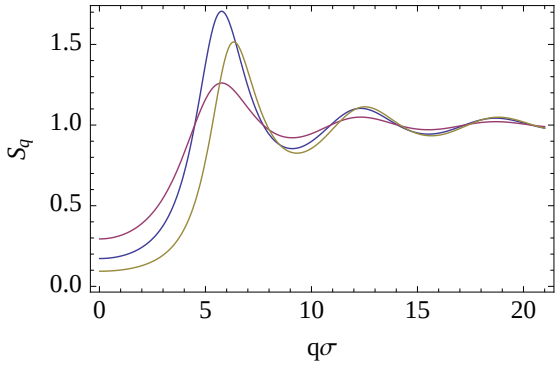

Figure 1: The structure factor of a hard sphere fluid of volume fraction $\phi = 0.3$ (purple) and $\phi = 0.6$ (blue) as estimated by the simplistic procedure described in the main text, which uses the hard sphere Mayer function $f(r) = \theta(r - \sigma) - 1$ as a first approximation for the direct correlation function $c(r)$ as its only input. While not quantitatively useful, it captures the qualitative features of the exact result (and, in fact, of the structure factor of any simple fluid) surprisingly well, as demonstrated by the comparison with the quite accurate Percus–Yevick result, Eq. (40) for $\phi = 0.3$ (yellow).

4 Density functional theory

The 2-lane stairway of correlations & response

The field theory formalism to be introduced in this section may be familiar to some readers from other areas of physics (e.g. QFT). It provides the formal grounds for the Ornstein–Zernike equation and also for the discussion of the fluctuation-dissipation theorem and the density functional theories in the remainder of this part of the lecture.

The whole formalism is nothing but a generalization of the double hierarchy of isothermal derivatives of the equilibrium free energy $F(T, V, N)$ and grand canonical potential $J(T, V, \mu)$, or rather their volume densities $\mathfrak{f}$ and $\mathfrak{j}$, respectively,

$$\begin{aligned} \partial_n \mathfrak{f} &= \mu \ , & \partial_n^2 \beta \mathfrak{f} &= \partial_n \beta\mu = (n^2 k_B T \kappa_T)^{-1} \\ -\partial_\mu \mathfrak{j} &= n \ , & -\partial_{\beta\mu}^2 \beta \mathfrak{j} &= \partial_{\beta\mu} n = n S_{q\to 0} \ , \end{aligned} \tag{45}$$

where β and V are understood to be constant throughout. The procedure can clearly be continued to higher-order derivatives, which will however not be pursued in the following. Note that the compressibility sum rule, Eq. (18) is equivalent to the statement that the second derivatives of the potentials are inverse to each other,

$$(\partial_n^2 \beta \mathfrak{f})(-\partial_{\beta\mu}^2 \beta \mathfrak{j}) = (\partial_n^2 \mathfrak{f})(-\partial_\mu^2 \mathfrak{j}) = 1 \tag{46}$$

This double hierarchy becomes a very useful tool when it is upgraded to allow

for spatial variations of all quantities involved except for the temperature $T = 1/k_B\beta$, which parametrizes the local equilibrium, and the volume V used to turn all extensive quantities into local densities. Spatial variations can arise from external forces, here represented by an external potential $\mathcal{U}(\mathbf{r})$, or from the (pair-)interaction potential $\mathcal{V}(\mathbf{r})$. In a field-theoretic framework, it is useful to express the Hamiltonian in terms of the microscopic densities $\hat{n}(\mathbf{r})$, namely

$$\begin{aligned} H &= \sum_i \frac{\mathbf{p}_i^2}{2m} + \mathcal{V}(\{\mathbf{r}_i\}) + \mathcal{U}(\{\mathbf{r}_i\}) = \sum_i \frac{\mathbf{p}_i^2}{2m} + \sum_{i<j} \nu(\mathbf{r}_i - \mathbf{r}_j) + \sum_i u(\mathbf{r}_i) \\ &= \sum_i \frac{\mathbf{p}_i^2}{2m} + \frac{1}{2}\int \mathrm{d}\mathbf{r}\mathrm{d}\mathbf{r}'\, \hat{n}(\mathbf{r})\nu(\mathbf{r}-\mathbf{r}')\hat{n}(\mathbf{r}') - N\nu(0)/2 + \int \mathrm{d}\mathbf{r}\, \hat{n}(\mathbf{r})u(\mathbf{r}) \end{aligned} \tag{47}$$

The subtraction of $N\nu(0)/2$ and the prefactor $1/2$ in front of the interaction term help to avoid counting the self-interactions and double counting all pairs, respectively. One must not forget the magic hats on the density, since this would turn the microscopic densities $\hat{n}(\mathbf{r})$ into coarse-grained ensemble-averaged densities $n(\mathbf{r})$, and thereby the Hamiltonian into an approximate expression for the free energy (the so-called random-phase approximation).

The main difference of this local formalism compared to the above homogeneous free energies and their derivatives is that partial derivatives of the free energy densities now turn into functional derivatives of the free energies themselves and that multiplications have to be interpreted as convolutions. (By a Fourier transform, one can always get rid of this complication). The benefit is that derivatives generate correlation and response functions and not merely moments of some global quantities and response coefficients, respectively. With the notion of a spatially heterogeneous generalized chemical potential (known as "electrochemical potential" in solid state physics)

$$\mu(\mathbf{r}) \equiv \mu - u(\mathbf{r}) \tag{48}$$

one has via the grand potential route

$$\frac{-\delta J}{\delta\mu(\mathbf{r})} = n(\mathbf{r})\ , \quad \frac{-\delta^2\beta J}{\delta\beta\mu(\mathbf{r})\delta\beta\mu(\mathbf{r}')} = \frac{\delta n(\mathbf{r})}{\delta\beta\mu(\mathbf{r}')} = \langle\delta\hat{n}(\mathbf{r})\delta\hat{n}(\mathbf{r}')\rangle \equiv G(\mathbf{r},\mathbf{r}')\ , \tag{49}$$

with $\delta\hat{n}(\mathbf{r}) \equiv \hat{n}(\mathbf{r}) - \langle\hat{n}(\mathbf{r})\rangle$. Recall that the pair correlation function $G(\mathbf{r},\mathbf{r}')$ is essentially the Fourier transform of the structure factor (times the particle number).

To obtain the corresponding free energy route, one notices that after subtracting the average potential energy

$$\langle\mathcal{U}(\{\mathbf{r}_i\})\rangle = \int \mathrm{d}\mathbf{r}\, \langle\hat{n}(\mathbf{r})\rangle u(\mathbf{r}) = \int \mathrm{d}\mathbf{r}\, n(\mathbf{r})u(\mathbf{r}) \tag{50}$$

from the total free energy corresponding to the Hamiltonian in Eq. (47), the remaining *intrinsic free energy*

$$F[n(\mathbf{r})] = J + \int \mathrm{d}\mathbf{r}\, n(\mathbf{r})\mu(\mathbf{r}) \;, \tag{51}$$

is the Legendre transformation of the functional $J[\mu(\mathbf{r})]$ with respect to the generalized chemical potential $\mu(\mathbf{r})$. Its functional derivatives are

$$\frac{\delta F}{\delta n(\mathbf{r})} = \mu(\mathbf{r}) \;, \quad \frac{\delta^2 \beta F}{\delta n(\mathbf{r}) \delta n(\mathbf{r}')} = \frac{\delta \beta \mu(\mathbf{r})}{\delta n(\mathbf{r}')} = G^{-1}(\mathbf{r}, \mathbf{r}') \;, \tag{52}$$

so that

$$\int \mathrm{d}\mathbf{r}'' \, \frac{\delta^2 F}{\delta n(\mathbf{r}) \delta n(\mathbf{r}'')} \frac{-\delta^2 J}{\delta \mu(\mathbf{r}'') \delta \mu(\mathbf{r}')} = \int \mathrm{d}\mathbf{r}'' \, G^{-1}(\mathbf{r}, \mathbf{r}'') G(\mathbf{r}'', \mathbf{r}') = \delta(\mathbf{r} - \mathbf{r}') \;. \tag{53}$$

It is often useful to isolate the exactly known ideal gas contribution (or, more generally, any other "known" reference free energy)

$$\beta F_{\mathrm{ig}}[n(\mathbf{r})] = \int \mathrm{d}\mathbf{r}\, n(\mathbf{r}) \big(\ln[n(\mathbf{r}) \lambda_T^3] - 1 \big) \tag{54}$$

with the derivatives

$$\frac{\delta F_{\mathrm{ig}}}{\delta n(\mathbf{r})} = k_B T \ln[n(\mathbf{r}) \lambda_T^3] \equiv \mu_{\mathrm{ig}}(\mathbf{r}) \;, \qquad \frac{\delta^2 \beta F_{\mathrm{ig}}}{\delta n(\mathbf{r}) \delta n(\mathbf{r}')} = \frac{1}{n(\mathbf{r})} \delta(\mathbf{r} - \mathbf{r}') \;. \tag{55}$$

This suggests to introduce the so-called *excess free energy* $F_{\mathrm{ex}} \equiv F - F_{\mathrm{ig}}$, with the derivatives

$$\begin{aligned} \frac{\delta F_{\mathrm{ex}}}{\delta n(\mathbf{r})} &= \mu(\mathbf{r}) - \mu_{\mathrm{ig}}(\mathbf{r}) \equiv \mu_{\mathrm{ex}}(\mathbf{r}) \;, \\ \frac{\delta^2 \beta F_{\mathrm{ex}}}{\delta n(\mathbf{r}) \delta n(\mathbf{r}')} &= \frac{\delta \beta \mu(\mathbf{r})}{\delta n(\mathbf{r}')} - \frac{1}{n(\mathbf{r})} \delta(\mathbf{r} - \mathbf{r}') = \frac{\delta \beta \mu_{\mathrm{ex}}(\mathbf{r})}{\delta n(\mathbf{r}')} \equiv -c(\mathbf{r}, \mathbf{r}'). \end{aligned} \tag{56}$$

By comparison with the second line of Eq. (47), $c(\mathbf{r}, \mathbf{r}')$ can be said to be the dressed version of the bare pair interaction $\nu(\mathbf{r} - \mathbf{r}')$ (the free energy looks like the Hamiltonian but with n and c in place of $\hat{n}$ and ν, respectively). The notation $c(\mathbf{r}, \mathbf{r}')$ is not an accident. The quantity thus defined, or rather $n(\mathbf{r}) c(\mathbf{r}, \mathbf{r}')$, is seen to encode "excess" correlations beyond the δ-correlations of the ideal gas. Indeed, it reduces to the direct correlation function $n\, c(\mathbf{r} - \mathbf{r}')$, introduced above, in the special case of a translation invariant system. Inserting Eq. (56) and the *total (pair) correlation function*

$$n(\mathbf{r}) n(\mathbf{r}') h(\mathbf{r}, \mathbf{r}') \equiv n(\mathbf{r}, \mathbf{r}') - n(\mathbf{r}) n(\mathbf{r}') = G(\mathbf{r}, \mathbf{r}') - n(\mathbf{r}) \delta(\mathbf{r} - \mathbf{r}') \;, \tag{57}$$

with $n(\mathbf{r},\mathbf{r}')$ the usual 2-point correlation function without self-correlations, into Eq.(53), one finds (exercises):

$$h(\mathbf{r},\mathbf{r}') = c(\mathbf{r},\mathbf{r}') + \int \mathrm{d}\mathbf{r}''\, h(\mathbf{r},\mathbf{r}'')n(\mathbf{r}'')c(\mathbf{r}'',\mathbf{r}') \; . \tag{58}$$

This is, of course, nothing but the Ornstein–Zernike equation in new garment. The earlier versions are immediately recovered for a homogeneous system with constant density $n(\mathbf{r}) = n$, for which also the definition of $h(\mathbf{r},\mathbf{r}')$ reduces to that of $h(\mathbf{r}-\mathbf{r}')$.

This now further clarifies the pertinence of the OZE and the direct correlation function. The OZE constitutes a relation between the 2-point correlation and/or response functions of different hierarchies, one obtained along the free-energy route, the other along the grand-potential route. In terms of response functions, it simply states the (trivial) reciprocity of the excess parts of $\partial_\mu n$ and $\partial_n \mu$. The response of the density to an infinitesimal fluctuation of the chemical potential is the reciprocal of the response of the chemical potential to an infinitesimal density fluctuation. As the above discussion tried to convey, despite this seemingly trivial content, it can serve as a powerful door-opener to the complicated many-body problem.

Fluctuation-response theorem

As already pointed out, the second derivatives of the generalized thermodynamic functionals $F[n(\mathbf{r})]$ and $J[\mu(\mathbf{r})]$ in Eqs. (49) and (52) can be interpreted as spatially varying susceptibility functions or correlation functions, respectively. These equations thus generalize results about the equivalence of fluctuations and response coefficients; e.g. the relation between grand canonical number fluctuations and the compressibility derived in introductory texts on statistical mechanics, or the compressibility sum rule in Eq. (18). They can also be understood as a local, differential version of the virial equation from Sec. 1 for spatially variable pressure. The relation between packing structure, thermal fluctuations, and macroscopic material properties is thereby cast into a form that includes detailed spatial information on both the structural and material side, to leading order. To bring it into a more familiar form, which also exposes more clearly its perturbative nature, it shall now be re-derived for the special case of a homogeneous fluid. For the sake of the argument, the external perturbation is assumed to be periodic (a Fourier component of a weak but otherwise arbitrary perturbing electric or gravitational potential, say),

$$u(\mathbf{r}) = \frac{u_q}{V} e^{i\mathbf{q}\cdot\mathbf{r}} \; . \tag{59}$$

This corresponds to the perturbation Hamiltonian $\mathcal{U} = u_q \hat{n}_{-q}/V$, with $\hat{n}_q = \sum_i e^{-i\mathbf{q}\cdot\mathbf{r}_i}$ the Fourier transformed microscopic density. Then, the resulting density field $\langle \hat{n}_q \rangle_{\mathcal{U}}$, in presence of the perturbation $\mathcal{U}$, is obtained to leading order in

the perturbing field as

$$\langle\hat{n}_q\rangle_{\mathcal{U}} = \frac{\langle\hat{n}_q e^{-\beta\mathcal{U}}\rangle}{\langle e^{-\beta\mathcal{U}}\rangle} \sim \frac{\langle\hat{n}_q(1-\beta\mathcal{U})\rangle}{\langle 1-\beta\mathcal{U}\rangle} \sim n_q + \frac{\beta u_q}{V}\Big(\langle\hat{n}_q\rangle\langle\hat{n}_{-q}\rangle - \langle\hat{n}_q\hat{n}_{-q}\rangle\Big) \; .$$

Here and in the following, quantities calculated in, or pertaining to the perturbed state are marked with a subscript $\mathcal{U}$ to distinguish them from corresponding quantities in the reference fluid. Note that the last term is, up to a missing factor $1/\langle N\rangle$, actually the definition of the structure factor. The strength of the deviations from the homogeneous reference state are controlled by the structure factor S_q of the unperturbed system, which—at the same time—characterizes the fluctuations and packing structure,[11]

$$\Delta n_q^{(\mathcal{U})} \equiv \langle\hat{n}_q\rangle_{\mathcal{U}} - \langle\hat{n}_q\rangle = -\frac{\beta u_q}{V}\langle\delta\hat{n}_q\delta\hat{n}_{-q}\rangle = -\beta u_q n S_q \; . \tag{60}$$

The local susceptibility generalizing the overall isothermal compressibility κ_T is the functional derivative of the local density with respect to the perturbing potential, which turns into an ordinary partial derivative in Fourier space,

$$\chi(\mathbf{r},\mathbf{r}') \equiv \delta n(\mathbf{r})/\delta u(\mathbf{r}') = -\beta G(\mathbf{r},\mathbf{r}') \; , \qquad \chi_q = \partial n_q/\partial u_q = -\beta n S_q \; . \tag{61}$$

The structure factor, the two-point correlation function of the density fluctuations, is at the same time the susceptibility controlling the density change in response to an external perturbing potential. This is the *fluctuation-response theorem*, which contains the compressibility sum rule as the special case $q \to 0$, and which is itself a specialization (to temporally stationary situations) of the more general (dynamic) fluctuation-dissipation theorem (FDT).

Basic notions of density functional theory

Density functional theory (DFT) is a very successful and popular framework based on the above formalism that extends (and includes as a special case) the Ginzburg–Landau theory usually discussed in statistical mechanics lectures. Although it exploits and builds on the above formally exact relations and admits fluctuations via the spatially varying density field $n(\mathbf{r})$, it is mean-field like in practice. The approximation schemes required to address real-life applications introduce some uncontrolled errors in the direct correlation function that spoil the critical behavior and other subtle correlation effects. Another limitation of DFT is that it usually does not get rid of some guessing of trial functions or, in more elaborate versions, at least of some free parameters. With respect to the task of obtaining numerically precise predictions this freedom may suit the

[11] Note the (initially confusing but common) overloading of the symbol S_q (with or without the forward scattering at $q = 0$) and the prefix δ (delta function, functional derivative and variation $\delta\hat{n} \equiv \hat{n} - n$ around some local or global average density $n \equiv \langle\hat{n}\rangle$).

practitioner, while it is somewhat less satisfying with respect to the task of generating insight into fundamental physical mechanisms. Examples that serve as paradigms for applications in many areas of physics are the Landau theory, the freezing and melting transition in simple fluids, the isotropic-nematic transition, and the Poisson–Boltzmann and Debye–Hckel theory. Appropriately extended versions of DFT involving particle exchange effects are very useful in quantum mechanical many-body problems, e.g. in describing electrons and more complex quasi-particles, e.g. in (semi-)conductors and large atoms, which are not considered here.

Inhomogeneous ideal gas

Basically the only exactly known density functional of an inhomogeneous fluid is that of the inhomogeneous ideal gas. It is obtained by replacing the constant density n by the spatially varying field $n(\mathbf{r})$ in the known bulk formula,

$$\beta F_{\rm ig}[n(\mathbf{r})] = \int \mathrm{d}\mathbf{r}\, n(\mathbf{r})\big(\ln[n(\mathbf{r})\lambda_T^3] - 1\big) \;\Rightarrow\; \frac{\beta\delta^2 F_{\rm ig}}{\delta n(\mathbf{r})\delta n(\mathbf{r}')} = \frac{1}{n(\mathbf{r})}\delta(\mathbf{r}-\mathbf{r}') \;. \quad (62)$$

In the homogeneous state the fields degenerate to $n(\mathbf{r}) = n$, $G(\mathbf{r},\mathbf{r}') = n\delta(\mathbf{r}-\mathbf{r}')$, and hence $ng(\mathbf{r}) = n$, $h(\mathbf{r}) = c(\mathbf{r}) = 0$, and $S_q \equiv 1$.

Slightly inhomogeneous fluids

Even for a strongly interacting many-body system, weak fluctuations around a homogeneous reference state may often be treated as a weakly interacting gas. The corresponding model of a slightly inhomogeneous fluid is among the most commonly applied models in many-body physics. It is the (classical) basis for the quantized elementary excitations and quasi-particles that govern the world of solid-state physics, but it is equally useful in soft matter physics. The inhomogeneous part of the free energy in terms of the density fluctuations $\delta n(\mathbf{r}) = n(\mathbf{r}) - n$ (around a global average density n) is defined as the intrinsic free energy minus its homogeneous part, i.e., with $n(\mathbf{r}) \equiv n$. Subtracting $N[\ln(n\lambda_T^3) - 1]$ from Eq. (62) gives the contribution of the ideal gas to the inhomogeneous free energy $\beta F_{\rm ih}$. And the interaction or excess part is written as a quadratic form in the small quantities $\delta n(\mathbf{r})$ that reproduces Eq. (56) upon differentiation. The direct correlation function $c(\mathbf{r},\mathbf{r}')$ is taken to be that of the homogeneous reference state (i.e., it may depend on $\mathbf{r}-\mathbf{r}'$ and on n but not on $\mathbf{r}$ and $\mathbf{r}'$ independently and on δn) and assumed to be known from somewhere (e.g. from the OZE, or estimated via the random-phase approximation). Hence, altogether one has

$$\beta F_{\rm ih} = \int \mathrm{d}\mathbf{r}\; \{n(\mathbf{r})\ln[n(\mathbf{r})/n] - \delta n(\mathbf{r})\} - \frac{1}{2}\int \mathrm{d}\mathbf{r}\mathrm{d}\mathbf{r}'\, c(\mathbf{r}-\mathbf{r}')\delta n(\mathbf{r})\delta n(\mathbf{r}') \;. \quad (63)$$

(The last term in the curly brackets actually vanishes upon integration, but is kept here as a gauge term for later cancellations with the first term.) A familiar example for such theories is the square-gradient expansion familiar from the Ginzburg–Landau free energy for the fluctuations, that amounts to the additional small wave vector approximation $c_q \sim c_0 + c_1 q^2/2$. Here, $c_1/4\beta$ would become the coefficient in front of the square gradient term in the free energy after Fourier back transformation.

The minimum condition for the grand potential reads

$$\frac{J}{\delta n(\mathbf{r})} = 0 \quad \Rightarrow \quad \frac{\beta\delta F_{\rm ih}}{\delta n(\mathbf{r})} = \beta\mu_{\rm ih}(\mathbf{r}) = \ln[n(\mathbf{r})/n] - \int \mathrm{d}\mathbf{r}'\, c(\mathbf{r},\mathbf{r}')\delta n(\mathbf{r}') \; . \qquad (64)$$

The last expression has to vanish or to balance an external potential $-\beta u(\mathbf{r})$, if present — given that the overall chemical potential μ is already taken care of by the reference fluid. In other words, the spatial density profile $n(\mathbf{r}) = n + \delta n(\mathbf{r})$ obeys the self-consistency relation

$$n(\mathbf{r}) = n e^{-\beta u_{\rm eff}(\mathbf{r})} \quad \text{with} \quad \beta u_{\rm eff}(\mathbf{r}) = \beta u(\mathbf{r}) - \int \mathrm{d}\mathbf{r}'\, c(\mathbf{r}-\mathbf{r}')\delta n(\mathbf{r}') \qquad (65)$$

a position dependent effective potential, which is self-generated by the interactions. This generalizes the well-known self-consistency equation (usually discussed in the mean-field theory for the Ising model in introductory statistical-mechanics texts) to a spatially varying mean field and incidentally improves it by replacing the bare pair interaction potential with the direct correlation function. For vanishing interactions the barometer equation is recovered. The calculation of the density for an interacting fluid thus parallels the solution of the barometer equation for an ideal gas with the additional problem of finding a consistent self-generated "mean field" (the last term in the equation), which encodes the corrections due to the self interactions in the linear-response approximation for small density variations. As usual, if the direct correlation function of the homogeneous reference state is not yet known (e.g. from the OZE), it can be replaced by the bare potential or by the Mayer function, in the random-phase approximation. In any case, such an approach will become poor if the self-induced density fluctuations become too pronounced.

5 Applications: mesophase transitions, freezing, screening

Onsager 1949: nematic transition, mesophases

A historically most significant early example of a density functional theory is Onsager's theory from 1949 for the isotropic-nematic transition in fluids or solutions

of rod-shaped macromolecules. It is instructive in various ways: it combines two independent theoretical concepts introduced above, the low-density approximation and density functional theory; it is a paradigm of partial ordering (orientational ordering without positional ordering) into a so-called micro- or mesophase, a theme with countless variations in (soft) condensed matter theory; and finally it is an early example for a purely entropic or "geometric" transition. Thereby, it anticipates later theories of freezing and melting of simple fluids.

The essential physics of the nematic transition is that isotropic rods of length L and diameter a jam up at high densities, as familiar from the mikado game. To avoid an entropy crisis, i.e., a complete loss of conformational entropy at the isotropic jamming density $n = n_c$, the system sacrifices a bit of its orientational disorder to retain some more of its translational freedom. This trick only works if a macroscopic fraction of the molecules can agree on an average preferred orientation. In other words, spontaneous long-range orientational order has to emerge. In contrast, no positional long-range ordering occurs in the nematic phase. The center-of-mass coordinates retain their fluid-like (or liquid-like) distribution, whence the name *liquid crystal*.

For idealized symmetric (non-polar) molecules there is no preferred direction, only a preferred orientation, which is mathematically represented by the tensor

$$\mathbf{\Psi} = \langle (3\mathbf{uu} - \mathbf{1})/2 \rangle = \psi (3\hat{\mathbf{d}}\hat{\mathbf{d}} - \mathbf{1})/2 \tag{66}$$

constructed from a unit vector $\mathbf{u}$, the "direction" of a representative molecule, which should not be confused with the potential u. The strength of the orientational order is measured by the scalar order parameter

$$\psi \equiv \langle \hat{\mathbf{d}} \cdot \mathbf{\Psi} \cdot \hat{\mathbf{d}} \rangle = \big(3\langle (\mathbf{u} \cdot \hat{\mathbf{d}})^2 \rangle - 1\big)/2 = \big(3\langle \cos^2 \theta \rangle - 1\big)/2 \ \in \ [0, 1] \,, \tag{67}$$

the component of $\mathbf{\Psi}$ parallel to the average orientation of the molecules. The tensor

$$\hat{\mathbf{d}}\hat{\mathbf{d}} \propto \sum_i \mathbf{u}_i \mathbf{u}_i = \langle \mathbf{uu} \rangle = \int \mathrm{d}\mathbf{u}\, p(\mathbf{u}) \mathbf{uu} \tag{68}$$

pointing along the average orientation[12] of the molecules (or also the vector $\hat{\mathbf{d}}$) is called the "director". Here, $p(\mathbf{u})$ denotes the normalized orientational distribution of the rods. In the limit of total alignment, $\mathbf{u} \cdot \hat{\mathbf{d}} = \pm 1$, the angle θ between $\mathbf{u}$ and $\hat{\mathbf{d}}$ vanishes (or becomes π) as the angular distribution $p(\mathbf{u})$ degenerates to a $\delta-$function, so that $\psi \to 1$. For the isotropic state $\cos\theta$ is evenly distributed, so that $p(\mathbf{u}) = 1/4\pi$, $\langle \cos^2 \theta \rangle = 1/3$, $\psi = 0$, and the director $\hat{\mathbf{d}}$ is not defined.

Onsager realized that, for extreme aspect ratios a/L of the rods, the nematic transition in a gas of hard rods occurs at very low densities, a fact familiar from the mikado game. With a careful analysis of the virial series, he proved that

[12] A slight intervention to break ergodicity, as familiar from the discussion of ferromagnetic order, is tacitly assumed in the formulation involving the ensemble average.

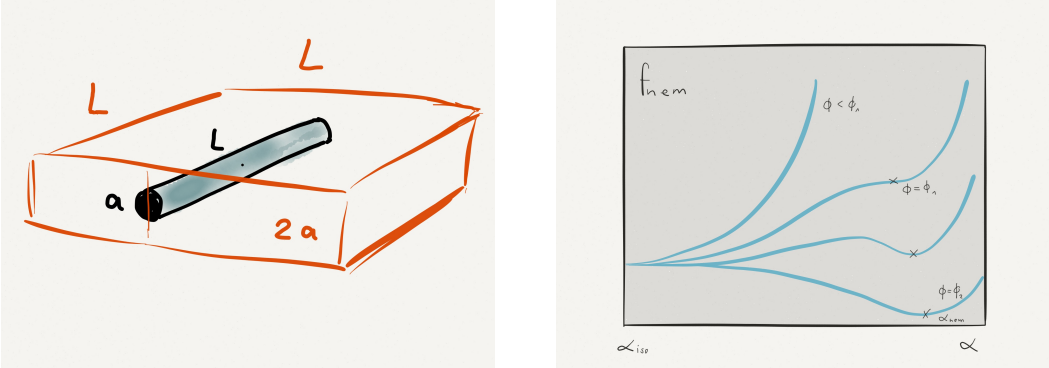

Figure 2: The nematic transition of slender rods. *Left:* Excluded volume for the centers of mass of a pair of slender hard rods. *Right:* The free energy cost $f_{\rm ih}$ to turn the isotropic state into an inhomogeneous state as a function of the parameter α quantifying the strength of the nematic order. Up to a critical volume fractions ϕ_1 there is only the global minimum corresponding to the isotropic state ($\alpha = \alpha_{\rm iso} = 0$). At higher volume fractions a metastable second local minimum emerges that corresponds to a partially ordered nematic phase. With increasing particle concentration, it gains stability. At $\phi = \phi_2$, the isotropic phase eventually becomes unstable. In the intermediate concentration range, the free energy can be lowered further by partitioning the fluid into coexisting isotropic and nematic phases.

in the limit $a/L \to 0$ simultaneous multiple collisions become rare. The pair interactions between the rods may then, right up to the nematic transition, be treated on the two-particle level (i.e. in low-density approximation). The direct correlation function is thus given by the Mayer function

$$c(\mathbf{r}, \mathbf{u}; \mathbf{r}', \mathbf{u}') \sim e^{-\beta\nu(\mathbf{r},\mathbf{u};\mathbf{r}'\mathbf{u}')} - 1 \; , \tag{69}$$

which, for hard rods, takes the value -1 upon overlap and vanishes otherwise.

Because of the low density at the transition, one expects the center-of-mass degrees of freedom to remain essentially gas-like up to the transition, while some nontrivial behavior should arise in the orientational degrees of freedom controlled by the weight $p(\mathbf{u})$, as indeed experimentally observed[13]. Hence, the generalized density $n(\mathbf{r}, \mathbf{u})$ of rods with orientation $\mathbf{u}$ at position $\mathbf{r}$ simplifies to

$$n(\mathbf{r}, \mathbf{u}) \to n\, p(\mathbf{u}) \; . \tag{70}$$

As an immediate consequence, the spatial integrals in the excess free energy will only contain the direct correlation function in Eq. (69), which then moreover only

[13]In fact, near the critical density, the isotropic and nematic phases turn out to coexist and have slightly different densities, but this can be taken into account later.

depends on the relative positions $\mathbf{r}_{12}$. After the positional degrees of freedom have been integrated out, what remains is the orientational direct correlation function

$$c(\mathbf{u},\mathbf{u}') \equiv \int \mathrm{d}\mathbf{r}\mathrm{d}\mathbf{r}'\, c(\mathbf{r}-\mathbf{r}';\mathbf{u},\mathbf{u}') = V\int \mathrm{d}\mathbf{r}_{12}\,[e^{-\beta\nu(\mathbf{r}_{12},\mathbf{u},\mathbf{u}')}-1] \tag{71}$$

From the sketch in Fig. 2 one quickly convinces oneself that

$$c(\mathbf{u},\mathbf{u}') = -2aL^2V|\mathbf{u}\times\mathbf{u}'| = -2aL^2V|\sin\theta|\,, \tag{72}$$

which is identified as the (negative) excluded volume, which depends on the relative orientation, i.e. on the angle θ between the considered pair of rods. These arguments are now put to work.

In the homogeneous and isotropic reference state, $p(\mathbf{u}) = 1/4\pi$ and the free energy per particle is given by the ideal gas contributions from the center-of-mass degrees of freedom (the constant contribution from the orientational degrees of freedom can be gauged away), plus the excess part of the free energy:

$$\begin{aligned}\beta F_{\mathrm{ex}} =& -\frac{1}{2}\int \mathrm{d}\mathbf{r}\mathrm{d}\mathbf{u}\mathrm{d}\mathbf{r}'\mathrm{d}\mathbf{u}'\, c(\mathbf{r}-\mathbf{r}';\mathbf{u},\mathbf{u}')n(\mathbf{r},\mathbf{u})n(\mathbf{r}',\mathbf{u}') \\ =& -\frac{n^2}{2}\int \mathrm{d}\mathbf{u}\mathrm{d}\mathbf{u}'\, c(\mathbf{u},\mathbf{u}')p(\mathbf{u})p(\mathbf{u}') \\ =& \, aL^2Vn^2\int\frac{\mathrm{d}\mathbf{u}}{4\pi}\,|\sin\theta| = B\,n^2V\end{aligned} \tag{73}$$

with the second virial coefficient $B = \pi aL^2/4$. The total free energy per particle in the homogeneous and isotropic reference state is thus (not very surprisingly)

$$\beta f_{\mathrm{iso}} = \ln(n\lambda_T^3) - 1 + B\,n\,. \tag{74}$$

So this is the rare case of a simple (and in the limit $a/L \to 0$ exact) analytical result for an interacting many-body system.

Now comes the hard part, namely dealing with the possible anisotropies. From Eq. (63), the inhomogeneous free energy per particle βf_{ih} (the excess over the isotropic state) reads

$$\beta f_{\mathrm{ih}} = \int \mathrm{d}\mathbf{u}\,\big[p(\mathbf{u})\ln 4\pi p(\mathbf{u}) - \delta p(\mathbf{u})\big] - \frac{n}{2V}\int \mathrm{d}\mathbf{u}\mathrm{d}\mathbf{u}'\, c(\mathbf{u},\mathbf{u}')\delta p(\mathbf{u})\delta p(\mathbf{u}')\,, \tag{75}$$

with $\delta p(\mathbf{u}) \equiv p(\mathbf{u}) - 1/4\pi$ the anisotropic part of the orientational distribution. The self-consistency relation for $p(\mathbf{u})$, Eq. (65), which results from minimizing the total free energy (corresponding to $f_{\mathrm{iso}} + f_{\mathrm{ih}}$) is

$$4\pi p(\mathbf{u}) = e^{-\beta u_{\mathrm{eff}}(\mathbf{u})} \quad \text{with} \quad \beta u_{\mathrm{eff}}(\mathbf{u}) = \phi\frac{8L}{\pi a}\int \mathrm{d}\mathbf{u}'\,|\mathbf{u}\times\mathbf{u}'|\;\delta p(\mathbf{u}')\,, \tag{76}$$

with the volume fraction $\phi = \pi(a/2)^2 L\, n$. Both Eqs. (75) and (76) are still formally exact for $a/L \to 0$, if the emerging orientational order is weak enough to justify the quadratic form of the free energy. However, in contrast to the homogeneous case, Eq. (74), all that is known about the excess orientational distribution $\delta p(\mathbf{u})$ is that it vanishes upon integration over all directions, and also for small values of the control parameters $\phi L/a \to 0$ (hence weak mean field). To allow for a nematic transition, it somehow has to develop a peaked structure. As a consequence, f_{ih} should turn negative above some critical volume fraction ϕ_c and thus yield the isotropic state unstable in favor of nematic ordering. In other words, one is looking for a bifurcation in a somewhat daunting infinite dimensional nonlinear eigenvalue problem.

This is, where uncontrolled approximations come into play. One invents a parameter-dependent trial function $p_\alpha(\mathbf{u})$ which reduces the problem to a low-dimensional eigenvalue problem. A reasonable guess for $p_\alpha(\mathbf{u})$ could be a Gaussian of width α^{-1} centered around the director, and one may expect that Onsager tried this first. In his paper, he proposed the ansatz

$$p_\alpha(\theta) = \frac{\alpha}{4\pi} \frac{\cosh(\alpha \cos\theta)}{\sinh \alpha} \tag{77}$$

instead, which has also only a single free parameter α, is similarly analytically tractable, and lowers the total free energy after minimization even further than the Gaussian. The dependence of the order parameter on α is readily obtained

$$\psi = 1 - 3(\coth \alpha - \alpha^{-1})/\alpha \; . \tag{78}$$

The limits $\alpha = \alpha_{\mathrm{iso}} = 0$ and $\alpha \to \infty$ correspond to an isotropic and perfectly oriented system, respectively. By minimizing the free energy with the trial function, Onsager indeed found a certain critical volume fraction $\phi_c \simeq a/L$, where the inhomogeneous contribution to the free energy turned negative for some $\alpha = \alpha_c > 0$ indicating a discontinuous ("first order") phase change with a corresponding jump in the order parameter.

At this point, many studies of mesophase transitions would be satisfied. Upon closer inspection, the situation turns out to be a bit more complex, though. The shape of the inhomogeneous free energy contribution f_{ih} as a function α undergoes qualitative changes from a convex monotonic to a "$\sim$"-shaped and finally "$\cup$"-shaped form upon increasing the control parameter $\phi L/a$ (sketch). Initially, it has a single minimum at $\alpha = \alpha_{\mathrm{iso}} = 0$. At $\phi = \phi_1 = 3a/L$ it first develops a second local minimum at $\alpha = \alpha_{\mathrm{nem}}(\phi) > 0$, which deepens and shifts to higher α upon further increase of $\phi L/a$, until the first minimum vanishes at $\phi_2 = 4a/L$. Hence, in a certain concentration range around ϕ_c there is a chance that the system lowers its *total* free energy by partitioning into domains of densities that are slightly higher and lower than the overall average density, respectively. In other words, there will be a coexistence region, where isotropic and nematic domains

coexist.[14] As apparent from a sketch of the total free energies corresponding to the local minima, $f_{\rm iso} \equiv f(\phi, \alpha_{\rm iso})$ and $f_{\rm ih} \equiv f(\phi, \alpha_{\rm nem})$ over the volume fraction ϕ, appropriate amounts of the two phases have to be present for this to happen. The volume fractions $\phi_{\rm iso}$, $\phi_{\rm nem}$ and particle numbers $N_{\rm iso}$, $N_{\rm nem}$ corresponding to the absolute minimum of the free energy follow from the lever rule

$$Nf = N_{\rm iso} f_{\rm iso} + N_{\rm nem} f_{\rm ih} \ , \quad f = \frac{\phi_{\rm nem} - \phi}{\phi_{\rm nem} - \phi_{\rm iso}} f_{\rm iso} + \frac{\phi - \phi_{\rm iso}}{\phi_{\rm nem} - \phi_{\rm iso}} f_{\rm ih} \ . \tag{79}$$

The concentration $\phi_{\rm iso} \approx 3.3a/L$ and $\phi_{\rm nem} \approx 4.5a/L$ of the coexisting phases follow from the Maxwell construction.

Recall that the whole discussion applies to extreme aspect ratios a/L. In practice, it is found to give a fair description for $L/a > 10^2$. Otherwise, the numerical values deviate substantially and other phases ("smectic", "plastic", crystalline) appear in the phase diagram. Together with the Thomas–Fermi theory for atoms with many electrons, Onsager's ground breaking work has been a paradigm for many later DFTs in condensed matter physics[15].

"Ordinary" fluid-crystal coexistence

Following Onsager, in 1979, Ramakrishnan und Yussouff used Eq. (63) with good success to elucidate the geometric nature of the freezing and melting transitions in classical fluids, explain the universality of the packing structure near these transitions, and numerically compute quantitative predictions for the phase diagram. Their analysis provided a theoretical basis for successful phenomenological rules of thumb, such as the Verlet rule and the Lindemann criterion, which are widely used in practical applications. The *Lindemann criterion* states that crystals melt if the mean-square fluctuations of the atoms exceed 10% of their average next-neighbor distance (the lattice unit), and the *Hansen–Verlet rule* states that fluids freeze if the height of the main peak in their structure factor exceeds 3, thereby hinting at different underlying mechanisms for both transitions.

Their DFT approach regards the crystal as a (not so) slightly inhomogeneous fluid. The procedure can be characterized as "fishing for crystal structures". Briefly, one looks for instances of a non-zero order parameter $n_{\mathbf{K}_i} \equiv \langle \sum_j e^{i\mathbf{K}_i \cdot \mathbf{r}_j} \rangle = \mathcal{O}(N)$ ("Bragg peaks") in a preferably exhaustive set of possible reciprocal lattice vectors $\mathbf{K}_i$. To this end one needs an ansatz. A sum of Gaussian distributions of width a centered at the lattice sites $\{\mathbf{R}\}$

$$n(\mathbf{r}) = n_s \big(\sqrt{\pi} a/a_0\big)^{-3} \sum_{\{\mathbf{R}\}} e^{-(\mathbf{r}-\mathbf{R})^2/2a^2} \tag{80}$$

[14] This is not a peculiarity of the nematic transition, but is in fact the generic situation in any discontinuous ("first order") phase transition, and should be familiar from the van der Waals model, which is usually discussed in introductory thermodynamics lectures.

[15] See Phys. Rev. Lett. **102**, 018302 (2009) for a closely related more recent example.

is plugged into Eq. (63). Local minima of the resulting free energy other than the homogeneous fluid reference state are then searched by varying the model parameters n_s, a_0, and a for a prescribed trial crystallographic lattice $\{\mathbf{R}(a_0)\}$ such as BBC, FCC, etc., and the one with the lowest free energy is then proposed as the equilibrium structure. While the average lattice constant a_0 refers to the abstract lattice, the density n_s refers to the actual mass sitting on this lattice. If it is treated as an independent parameter, the ansatz can account for vacancies.

Poisson–Boltzmann and Debye screening

Another useful and widely used application of the self-consistency relation Eq. (65) is to dilute plasmas, represented by a mixture of two ideal gases of oppositely charged particles that interact via the Coulomb interactions. The densities of the particles are denoted by $n_+(\mathbf{r})$ and $n_-(\mathbf{r})$ and assumed to vary around the same average $n/2$ to ensure neutrality. Only interactions of local excess charges are considered, disregarding the (divergent) interaction energies within the homogeneous background. Each species obeys a self-consistent Barometer equation of the type in Eq. (65) with a factor $n/2$ (instead of n) in front of the exponential and $\pm\delta n(\mathbf{r})$ (the sign depending on the species considered) replaced by the net charge density $n_e(\mathbf{r}) \equiv n_+(\mathbf{r}) - n_-(\mathbf{r})$, as it is only via the charges that the particles interact. The direct correlation function is approximated, in random-phase approximation, by the bare Coulomb potential. In absence of external fields, the effective potential for the species densities $n_\pm(\mathbf{r})$ is then given by

$$\pm\beta u_{\text{eff}}(\mathbf{r}) = \int \mathrm{d}\mathbf{r}' \, \frac{z^2 \ell_B}{|\mathbf{r} - \mathbf{r}'|} n_e(\mathbf{r}') \; . \tag{81}$$

Here, the *Bjerrum length* $\ell_B \equiv \beta e^2$ emerges as the natural length scale that distinguishes short distances (governed by the Coulomb force) from long distances (governed by thermal forces). Subtracting the self-consistency equations for both charge species from each other, and using the Poisson equation to express $n_e(\mathbf{r})$ in terms of the self-generated electrical potential $u_{\text{eff}}(\mathbf{r})$, gives the so-called Poisson–Boltzmann equation,

$$-4\pi z^2 \ell_B n_e(\mathbf{r}) = \nabla^2 \beta u_{\text{eff}}(\mathbf{r}) = \varkappa^2 \sinh \beta u_{\text{eff}}(\mathbf{r}) \; , \tag{82}$$

with $\varkappa^2 \equiv 4\pi z^2 \ell_B n$. Note that the *Debye screening length* $\varkappa^{-1}$ sets the natural scale for the spatial derivative ∇, and therefore for any inhomogeneities in the charge density, which are expected to vanish for $\varkappa r \gg 1$). This indicates the effect of "screening". The Coulomb force exerted by a charge fluctuation onto the surrounding plasma induces a compensating charge cloud that neutralizes and screens it for distant observers.

To pin down the effect more clearly, consider the OZE in the random-phase approximation, i.e. with $c(r) \approx -\beta\nu(r) = z^2 \ell_B / r$, which becomes $-4\pi z^2 \ell_B / q^2$ in

Fourier space. The OZE then gives the charge structure factor and fluctuation function

$$S^e_q = \frac{q^2}{\varkappa^2 + q^2} \quad \Longrightarrow \quad h^e_q = S^e_q - 1 = -\frac{\varkappa^2}{\varkappa^2 + q^2} \tag{83}$$

The vanishing of the "charge compressibility" $S^e_{q\to 0}$ is of course nothing but a reformulation of global charge neutrality. Fourier back transformation Eq. (83) yields the Debye–Hckel form of $h^e(r)$, which can, to the present order of approximation, be identified with the (charge) potential of mean force $\beta w^e(r)$

$$h^e(r) \approx -\beta w^e(r) \approx -\frac{z^2\ell_b}{r}\exp(-\varkappa r)\ . \tag{84}$$

So the actual interaction potential between two charge fluctuations embedded in a plasma is not the bare Coulomb potential, but a screened (or "dressed") version that decays exponentially over a distance $\varkappa^{-1}$. It is Coulombic at short distances $r \ll \varkappa^{-1}$ but vanishes at large distances $r \gg \varkappa^{-1}$. A charge fluctuation is thus not visible from large distances. The result can also be interpreted in terms of the "solvent contributions" encoded in $\Delta w(\mathbf{r}) = z^2\ell_b(e^{-\varkappa r} - 1)/r$, which suppress the long-range part of the bare Coulomb potential.

Part II
Soft-Matter Paradigms: Complex Fluids, Soft Solids, Active Matter

Along with the general principles of many-body physics, the first part of the lecture already briefly introduced some important model systems of soft matter physics, such as the hard sphere fluid and liquid crystals. They serve well to elucidate why and how soft matter is soft and slow and prone to large deformations and fluctuations. Namely, the softness of a hard sphere crystal, which has an elastic modulus on the order of k_BT/ℓ^3, is primarily due to its large lattice constant ℓ (on the order of 100 nm, say) and, to a lesser degree, also to its weak entropic interaction strength (given by the thermal energy k_BT itself). Together with the viscous damping due to the solvent that usually dominates over inertia effects, this also accounts for the relative slowness of the dynamics compared to conventional hard-matter systems. This observation is very general and carries over to a vast class of material structures, with only minor modifications. It also rightly suggests that soft matter systems may take the role of an upscaled and slowed-down laboratory for many of the physical principles at work in hard matter systems.

The main aim of the present part of the lecture is to provide a slightly more specific perspective on other paradigmatic properties of soft materials. Even if a liquid froth or a dense solution of swimming bacteria, say, may share some intriguing similarities with the packing of hard spheres, one would not expect that their physics can entirely be understood by this analogy, alone. At some point, additional aspects, such as surface tension, surfactants, wet electrostatics, fluid flow, and self-propulsion will enter the stage and claim to make a difference. And these effects are so ubiquitous and entail such a wide variety of phenomena that their omission would amount to throwing out the baby with the bath water. As a *pars pro toto* for such additional important (and still reasonably general) aspects, the remainder of the lecture focusses on the floppy internal degrees of freedom of low-dimensional mesostructures (such as phase boundaries, biological membranes, or macromolecules[16]) and the dynamics of the solvent in which they are dispersed, and eventually adds activity to the story. Many soft materials, and in particular all living ones, are well characterized as fluids with some inter-dispersed low-dimensional elastic mesoscale structures (or *vice versa*), and possibly activity. Elements of the theories of (fluctuating) hydrodynamics and of the elasticity of low-dimensional manifolds, both near and far from equilibrium, are therefore often useful companions in soft matter physics.

[16] Also magnetic flux lines in type-II superconductors could be mentioned as an example.

6 Principles of hydrodynamics

Hydrodynamics is the general name for the dynamics of the slow variables of a macroscopic material, if the emphasis is more on mechanical rather than thermal properties[17]. The classical field theories discussed in the first part of the lecture provide good examples for theories that one might subsume under the names of generalized hydrodynamics and (continuum) elasticity. Yet, it is of some interest to have a closer look at hydrodynamics in the narrower sense, namely at the dynamic flow of simple (and not so simple) liquids. Technically speaking, hydrodynamic theories are phenomenological descriptions of material behavior based on symmetries and conservation laws. They become exact in the long-wavelength limit but do not give a clue as to the microscopic scale where they might fail to apply. This is generally a great advantage, because it allows for an exact discussion of swimming without resorting to the microscopic details hidden in the numerical values of some phenomenological coefficients (masses, couplings, moduli, viscosities ...). It can be a nuisance if you need to decide whether it is worthwhile to build an expensive particle accelerator supposed to discover these hidden details behind the (essentially hydrodynamic) standard model of particle physics. In practice, hydrodynamics often works reliably almost all the way down to the omitted "molecular" scale itself. If the microscopic physics is known, one can choose to approach the hydrodynamic equations either from a phenomenological (thermodynamic) or microscopic starting point.

Phenomenological approach

The phenomenological approach does not require knowledge of any atomistic details of a material. It rather builds on a macroscopic formulation of exact conservation laws (which express the symmetries of the problem) in terms of continuity equations. If the latter do not exhaust the degrees of freedom, material laws (equations of state) are additionally required to arrive at a closed set of equations.

The local conservation of a quantity X, say the particle number N, implies

$$\partial_t \rho^X + \nabla \cdot \mathbf{J}^X = 0 \tag{85}$$

with $\rho^X(\mathbf{r}, t)$ and $\mathbf{J}^X(\mathbf{r}, t)$ the density and flux of the conserved quantity X, respectively. In Fourier space, this becomes

$$\partial_t \rho^X_{\mathbf{q}} = i\mathbf{q} \cdot \mathbf{J}^X_{\mathbf{q}} \ , \tag{86}$$

which shows that long-wavelength modes ($\mathbf{q} \to 0$) of conserved quantities relax slowly in time. They are therefore the natural candidates for good hydrodynamic

[17] Otherwise also known as nonequilibrium/dissipative thermodynamics.

variables that can live a tranquil life of their own while the fast and furious microscopic degrees of freedom have long established their perfect local equilibrium under the quasi-static constraints imposed by the slow variables. Other natural candidates for slow variables are broken-symmetry variables. These could be said to be accidentally slow, as the restoring forces that confine their fluctuations happen to be weak because of a nearby critical point. Think of the orientation of the director of a nematic liquid crystal. It costs no energy to turn it globally and therefore also not much to induce a slight bend, twist, or splay — which is why such deformations are easy to achieve and relax slowly.

If the flux $\mathbf{J}$ in Eqs. (85), (86) is not externally prescribed or itself a conserved quantity (a case deferred to further below), one has to find a closure, so that the number of equations equals the number of unknown variables. The flux will in general depend on the density and possibly on other quantities for which one would need additional equations. In the simplest case, someone provides a closure of the form $\mathbf{J}^X[\rho^X]$. In fact, on the phenomenological level, this is not necessarily very hard, as the following simple example demonstrates[18]. Take X to be the number N of colloidal particles suspended in an isothermal isobaric liquid solvent at rest. Then the form of the closure $\mathbf{J}[n(\mathbf{r})]$ for the flux in terms of the number density $n(\mathbf{r},t) \equiv \rho^N(\mathbf{r},t)$ is largely constrained by symmetry. First, Galilei invariance suggests that a flux can be generated by looking at some fluid of density $n(\mathbf{r},t)$ in a comoving frame, so that

$$\mathbf{J}[n(\mathbf{r})] = n(\mathbf{r})\mathbf{v}(\mathbf{r},t) \tag{87}$$

But this only defers the closure problem from the flux $\mathbf{J}$ to the hydrodynamic velocity $\mathbf{v}$. One still needs to relate either vector to the scalar n. This requires another vector to take a scalar product, but there is none around in a homogeneous and isotropic fluid, so that $\mathbf{J}$ must vanish. A more interesting closure results if there happens to be a density gradient ∇n which provides the sought-after vector. Assuming moreover that the gradient is small (as appropriate for a long-wavelength theory), the only possible closure

$$\mathbf{J}(\mathbf{r},t) = -D\nabla n(\mathbf{r},t) \tag{88}$$

with a phenomenological transport coefficient $D(T,n)$ that can only depend on the average density n but not on the density variations. By combining this with particle conservation, Eq. (85), a closed hydrodynamic equation is obtained, namely the diffusion equation

$$\partial_t n(\mathbf{r},t) = D\nabla^2 n(\mathbf{r},t)\ . \tag{89}$$

Thermodynamics and statistical mechanics can provide some additional insight. The thermodynamic approach starts from the second law, which suggests

[18] . . . but it quickly gets very laborious if more hydrodynamic variables enter the game

that non-conserved (dissipative or entropy-producing) currents should always flow "downhill" until the gradient is gone and the appropriate free energy is minimized. For the chosen example of an isothermal isobaric colloidal suspension, the appropriate potential is the Gibbs free energy (per constant coarse-graining volume), $G/V = \mu n$ with[19]

$$\mathrm{d}(\mu n)_{T,p} = \mu \mathrm{d}n \tag{90}$$

Its time derivative is thus

$$\partial_t(\mu n)_{T,p} = \mu \partial_t n = -\mu \nabla \cdot (n\mathbf{v}) = -\nabla \cdot (\mu n \mathbf{v}) + n\mathbf{v} \cdot \nabla \mu \; . \tag{91}$$

This amounts to a continuity equation for the Gibbs free energy with a sink (it must be a sink according to the second law), namely,

$$\partial_t(\mu n) + \nabla \cdot (\mu n \mathbf{v}) = n\mathbf{v} \cdot \nabla \mu \leq 0 \; . \tag{92}$$

and is prototypical of the equations of irreversible thermodynamics. One concludes that spontaneous particle fluxes $n\mathbf{v}$ (that are not excited by some means from outside) always run in the direction of negative gradients in the chemical potential, i.e. they can be understood to be driven by these gradients, which thus play a role akin to external driving forces. This is indeed what Eq. (90) says, namely that the force conjugate to a homogeneous density change is the chemical potential. Chemical potential gradients excite fluxes of the density, accordingly. Denoting by Γ the kinetic coefficient (acting as its friction coefficient) that fixes the time scale for this flux, one thus has

$$\mathbf{J} = n\mathbf{v} = -\Gamma \nabla \mu = -\Gamma \partial_n \mu)_T \nabla n \; . \tag{93}$$

Using $\partial_n \mu)_T = n^{-2}\kappa_T^{-1}$ with the isothermal compressibility κ_T, the diffusion coefficient

$$D(T,n) = \Gamma \partial_n \mu)_T = \Gamma n^{-2} \kappa_T^{-1} \tag{94}$$

in Eq. (89) is seen to encode some kinetic (Γ) and some thermodynamic ($n^2\kappa_T$) information. In particular, for an ideal gas, $D \propto k_B T/n$, which indicates that diffusion is an entropic transport process, driven by thermal fluctuations. According to Eq. (94), it slows down dramatically at a critical point, where the compressibility diverges (so-called "critical slowing-down"). Moreover, it may reverse its direction ("uphill diffusion") in a spinodal instability, where κ_T changes sign, so that time may seem to run backwards for a while, when the particles gather from a homogeneous dilute solution into dense clusters or droplets.

Microscopic approach

A recipe for deriving Eq. (88) microscopically from statistical mechanics would roughly proceed along the lines introduced in the first part of the lecture, which

[19] Recall that $\mathrm{d}G)_{T,p} = \mu \mathrm{d}N$.

is not further pursued here, since it would only lead to equilibrium closure relations[20]. However, the softness of soft matter implies that it is easily driven far from equilibrium. Therefore, the aim is to venture beyond equilibrium. This subsection thus follows the microscopic approach only up to the point where closures come into play. In a microscopic approach the conservation laws are encoded in the microscopic equations of motion. They have then to be coarse-grained to arrive at the hydrodynamic equations, i.e. atomistic details have to be blurred. If one can assume local equilibrium, it is easy to go from microscopic densities to the local densities of hydrodynamics, as usual ($X = \sum_i x_i$):

$$\hat{\rho}^X(\mathbf{r},t) = \sum_i \hat{x}_i \delta[\mathbf{r} - \hat{\mathbf{r}}_i(t)] \quad \rightarrow \quad \rho^X(\mathbf{r},t) = \langle \hat{\rho}^X(\mathbf{r},t) \rangle \; . \tag{95}$$

But, as pointed out, one has to bear in mind that this local equilibrium is generally a perturbed one (by the hydrodynamic flow) compared to the fluid at rest. More generally, one might want to deal with a general nonequilibrium distribution that is of course *a priori* unknown. Or one might resort to spatial coarse-graining by introducing a low-pass filter, a normalized positive real space function that has vanishing Fourier coefficients for wave vectors beyond a certain coarse-graining scale. To obtain the hydrodynamic densities from the microscopic densities, the latter are then convoluted with the filter function. With a slight overloading of the symbol $\langle \dots \rangle$, the definitions of hydrodynamic quantities look the same with such a dynamic coarse-graining as with the nonequilibrium or local equilibrium ensemble averages.

Focussing on the example of a simple one-component liquid (or gas) with particle mass m one has the mass density

$$\hat{\rho}^M(\mathbf{r},t) = m \sum_i \delta[\mathbf{r} - \hat{\mathbf{r}}_i(t)] \tag{96}$$

with its time derivative ($\hat{\mathbf{v}}_i = \partial_t \hat{\mathbf{r}}_i$)

$$\partial_t \hat{\rho}^M(\mathbf{r},t) = -\nabla \cdot \sum_i m \hat{\mathbf{v}}_i(t) \delta[\mathbf{r} - \hat{\mathbf{r}}_i(t)] \; . \tag{97}$$

The microscopic mass flux is thereby identified as

$$\hat{\mathbf{J}}^M(\mathbf{r},t) = \sum_i m \hat{\mathbf{v}}_i(t) \delta[\mathbf{r} - \hat{\mathbf{r}}_i(t)] \; , \tag{98}$$

so that Eq. (97) is recognized as a microscopic continuity equation. The hydrodynamic continuity equation (85) is recovered upon coarse-graining. Also the hydrodynamic transport velocity $\mathbf{v}(\mathbf{r},t)$ is defined, using the coarse graining operation $\langle \dots \rangle$,

$$\langle \hat{\rho}^M(\mathbf{r},t) \rangle \mathbf{v}(\mathbf{r},t) \equiv \langle \hat{\mathbf{J}}^M(\mathbf{r},t) \rangle \; . \tag{99}$$

[20] Microscopic approaches to conditions far from equilibrium are still under development.

In case of particles in vacuum, the mass flux $\mathbf{J}^M$ is a conserved quantity itself, namely the momentum density

$$\hat{\rho}^{\mathbf{P}}(\mathbf{r},t) = \hat{\mathbf{J}}^M(\mathbf{r},t) \; . \tag{100}$$

In the absence of external forces, using Newton's law of motion, one then has

$$\partial_t \hat{\rho}^{\mathbf{P}}(\mathbf{r},t) = -\nabla \cdot \sum_i m \hat{\mathbf{v}}_i \hat{\mathbf{v}}_i \delta(\mathbf{r}-\hat{\mathbf{r}}_i) + \sum_i \hat{\mathbf{F}}_i \delta(\mathbf{r}-\hat{\mathbf{r}}_i) \; . \tag{101}$$

with $\hat{\mathbf{F}}_i(t)$ the force exerted at time t on particle i by all other particles. (Some time arguments are suppressed for brevity.) The equation for the momentum density does not yet have the expected form of a continuity equation. Note, however, that the mutual forces within any volume element cancel each other exactly up to surface[21] contributions arising from the interactions with particles outside the volume element. This is Newton's action-reaction law. Therefore, integrating the force density over any volume element will contribute a surface integral to the overall force, which is another way of saying that the force density may be written as the divergence of a tensor.

Coarse-graining (locally averaging) Eq. (101) and omitting the mass index of the density, one has on the left hand side

$$\partial_t(\rho\mathbf{v}) = \rho\partial_t\mathbf{v} + \mathbf{v}\partial_t\rho = \rho\partial_t\mathbf{v} - \mathbf{v}\nabla\cdot(\rho\mathbf{v}) \; . \tag{102}$$

Using the definition of the transport velocity, (minus) the first term on the right hand side of Eq. (101) reads

$$\nabla\cdot\rho\mathbf{v}\mathbf{v} + \nabla\cdot\sum_i m\langle(\hat{\mathbf{v}}_i-\mathbf{v})(\hat{\mathbf{v}}_i-\mathbf{v})\delta(\mathbf{r}-\hat{\mathbf{r}}_i)\rangle \equiv \nabla\cdot\mathbf{J}^{\mathbf{P}} + \nabla\cdot\Pi^{\mathrm{ig}} \, . \tag{103}$$

Here, the first term is immediately identified as divergence of the hydrodynamic flux $\mathbf{J}^{\mathbf{P}}$ of the momentum density $\rho\mathbf{v}$. It partly cancels with the last term of Eq. (102) if written as $\mathbf{v}\nabla\cdot(\rho\mathbf{v}) + \rho\mathbf{v}\cdot\nabla\mathbf{v}$. The second term $\nabla\cdot\Pi^{\mathrm{ig}}$ is due to stresses arising from velocity fluctuations. It is labeled by "ig", because it is the only stress contribution that is already present for an ideal gas.

Finally, the mutual particle interactions represented by the last term on the right-hand side of Eq. (101) also must have a representation as a divergence of a tensor, as generally assured, above. Upon coarse-graining and partial integration it can indeed somewhat sloppily but suggestively[22] be rewritten as the divergence of the locally coarse-grained virial of the forces $\hat{\mathbf{F}}_i$ acting on particles i in the coarse-graining volume,

$$\langle\sum_i[\nabla_i\cdot\hat{\mathbf{r}}_i]\hat{\mathbf{F}}_i\delta(\mathbf{r}-\hat{\mathbf{r}}_i)\rangle = \nabla\cdot\langle\sum_i\hat{\mathbf{r}}_i\hat{\mathbf{F}}_i\delta(\mathbf{r}-\hat{\mathbf{r}}_i)\rangle \equiv -\nabla\cdot\Pi^{\mathrm{int}} \; . \tag{104}$$

[21] Assume finite range interactions.

[22] An explicit integration (using Newton's 3rd law) requires a bit more work. The mnemotechnic shortcut exploits that boundary terms on adjacent coarse-graining cells cancel, that $\nabla_i\hat{\mathbf{F}}_i\delta(\mathbf{r}-\hat{\mathbf{r}}_i) = -\nabla\hat{\mathbf{F}}(\mathbf{r})\delta(\mathbf{r}-\hat{\mathbf{r}}_i)$, and it replaces $\nabla_i\cdot\hat{\mathbf{r}}_i$ in the $\langle\,\rangle$ by its isotropic average.

In principle, the task of explicitly calculating the interaction part $\Pi^{\rm int}$ of the stress tensor thus leads back to the virial equation of state discussed in the first part of the lecture. It has to be emphasized again that one will thereby only obtain equilibrium results, while the purpose of the hydrodynamic equations is of course mainly to deal with situations where equilibrium is only locally attained, with intensive parameters that slowly change in space and time and forces that deviate from those in equilibrium. To illustrate the point, consider the stress contributed by velocity fluctuations, i.e. the last term in Eq. (103). In a local equilibrium, the averaging should be performed with a Maxwell distribution, which yields the hydrostatic ideal gas pressure

$$\Pi^{\rm ig}(\mathbf{r},t) = P(\mathbf{r},t)\mathbf{1}\ , \qquad P = n(\mathbf{r},t)k_BT(\mathbf{r},t)\ . \qquad \text{(local equilibrium)} \quad (105)$$

Similarly, the stresses resulting from the local-equilibrium virial in Eq. (104) would be diagonal. This means that also the particle interactions only contribute to the scalar hydrostatic pressure, which is, per definition, indeed the only type of stress a fluid at rest can support.

Euler equation

Nevertheless, even on the level of a local equilibrium closure, and assuming $P(\rho)$ to be known from thermostatics, say, one obtains a practically useful hydrodynamic equation. Collecting the above results, and using $\partial_t(\rho\mathbf{v}) + \nabla\cdot(\rho\mathbf{v}\mathbf{v}) = \rho(\partial_t + \mathbf{v}\cdot\nabla)\mathbf{v}$, one obtains the so-called Euler equation. Taken together with the mass continuity equation, it represents a closed hydrodynamic model:

$$\partial_t\rho + \nabla\cdot(\rho\mathbf{v}) = 0\ , \qquad \partial_t(\rho\mathbf{v}) + \nabla\cdot(\rho\mathbf{v}\mathbf{v}) = \rho(\partial_t + \mathbf{v}\cdot\nabla)\mathbf{v} = -\nabla P(\rho)\ . \quad (106)$$

The total stress (or pressure) tensor $\Pi = \Pi^{\rm ig} + \Pi^{\rm int} = P(\rho)\mathbf{1}$ is diagonal. The operator in parentheses is known as the material derivative. The rate of change noticed by an observer in a frame co-moving with a streamline, or, in other words, by the streaming material itself, is different from the rate of change observed in the lab frame, where it is partly due to advection of the material by the flow. In other words, Eq. (106) is nothing but Newton's second law, $m\mathrm{d}_t\mathbf{v} = -\mathbf{F}$ for a fluid element of mass m, after reformulating it in the lab frame for a continuum fluid made up of many such fluid elements. This innocent-looking model describes all inviscid flows, also called "dry water" by Feynman, and is indeed stunningly successful in countless applications involving fast flows of liquids and gases on large scales.

A particularly simple approximate set of solutions that is easily read off from Eq. (106) by linearization, is that corresponding to sound modes. To leading order in powers of the derivatives of $\mathbf{v}$ and ρ, Eq. (106) reduces to the simple system (terms $\mathbf{v}\cdot\nabla\ldots$ are neglected, as not only derivatives of $\mathbf{v}$ but also $\mathbf{v}$ itself

is supposed to be small)

$$\partial_t \rho + \rho \nabla \cdot \mathbf{v} = 0 \tag{107}$$

$$\rho \partial_t \mathbf{v} + \nabla P = 0 \, . \tag{108}$$

Using the (local) equilibrium equation of state $P(\rho)$ for the hydrodynamic pressure, these equations can be recast into the form

$$\partial_t^2 \rho = c^2 \nabla^2 \rho \, , \qquad \partial_t^2 P = c^2 \nabla^2 P \tag{109}$$

obviously admitting sound waves $\rho(x - ct)$, $P(x - ct)$ with the sound velocity

$$c(\rho, T) \equiv (\partial_\rho P)_X^{1/2} = (\rho \kappa_X)^{-1/2} \tag{110}$$

as their solution. Notice the similarity with Eq. (94) — thermodynamics gives information about kinetic coefficients, e.g. that sound propagates with a velocity similar to the thermal velocity in an ideal gas, for which $\rho\kappa_X \simeq \rho\kappa_T = m/k_B T$. One distinguishes the idealized cases of adiabatic and isothermal sound propagation, depending on whether $X = S$ or $X = T$ provides a better approximation. (Sound attenuation could be studied, and seen to be of higher order in the wave vector, by taking into account the viscous terms discussed in the next paragraph.)

Navier–Stokes equation

As announced above, there will in general be some additional (non-equilibrium, possibly off-diagonal) dynamic contributions to the stress tensor Π, which remain to be specified. For the special case of dilute gases, the Boltzmann equation allows such dynamic contributions to be calculated, perturbatively[23]. For instance, it predicts a dynamic shear viscosity $\eta \propto \sqrt{m k_B T}$ that is to a first approximation independent of the density of the gas but increases as a function of the particle mass and temperature (a prediction first derived and then tested by Maxwell himself). But such calculations cannot be extended to dense fluids, which exhibit the same universal hydrodynamic behavior. This observation clearly calls for a more general strategy. Again, one can use symmetry arguments and the long-wavelength (or "hydrodynamic") limit of slowly changing hydrodynamic variables.

In this way, one obtains the next more complex model of fluid flow, appropriate to so-called Newtonian viscous fluids, which have diagonal and off-diagonal nonequilibrium stress contributions that account for viscous damping of the flow. These new stresses are a dynamical friction caused by the fluid flow and should thus, in the simplest case, depend on (powers of) the instantaneous velocity, so that the model remains local in time or "Markovian". This means that state changes depend only on the present state and not on its preceding history. However, to respect the global Galilei invariance, which is the fundamental symmetry

[23] See, e.g., Kerson Huang: Introduction to Statistical Mechanics.

of any non-relativistic dynamics, only gradients of the velocity can matter (the physical friction force must not depend on the inertial frame of an observer). To lowest order[24] in the hydrodynamic variables ρ and $\mathbf{v}$, the dynamic stresses have to be of order $\mathcal{O}(\nabla\mathbf{v})$. Moreover, to avoid that a solid body rotations give rise to internal stresses, this expression has to be made symmetric in the coordinate indices: $\partial_\alpha v_\beta + \partial_\beta v_\alpha$. This symmetric matrix now has diagonal and off-diagonal contributions. Also a renaming of the indices cannot change the physics, hence components related by a coordinate rotation are equivalent and must have the same kinetic coefficient. But the kinetic coefficients for volume preserving shear and uniform compression/dilation, corresponding to the trace-less parts and the trace of the tensor, should generally be allowed to have different values, say η and ζ, respectively, because they correspond to physically distinct types of deformation. Altogether, one thus arrives at the following closure (the negative sign is chosen to account for the fact that the viscous stress counteracts spatial velocity variations),

$$\Pi_{\alpha\beta} = P\delta_{\alpha\beta} - \eta[\partial_\alpha v_\beta + \partial_\beta v_\alpha - (2/3)\delta_{\alpha\beta}\nabla\cdot\mathbf{v}] - \zeta\delta_{\alpha\beta}\nabla\cdot\mathbf{v}\ , \tag{111}$$

corresponding (for spatially constant viscosities) to the *compressible Navier–Stokes* equation

$$\rho(\partial_t + \mathbf{v}\cdot\nabla)\mathbf{v} = -\nabla P + \eta\nabla^2\mathbf{v} + (\zeta + \eta/3)\nabla\nabla\cdot\mathbf{v} \tag{112}$$

Together with the continuity equation for the density and an equation of state for the hydrostatic pressure $P(\rho)$, this provides another complete hydrodynamic model. If supplemented by boundary conditions (the microscopic derivation of which is an equally challenging task as the derivation of the equations of state) and initial conditions, it can in principle be solved to yield predictions for the flow of any simple liquid or gas. It is important to say "in principle", because in practice one is somewhat limited by the lack of mathematical proofs that such solutions exist and are unique etc. The millenium prize of one million dollars for any relevant progress in this direction has not been awarded so far (though unsuccessfully claimed), and the corresponding warnings[25] in Gallavotti's book

[24]The introduction of higher order terms or transport coefficients is a subtle issue, because of what R. Zwanzig called "Dorfman's lemma": all relevant fluxes are non-analytics functions of all relevant variables. So seemingly innocent power- or gradient expansions are not the way to go (J. A. McLennan, Introduction to Non-Equilibrium Statistical Mechanics, 1988).

[25]Fearless engineers write gigantic codes that are supposed to produce solutions to the equations: they do not care the least (when they are conscious of the problem, which unfortunately seems to be seldom the case) that what they study are *not* the Navier Stokes equations, but just the informatic code they produced. *No one* is, to date, capable of writing an algorithm that, in an *a priori* known time and within prefixed approximation, will produce the calculation of any property of the equations' solution following an initial datum and forces which are not "very small" or "very special". Statements to the contrary are not rare, and they may appear even on the news: but they are wrong. (Giovanni Gallavotti, Foundations of Fluid Mechanics)

on fluid mechanics are not yet outdated. In return, if you can find solutions of the Navier–Stokes equations, these tend to be of great generality. Namely, these equations essentially exhaust the world of "ordinary" fluid dynamics (all simple liquids and gases).

For flows that are slow compared to the sound velocity ($\mathbf{v} \ll c$), density fluctuations have relaxed. In absence of externally imposed pressure gradients, the density is then also homogeneous, and one can take $\rho =$ constant, hence $\nabla \cdot \mathbf{v} = 0$. The last term in Eq. (112) then vanishes and one is left with the *incompressible Navier–Stokes* equation

$$\rho(\partial_t + \mathbf{v} \cdot \nabla)\mathbf{v} = -\nabla P + \eta \nabla^2 \mathbf{v} \,. \tag{113}$$

Note that the role of the pressure has now changed compared to the compressible case. It is no longer to be understood as a thermodynamic function of the (now constant) density. Instead it plays the role of a dynamic Lagrange multiplier to account for the auxiliary condition $\nabla \cdot \mathbf{v} = 0$. It makes sense to divide the whole equation by the constant density ρ and introduce the (reduced) dynamic pressure $\tilde{P} \equiv P/\rho$ as a new Lagrange parameter and the *kinematic viscosity*[26] $\nu \equiv \eta/\rho$ as the only material parameter that matters for divergence-free flows of any given Newtonian liquid or gas:

$$(\partial_t + \mathbf{v} \cdot \nabla)\mathbf{v} = -\nabla \tilde{P} + \nu \nabla^2 \mathbf{v} \,, \qquad \nabla \cdot \mathbf{v} = 0 \,. \tag{114}$$

So these equations together represent a complete one-parameter hydrodynamic model, and arguably one of the most powerful and most striking dynamic models in all of physics. As mentioned above, exact mathematical knowledge about its possible solutions is severely limited.

Reynolds number

Another instructive way of writing the Navier–Stokes equation is in dimensionless form, using natural units. Measuring lengths as multiples of a characteristic linear dimension L (e.g. a particle or container size) and velocity in terms of a characteristic or typical flow speed u (and therefore time, accordingly, in units of L/u), one has after dividing Eq. (114) with u^2/L

$$(\partial_t + \mathbf{v} \cdot \nabla)\mathbf{v} = -\nabla \tilde{P} + \mathrm{Re}^{-1} \nabla^2 \mathbf{v} \,, \qquad \text{(reduced units)} \,, \tag{115}$$

with yet another (now dimensionless) Lagrange multiplier $\tilde{P}$ and the Reynolds number

$$\mathrm{Re} \equiv uL/\nu \tag{116}$$

This form makes it clear that solutions of the equation should be invariant under transformations of space and time that leave the Reynolds number invariant. A

[26] $\nu \approx 10^{-6}$ m^2/s for water and about 15 times higher for air, at about room temperature.

small fast submarine and a large slow submarine should create the same flow patterns. At extreme values of the Reynolds number, things should become even simpler: all large and fast moving objects of the same shape should create the same flow pattern, as should all small and slow ones. These statements turn out to be quite useful in engineering and for the movies industry. The Reynolds number can be understood as an index used to characterize the typical ratio of the inertial and dissipative terms $\mathbf{v}\cdot\nabla\mathbf{v}$ and $\nu\nabla^2\mathbf{v}$, in Eq. (114), for any given flow. If Re is large, momentum conservation is only weakly violated by the dissipative term and provides the dominant transport mode. The flow is inertial. If the Reynolds number is small, instead, the dynamics is highly dissipative and momentum diffusion is the dominant transport mode, while there is no inertia. The flow is viscous or over-damped. Typical Reynolds numbers are about $\mathrm{Re}=10^6$ for a human swimmer and $\mathrm{Re}=10^{-3}$ for a microbic swimmer in water. The two extreme cases of inertial flows with $\mathrm{Re}^{-1}=0$ and viscous "creeping" flows with $\mathrm{Re}=0$ lead to the Euler and Stokes equations, respectively,

$$(\partial_t+\mathbf{v}\cdot\nabla)\mathbf{v}=-\nabla\tilde{P}\,,\qquad(\mathrm{Re}=\infty\,,\ \mathrm{Euler}) \tag{117}$$

$$\partial_t\mathbf{v}=-\nabla\tilde{P}+\nu\nabla^2\mathbf{v}\,,\qquad(\mathrm{Re}=0\,,\ \mathrm{Stokes})\,. \tag{118}$$

Both need to be closed by the equation of state, $\nabla\cdot\mathbf{v}=0$ for incompressible (or stationary) flows, which is used to eliminate the pressure. And they need to be supplemented by suitable boundary conditions. Because of the different order of the spatial derivatives, the Euler equation only allows for the specification of one velocity component at a boundary (typically no-influx, $\mathbf{v}_\perp=0$), while the Stokes equation for all velocity components (typically no influx and no-slip, $\mathbf{v}_\perp=0$, $\mathbf{v}_\parallel=0$). Stokes flows have long-ranged velocity correlations, due to the diffusive spread of momentum and because the fluid layers stick to each other. In contrast, Euler flows can in principle be very erratic, since there is nothing to prevent arbitrary changes of the flow speed to occur in adjacent fluid layers and at solid boundaries. Indeed, flows at high Reynolds numbers tend to be turbulent (full of turbulent structures or "eddies") and very irregular.

7 Rheology of simple and complex fluids

Rheology is the lore of flows, including very complex flows not described by the Navier-Stokes equations. Rheometry is the technique used to deduce material properties from flow measurements. Various designs are used in practice. Microrheology employs microspheres to investigate the viscous and viscoelastic properties of small samples and inside living organisms. Couette and cone-plate cells are used to measure macroscopic sample volumes. Obviously, the precise flow pattern excited by a rheometer should be known in order to safely deduce properties of the measured fluids from the recorded stresses and strain rates. So,

one clearly faces a difficult hen-egg problem. To provide a first idea, this subsection, together with the accompanying exercises, introduces some paradigmatic flow types. Euler flows are ubiquitous in Newtonian liquids and gases flowing on macroscopic scales in natural environments and in large devices. In contrast, Stokes flows prevail in microscopic, biophysical applications, and in narrow boundary layers near solid boundaries, in high-Re flows.

Some basic notions and Newtonian flows

If the divergence of the velocity vanishes identically, the most obvious thing of interest left is its curl, the *vorticity* $\boldsymbol{\Omega} \equiv \nabla \times \mathbf{v}$, which measures the local spinning of the fluid flow. The vorticity naturally shows up in the Euler equation, if the vector identity

$$\nabla(\mathbf{v}^2/2) = \mathbf{v} \cdot \nabla \mathbf{v} + \mathbf{v} \times \boldsymbol{\Omega} \tag{119}$$

is used, so that the Euler equation in an external potential $\mathcal{U}$ (normalized by the fluid particles' mass) reads

$$\partial_t \mathbf{v} + \boldsymbol{\Omega} \times \mathbf{v} = -\nabla(\tilde{P} + \mathbf{v}^2/2 + \mathcal{U}) \, . \tag{120}$$

For a stationary Euler flow (with $\partial_t \mathbf{v} = 0$), multiplication by $\mathbf{v}$ shows that

$$\mathbf{v} \cdot \nabla(\tilde{P} + \mathbf{v}^2/2 + \mathcal{U}) = 0 \, , \qquad \text{(Bernoulli)} \tag{121}$$

so that the sum $P + \rho \mathbf{v}^2/2 + \rho \mathcal{U}$ of kinetic and potential energy densities is seen to be conserved along streamlines (i.e., in a frame co-moving with the mass elements). Moreover, Eq. (120) shows that taking the curl of the Euler and Stokes equations (117), (118) yields

$$\partial_t \boldsymbol{\Omega} + \nabla \times (\boldsymbol{\Omega} \times \mathbf{v}) = 0 \quad \Rightarrow \quad (\partial_t + \mathbf{v} \cdot \nabla)\boldsymbol{\Omega} = \boldsymbol{\Omega} \cdot \nabla \mathbf{v} \, , \qquad (\mathrm{Re} = \infty) \tag{122}$$

$$\partial_t \boldsymbol{\Omega} = \nu \nabla^2 \boldsymbol{\Omega} \, , \qquad (\mathrm{Re} = 0) \, . \tag{123}$$

The second line is easier to interprete. It says that any Stokes flow amounts to a diffusive spread of vorticity with the diffusivity ν. So the vorticity and its associated momentum are locally conserved but dispersed by the dynamics so that they leak out to infinity, thereby revealing the physical interpretation of the kinematic viscosity as a diffusion coefficient for the vorticity. This insight provides an easy way to anticipate or even compute the solutios of the Stokes equation—if one manages to formulate the boundary conditions and initial conditions in terms of the vorticity rather than in terms of the velocity, as usual. The consequences of the Euler equation for the vorticity in the first line are a bit less obvious. First, notice that the second form of the Euler equation in Eq. (122) implies that in planar flows, for which the vorticity is perpendicular to the velocity and its gradient, vorticity is again conserved and passively advected along with the flow. Planar incompressible Euler flows thus conserve the vorticity of each volume

element—and along streamlines if steady. This has important consequences for the stability of locally straight vortex lines (or tubes), as they emanate from the wings of airplanes, for example. They govern the complicated turbulent flows at high Reynolds numbers. Ultimately, vorticity will slowly diffuse away, of course, if the neglected viscous term $\nu\nabla^2\mathbf{\Omega}$ is taken into account. But before this happens, the vortex lines can be stretched, coiled and knotted into complex tangles reminiscent of polymer networks. In general non-planar Euler flows, one still has $\mathbf{\Omega}(t) \equiv 0$ if $\mathbf{\Omega}(0) \equiv 0$: initially irrotational flows stay irrotational forever—without automatically being trivial, as it would be the case in the Stokes limit, where vorticity is everything. This hints at a reason why the viscous term is important for the qualitative nature even of high-Reynolds-number flows, that is even if its direct consequences on the flow are minute. It can contaminate the flow with vorticity that it creates e.g. near a no-slip boundary, where a narrow shear layer resides in which the Stokes equation applies.

Incompressible and irrotational flows are called *potential flows*, because irrotational fields may be represented as the gradient of a potential, which, for incompressible flow, solves the Laplace equation,

$$\nabla \times \mathbf{v} = 0 \quad \Rightarrow \quad \mathbf{v} = \nabla\varphi \tag{124}$$

$$\nabla \cdot \mathbf{v} = 0 \quad \Rightarrow \quad \nabla^2\varphi = 0\,. \tag{125}$$

Stationary potential flows have electrostatic analogies, as they obey the equations of electrostatics. They conserve the total energy density $P + \rho\mathbf{v}^2/2 + \rho\mathcal{U}$ globally (not only along streamlines). Since they do not account for viscous friction and other characteristic features of fluids, such as vorticity, turbulence, and sound waves, von Neumann and Feynman introduced the name "dry water" for them. A classical example is the Euler flow around a sphere or cylinder, which differs markedly from the Stokes flow around the same obstacles and gives rise to the d'Alembert paradox (no frictional resistance), but also to the more interesting concept of a renormalized mass (see exercises).

Stokes' "creeping" flow

Most soft-matter and all microbiological applications of hydrodynamics involve shear flows at low Reynolds numbers. Since colloidal particles, proteins and low-dimensional meso-structures like polymers and membranes all diffuse slowly compared to the vorticity of the solvent, it is moreover usually sufficient to deal with the solvent dynamics on the stationary level, i.e., one can idealize the reaction of the fluid as an instantaneous action at any distance. This statement can be anticipated by rewriting Eq. (123) in natural units, namely

$$\partial_t\Omega = \mathrm{Re}^{-1}\nabla^2\Omega\,. \tag{126}$$

To leading order, the term $\mathrm{Re}\partial_t\Omega$ can be dropped. The interpretation is that "frequencies are much larger than wave vectors", so that vorticity relaxes quickly

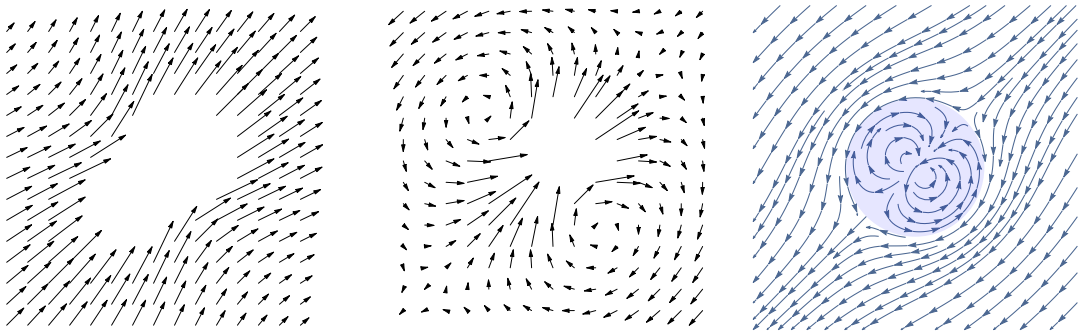

Figure 3: The Stokeslet, Eq. (134), fundamental solution (or Green function) of the Stokes equation, is the flow field excited by a point force at the origin, here pointing into the upper right corner. In the lab frame (left), the flow velocity everywhere has a component in the same direction. In a slowly co-moving frame (middle) one gets a more direct visual impression of the generated vorticity and "backflow". The flow around a uniformly translating sphere differs from the Stokeslet by the source-doublet, Eq. (135), which helps to realize the no-slip/no-influx boundary condition on the solid surface, as a revealed by a plot of the full flow field in a comoving frame (right).

over large distances and can be assumed to be stationary, i.e. a solution of the Laplace equation $\nabla^2\Omega = 0$. Equation (126) then amounts to the (incompressible) stationary Stokes equation for the velocity. In an external force field $\mathbf{f}(\mathbf{r})$:

$$\eta\nabla^2\mathbf{v} - \nabla P = \mathbf{f}(\mathbf{r}) \,, \qquad \nabla\cdot\mathbf{v} = 0 \,. \tag{127}$$

In Fourier space,

$$\eta q^2\mathbf{v}_\mathbf{q} + i\mathbf{q}P_\mathbf{q} = \mathbf{f}_\mathbf{q} \,, \qquad i\mathbf{q}\cdot\mathbf{v}_\mathbf{q} = 0 \,. \tag{128}$$

Multiplying the Stokes equation by $-i\mathbf{q}$ allows the pressure to be eliminated, so that the velocity as a function of the force density is obtained (writing $\hat{\mathbf{q}} \equiv \mathbf{q}/|\mathbf{q}|$)

$$\mathbf{v}_\mathbf{q} = \frac{\mathbf{1} - \hat{\mathbf{q}}\hat{\mathbf{q}}}{\eta q^2}\cdot\mathbf{f}_\mathbf{q} \equiv \mathbf{H}_\mathbf{q}\cdot\mathbf{f}_\mathbf{q} \,. \tag{129}$$

For the Fourier back-transformation of the mobility matrix $\mathbf{H}_\mathbf{q}$ to real space, one makes the ansatz $\mathbf{H}(\mathbf{r}) = a\mathbf{1} + b\hat{\mathbf{r}}\hat{\mathbf{r}}$ (exploiting that $\mathbf{r}$ is the only available vector to construct tensors other than the unit tensor.) To fix the coefficients, it is enough to fix two independent scalars, namely the trace $\mathrm{tr}\mathbf{H}(\mathbf{r}) = 3a + b$ and $\hat{\mathbf{r}}\cdot\mathbf{H}(\mathbf{r})\cdot\hat{\mathbf{r}} = a + b$. After doing the corresponding Fourier integrals,

$$3a + b = \int\frac{\mathrm{d}\mathbf{q}}{(2\pi)^3}\,\frac{2}{\eta q^2}e^{i\mathbf{q}\cdot\mathbf{r}} \,, \qquad a + b = \int\frac{\mathrm{d}\mathbf{q}}{(2\pi)^3}\,\frac{1-(\mathbf{q}\cdot\hat{\mathbf{r}})^2}{\eta q^2}e^{i\mathbf{q}\cdot\mathbf{r}} \tag{130}$$

one finds the fundamental solution or Green function of Eq. (127) to be given by the so-called *Oseen mobility matrix* in real space

$$\mathbf{H}(\mathbf{r}) = \frac{\mathbf{1} + \hat{\mathbf{r}}\hat{\mathbf{r}}}{8\pi\eta r} \,. \tag{131}$$

The velocity field generated by an arbitrary force field $\mathbf{f}(\mathbf{r}')$ is thus obtained via the convolution

$$\mathbf{v}(\mathbf{r}) = \int \mathrm{d}\mathbf{r}' \, \mathbf{H}(\mathbf{r} - \mathbf{r}') \cdot \mathbf{f}(\mathbf{r}') = \int \mathrm{d}\mathbf{r}' \, \frac{\mathbf{1} + \frac{\mathbf{r}-\mathbf{r}'}{|\mathbf{r}-\mathbf{r}'|}\frac{\mathbf{r}-\mathbf{r}'}{|\mathbf{r}-\mathbf{r}'|}}{8\pi\eta|\mathbf{r} - \mathbf{r}'|} \cdot \mathbf{f}(\mathbf{r}') \,. \tag{132}$$

In particular, for the point force $\mathbf{f} = \mathbf{F}\delta(\mathbf{r})$, the velocity field $\mathbf{v}(\mathbf{r})$ is given by the fundamental solution $\mathbf{H}(\mathbf{r}) \cdot \mathbf{F}$ itself, which is also called a "Stokeslet". It represents the far field solution $\mathbf{v}(\mathbf{r} \to \infty)$ for the flow around any finite object in uniform motion, or, equivalently, the flow disturbance caused by an infinitely small and fast particle. An illustration is provided by Fig. 3. In the lab frame (left), the enhanced flow speed due to the projector accounting for the incompressibility condition ("in front and behind the origin") is apparent. The view from a slowly co-moving frame (right) reveals the vorticity created and dispersed by the flow.

Averaging the Stokeslet over a spherical shell of radius $r = R$ around the force center gives[27]

$$\langle \mathbf{v}(R) \rangle = \mathbf{F}/(6\pi\eta R) \tag{133}$$

So fluid shells of increasing radius (and mass) move with decreasing average speeds, as expected from momentum conservation. It is suggestive that the formula should also hold for a solid sphere of radius R pushed by the force $\mathbf{F}$. This is indeed true, but not entirely self-evident, since the flow field on the surface of a solid sphere cannot obey Eq. (131). For a solid sphere with no-slip and no-influx boundary conditions, the fluid velocity at the surface must exactly (and not only on average) be equal to the sphere's velocity. To account for the difference between the Stokeslet

$$\frac{3R}{4r}(\mathbf{1} + \hat{\mathbf{r}}\hat{\mathbf{r}}) \cdot \langle \mathbf{v}(R) \rangle \tag{134}$$

and the actual flow around the sphere one thus needs an additive correction term that has to obey a number of conditions. First and foremost, since perfect force/momentum balance is already guaranteed by the fundamental solution, the correction cannot give rise to any net momentum transfer through a concentric spherical shell around the sphere: its trace and spherical average must therefore vanish. This corroborates that Eq. (133) holds for the sphere. It thereby incidentally establishes Stokes' formula $\zeta = 6\pi\eta R$ for the friction coefficient without requiring the complete flow field, which is however easily found. Namely, in order

[27] Using spherical coordinates, check that $\langle \hat{\mathbf{r}}\hat{\mathbf{r}} \rangle = (1/3)\mathbf{1}$, as expected for a projector.

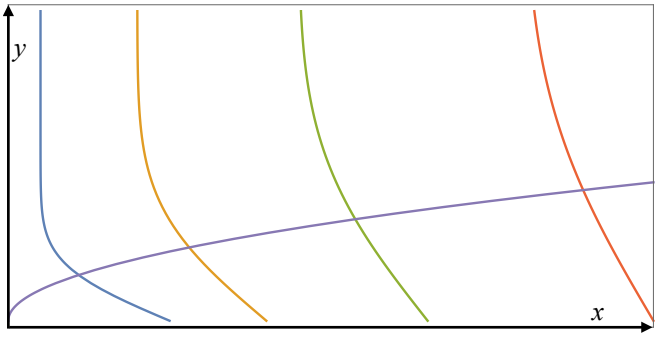

Figure 4: Emergence of a Stokes boundary layer flow with a linear shear profile (in $y-$direction) above a plane solid boundary that started moving with a constant velocity $\mathbf{v} = (v_0, 0, 0)^T$ in $x-$direction, at time $t = 0$. The flow is shown at successive times, to reveal the developing boundary layer of width $\Delta = \sqrt{\nu t}$.

to undo the relative tangential and normal flux of the Stokeslet on the surface of the sphere, the trace-less correction term must iron out the velocity variations caused by the projector $3\hat{\mathbf{r}}\hat{\mathbf{r}} \cdot \langle \mathbf{v} \rangle/4$ in Eq. (134), at $r = R$; i.e. it must have the form $(R/r)^m(\mathbf{1} - 3\hat{\mathbf{r}}\hat{\mathbf{r}}) \cdot \langle \mathbf{v} \rangle/4$. Requiring the divergence $(R/r)^m(2m-6)\hat{\mathbf{r}} \cdot \langle \mathbf{v} \rangle/4r$ to vanish to satisfy the incompressibility condition then yields the so-called source doublet,

$$\frac{R^3}{4r^3}(\mathbf{1} - 3\hat{\mathbf{r}}\hat{\mathbf{r}}) \cdot \langle \mathbf{v}(R) \rangle \; . \tag{135}$$

Summarizing, the flow velocity field $\mathbf{v}(\mathbf{r})$ around a sphere driven by a constant force $\mathbf{F} = 6\pi\eta R \langle \mathbf{v}(R) \rangle$ is given by the sum of Eqs. (134), (135). The result is illustrated in Fig. 3 (right) in a reference frame co-moving with the uniformly translating sphere, which clearly exposes the no-slip/no-influx boundary condition. Other superpositions of the two terms pertain if the no-slip condition is relaxed or the particle surface is not spherical, e.g., for soft or viscous solutes.

Equations (118), (123), (126) can be used to compute time-dependent creeping flows. As an example for a transient towards the stationary flow, consider the planar shear flow generated in the infinite half-space above a plane solid boundary in the $x - y-$coordinate plane, which starts to move with velocity v_0 in the $x-$direction at time t. This will excite a flow velocity field $\mathbf{v} = (v_x, 0, 0)^T$, directed along the $x-$direction and varying along the perpendicular $y-$direction, with $v_x(y, t)$ obeying $v_x(y, 0) = 0$ and $v_x(y = 0, t > 0) = v_0$. Because of mass conservation, $\partial_x v_x = 0$, the fluid velocity stays independent of the $x-$position for all times (and no momentum is scattered into the $y-$direction). So does the vorticity $\boldsymbol{\Omega} = (0, 0, \Omega_z)$ with $\Omega_z(y, t) = -\partial_y v_x(y, t)$ equal to the negative shear gradient. Since the velocity field at the onset of motion is given by a step function $v_x(y, 0+) = v_0\theta(-y)$, the initial condition for the vorticity field is $\Omega_z(y, 0+) = -\partial_y v_x = \delta(y)v_0$. The equation of motion for the vorticity, Eq. (126),

thus boils down to the scalar diffusion equation $\partial_t \Omega_z = \nu \partial_y^2 \Omega_z$ with the initial condition $\Omega_z(y,0) = v_0 \delta(y)$. Its solution is

$$\Omega_z(y,t) = \frac{v_0}{\sqrt{\pi}\Delta} e^{-y^2/(2\Delta^2)} , \quad \text{with} \quad \Delta = \sqrt{2\nu t} . \tag{136}$$

The vorticity thus diffuses out from the boundary into a boundary layer of growing thickness $\Delta \propto t^{1/2}$, while its value $\Omega_z(y \ll \Delta, t) \propto t^{-1/2}$ inside the boundary layer slowly decays in time. The velocity field is obtained by spatial integration over y (cf. Fig. 4),

$$\frac{v(y,t)}{v_0} = 1 - \operatorname{erf}\left[y/(\sqrt{2}\Delta)\right] \sim \begin{cases} 1 - (2/\pi)^{1/2} y/\Delta & (y \ll \Delta) \\ (2/\pi)^{1/2} e^{-y^2/(2\Delta^2)} \Delta/y & (y \gg \Delta) \end{cases} \tag{137}$$

Within the boundary layer ($y \ll \Delta$), the linear profile characteristic of steady shear flow in the Stokes regime[28] develops. Because of the spreading of the layer, this profile flattens out over time and the shear gradient decays, due to the dispersal of the vorticity. The decay could be stopped by inserting a parallel boundary at a certain height (i.e. putting a lid on the box). Thereby one could realize a strictly linear flow field, called plane Couette or simple shear flow, at late times. A simple way to see how this comes about, is to realize that the lid would affect the flow essentially by setting a cutoff length L for $\Delta(t)$, so that near the lower boundary

$$v(y, t \to \infty) \to v_0 (1 - y/L) . \tag{138}$$

At late times, this should extend across the whole box, as there is nothing special about the upper or lower boundary any more (up-down symmetry), as also directly inferred from the stress tensor $\sigma_{xy} = \eta \partial_y v_x = \text{const}$. Also note that one could alternatively stop the boundary layer from growing by imposing an oscillatory shear motion at frequency ω. Then the fixed boundary layer width $\Delta = \sqrt{2\nu/\omega}$ would play the role of a "skin depth" across which the flow decays, so that no vorticity or momentum would be transmitted to infinity.

The example showed that the slow diffusive transport of vorticity affords creeping flows with long-lived memory. This memory shows up in the form of a memory kernel in the equations of motion of Brownian particles. The paradigmatic example is provided by the (non-stationary) equations of motion for a sphere of mass m moving at a time-dependent velocity $\mathbf{u}(t)$ in a Newtonian liquid, the so-called Boussinesq solution of the Stokes equation, which reads

$$F(t) = \left(m + 2\pi\rho R^3/3\right) \dot{\mathbf{u}}(t) + 6\pi\eta R\, \mathbf{u}(t) + 6\sqrt{\pi\eta\rho} R^2 \int_{-\infty}^{t} \mathrm{d}t' \, \frac{\dot{\mathbf{u}}(t')}{\sqrt{t - t'}} . \tag{139}$$

[28] In contrast, highly turbulent shear flow develops a logarithmic velocity profile.

The instantaneous force $\mathbf{F}(t)$ cannot be specified by the instantaneous velocity $\mathbf{u}(t)$ alone, but depends on its whole history $\mathbf{u}(t \leq t')$. The flow has long-lived memory. Also notice that the mass of the sphere is renormalized by the accelerated fluid mass $2\pi\rho R^3/3$.

Viscoelastic fluids

As pointed out in the previous paragraph, memory appears in flows at low-Reynolds numbers as a consequence of the slow vorticity diffusion. In practice, the material behavior itself is another important source of memory, i.e., the viscosity need not be a constant coefficient but may itself be time-dependent. One then speaks of non-Newtonian (non-Markovian) or complex fluids. Two important idealized types of non-Newtonian fluids shall be discussed, in the following: linear viscoelastic fluids and nonlinear fluids. Real fluids usually exhibit both types of behavior under appropriate conditions.

Specializing to incompressible fluids, the discussion can be simplified by focussing on one off-diagonal component σ of the stress tensor (the σ_{xy} component, say) and the corresponding component[29] $\dot\gamma = \partial_x v_y + \partial_y v_x$ (called the shear rate) of the velocity-gradient tensor. Viscoelastic fluids are non-Markovian fluids, in which the stress at time t not only depends on the velocity gradients at the same time in the form $\sigma(\dot\gamma)$, but also on those at earlier times, i.e. $\sigma[\dot\gamma(t)]$. In other words, viscoelastic fluids are fluids with memory. Over a certain frequency range, they may appear to be solids and only reveal their fluidity at late times. Such ambivalent behavior can already be apparent in a linear-response experiment, where the strength of the perturbation is infinitely weak. In contrast, whether a fluid has non-trivial nonlinear behavior is only revealed at large deformations. Nonlinear fluids are conventionally characterized by their "flow curves", namely their rate-dependent viscosity $\eta(\dot\gamma)$ that typically decreases with increasing $\dot\gamma$ upon stationary shearing at a fixed rate $\dot\gamma$. This behavior is called shear-thinning and is now microscopically understood as an indirect signature of the tendency of the fluid to arrest at low temperatures[30]. The opposite trend of shear-thickening is also observed, particularly at high shear rates. It is usually attributed to flow-induced "jamming" of some meso-structures of the material. Figure 5 provides a somewhat selective overview over some common linear and nonlinear flow properties.

In the linear-response regime, i.e. for perturbations applied at a finite rate $\dot\gamma$ but with vanishing amplitude γ, the most general form of a viscoelastic constitutive relation is of the form

$$\sigma(t) = \int_{-\infty}^{\infty} \mathrm{d}t'\, G(t-t')\theta(t-t')\dot\gamma(t') \;, \tag{140}$$

[29] One of the two contributions to $\dot\gamma$ vanishes if the shear direction is aligned with an axis.

[30] M. Fuchs, M. E. Cates, Phys. Rev. Lett. 89 (2002) 248304

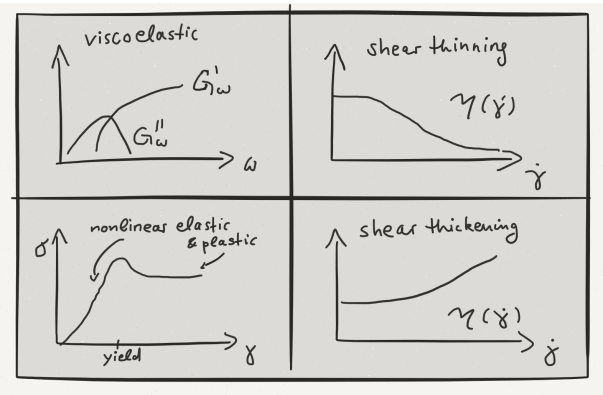

Figure 5: Schematic examples for linear and nonlinear rheometry. In oscillatory linear rheology (upper left panel), one varies the frequency of a periodic perturbation but takes the amplitude to zero. The obtained frequency-dependent moduli (stress- over strain amplitude) are properties of the unperturbed medium. Nonlinear rheology imposes perturbations with large or even infinite amplitude (e.g. stationary shear at a constant rate) and can reveal shear-thinning or shear-thickening behavior, as well as (transient) nonlinear elasticity and (irreversible) plastic flow. Note that stress-controlled, strain-, and strain-rate-controlled protocols generally all give different moduli, in nonlinear rheology.

with a causal memory kernel (proportional to the step function) that completely defines the linear viscoelastic behavior. The customary way of writing this relation in Fourier space is

$$\sigma_\omega \equiv G^*(\omega)\gamma_\omega \equiv (G'_\omega + iG''_\omega)\gamma_\omega \tag{141}$$

with

$$G^*(\omega) = i\omega \int_0^\infty \mathrm{d}t\, G(t) e^{-i\omega t} \tag{142}$$

A direct measurement of this relation employs oscillatory shear at varying frequency ω but vanishing amplitude $\gamma_\omega \to 0$. The real (in phase) and imaginary (out of phase) parts of the complex modulus $G^*(\omega)$, namely G'_ω and G''_ω, are called storage and loss modulus, respectively. The phase shift $\phi_\omega \equiv \arctan(G''_\omega/G'_\omega)$ between stress and strain can be interpreted as an indicator of the elastic ($\phi_\omega \to 0$) versus viscous ($\phi_\omega \to \pi/2$) character of the response. Note that the functional forms of the frequency-dependent moduli G'_ω and G''_ω are not independent, since they are both derived from the same real function $G(t)$. This interdependence holds for any frequency-dependent linear-response functions. It is formalized by the so-called Kramers–Kronig relations that exploit the causality of the kernel to

mutually express both functions in the form (exercises):

$$G''_\omega = -\frac{2\omega}{\pi}\,\mathcal{P}\!\int\!\mathrm{d}\omega'\,\frac{G'_\omega}{\omega'^2-\omega^2}\;, \qquad G'_\omega = \frac{2}{\pi}\,\mathcal{P}\!\int\!\mathrm{d}\omega'\,\frac{\omega' G''_\omega}{\omega'^2-\omega^2}\;. \tag{143}$$

As a special case, for power-law spectra $G'_\omega \propto G''_\omega \propto \omega^\alpha$, one quickly shows from the Kramers–Kronig relations that the phase angle is $\phi_\omega = \alpha\pi/2$, so that $G''_\omega \gtrless G'_\omega$ for $\alpha \gtrless 1/2$.

A paradigmatic example of a phenomenological viscoelastic fluid model is the Maxwell model. It interpolates between solid-like and fluid-like behavior. It can neatly be defined via its exponential memory kernel,

$$G(t) = G_0 e^{-t/\tau}\;. \tag{144}$$

Accordingly, $G(t) \approx G_0$ at short times $t \ll \tau$, and the Maxwell fluid behaves elastic, $\sigma \approx G_0\gamma$. For slow straining (on long time scales $t \gg \tau$), the memory has decayed, and $\sigma \approx \eta\dot\gamma$ with

$$\eta \equiv \int_0^\infty \mathrm{d}t\, G(t) = G_0\tau\;. \tag{145}$$

Another way of looking at the Maxwell model is in terms of its constitutive differential equation

$$\dot\gamma = \dot\sigma/G_0 + \sigma/\eta \tag{146}$$

or the corresponding susceptibility $\chi^*(\omega) = 1/G^*(\omega) = G_0^{-1} + (i\omega\eta)^{-1}$ that gives the Fourier amplitude of the strain upon multiplication with the Fourier amplitude of the stress. It implies that the model can be interpreted as a spring (an ideal linear elastic solid) and a dashpot (an ideal Newtonian fluid) in series. The complementary behavior of a soft solid that is dominated by viscous friction at high frequency, is in the simplest case represented by a spring and dashpot in parallel (an over-damped phonon), and commonly known as the Kelvin–Voigt model. The two models are the rheological analogues of the well-known electrical RC-circuits used to model complex electrical impedances.

Yet another way of looking at the Maxwell model is in terms of its complex spectrum $G^*(\omega)$,

$$G'_\omega = G_0\frac{\omega^2\tau^2}{1+\omega^2\tau^2}\;, \qquad G''_\omega = G_0\frac{\omega\tau}{1+\omega^2\tau^2}\;. \tag{147}$$

Viscous (solid) behavior emerges in the low- (high-)frequency limit

$$\lim_{\omega\to0} G^*(\omega) = \lim_{\omega\to0} iG''_\omega = i\omega\eta\;, \qquad \lim_{\omega\to\infty} G^*(\omega) = \lim_{\omega\to\infty} G'_\omega = G_0\;. \tag{148}$$

Also note that $G^*(\omega)/i\omega$ can be interpreted as a generalized, frequency-dependent viscosity $\eta^*(\omega)$. Certain real complex fluids that are indeed well described by the

Maxwell model, most notably so-called wormlike micelles, which are largely responsible for the viscoelastic properties of hair shampoos. Wormlike micelles are polymer-like micellar tubes. At sufficient (but actually very low) concentration, they form an entangled network that behaves rubber-like on short times scales. Beyond a certain characteristic time scale, the micelles can break and reform, so that the topological entanglement can evolve in time, and beyond this time scale they are found to behave like a Newtonian viscous liquid. In fact, all transient polymeric networks behave in a qualitatively similar way.

The single exponential decay of the Maxwell memory kernel gives rise to a so-called "Debye" or "Lorentz" peak in the spectrum G''_ω. It is best recognized (as a symmetric peak) in the log-log representation of G''_ω. Many real systems exhibit much broader spectra with a broad spectrum of relaxation modes, making the log-log representation even more compulsory. Their spectra are indicative of superpositions of Maxwell- or Kelvin–Voigt-elements (using more and more of those, any linear viscoelastic response can ultimately be composed). A particularly simple model idealizing such broad spectra is the so-called power-law fluid,

$$G^*(\omega) \propto (i\omega)^\alpha \ . \tag{149}$$

Apart from an overall scale factor (that is often of minor interest), this model is completely characterized by the single scalar parameter α. Paradoxically, living cells (arguably the most complex material on Earth — if one wants to speak of a material, at all, in this context), have been shown to exhibit power-law rheology, at least after large numbers of the individual noisy spectra taken for identically prepared single cells are superimposed[31]. The exponent α is found to be a small non-universal number.

8 Flexible polymers and renormalization

The rheological complexity of complex fluids is usually caused by some suspended mesostructures. The mesostructures might be globular, as in the case of colloidal spheres or emulsion droplets, which are reminiscent of up-scaled atoms but already exhibit a highly complex rheology, including an incompletely understood glass transition that has been studied for several decades. It might also be membrane-like, as in the case of phase boundaries, micro-emulsions, or biological cells. In many cases, e.g., for the mentioned wormlike micelles or for most rubbers and plastics, or most living tissues, the mesostructure is predominantly polymer-like. All low-dimensional mesostructures have in common that they are governed by large thermal fluctuations.

This section considers single polymers and polymeric fluids as a *pars pro toto* for all such mesostructures. Flexible polymers are widely employed as building

[31] B. Fabry *et al.* Phys. Rev. Lett. 87 (2001) 148102.

blocks of synthetic materials, whereas semiflexible and stiff fibrous elements prevail in living matter. In a material made of such polymers embedded in a solvent, some of the polymers will usually be bent and stretched, and move relative to the solvent background, when the material is deformed, and this will give rise to a viscoelastic response of the material. While there are many materials that exhibit a polymeric mesostructure, it is also interesting to note that even many non-polymeric materials owe certain material properties to polymer-like line tangles, namely, ordinary crystals (defect lines), high-T_c superconductors (flux lines), turbulent (magneto-)hydrodynamic flows (vortex lines), etc.

A toy model

A simple toy model for flexible polymers is the freely-jointed chain, a chain of freely hinged stiff rods. The little rods may be thought to represent the covalent bonds between adjacent atoms or small molecules that form the unit cell or monomer of the polymer. Great universality emerges from the large number of monomers (which may, in practice, range up to a few millions). This makes the concepts of statistical mechanics applicable on the level of a single macromolecule. Indeed, the statistical mechanics of a chain of hinged freely rotating rods (vectors $\mathbf{u}_n$) of length ℓ oriented along the unit vectors $\hat{\mathbf{u}}_n$ is equivalent to that of a classical spin chain. Its partition sum and the ensuing constitutive equation for the magnetization as a function of an external magnetic field are well know. The results can easily be translated to the polymer, by identifying the external magnetic field with a force $\mathbf{F}$ along the direction $\hat{\mathbf{F}}$ that pulls the ends of the polymer apart and thereby stretches its end-to-end vector

$$\mathbf{R} \equiv \mathbf{r}_N - \mathbf{r}_0 = \sum_{n=1}^{N} \mathbf{u}_n = \ell \sum_{n=1}^{N} \hat{\mathbf{u}}_n \tag{150}$$

(the equivalent of the magnetic moment), such that

$$\langle \mathbf{R} \rangle_{\mathbf{F}} = L\mathcal{L}(|\mathbf{F}|\ell/k_BT)\hat{\mathbf{F}} \qquad \text{with} \qquad \mathcal{L}(x) = \coth x - x^{-1} \,, \tag{151}$$

the Langevin function. For weak forces, this reduces to the equivalent of the Curie law,

$$\langle \mathbf{R} \rangle_{\mathbf{F}} = \frac{\ell^2 N}{3k_BT}\mathbf{F} = \frac{\langle \mathbf{R}^2 \rangle}{3k_BT}\mathbf{F} \,, \qquad \text{for } |\mathbf{F}| \ll k_BT/\ell \,. \tag{152}$$

In the linear approximation, the polymer is an entropic spring, as apparent from the proportionality of the spring stiffness to the thermal energy k_BT. (Its elastic response comes entirely from heat, which is the reason why a rubber band heats/cools upon stretch/release.) Here $\langle \dots \rangle$ denotes the unperturbed equilibrium average, which yields

$$\mathcal{R}^2 \equiv \langle \mathbf{R}^2 \rangle = \ell^2 \sum_{nm} \langle \hat{\mathbf{u}}_n \hat{\mathbf{u}}_m \rangle = \ell^2 \sum_{nm} \delta_{nm} = \ell^2 N = \ell L \,, \tag{153}$$

because the free polymer is a random walk of N steps. The short-hand notation for the equilibrium coil size $\mathcal{R} = \langle \mathbf{R}^2 \rangle^{1/2}$, introduced here, is practical for the following. Note that $\mathcal{R}$ is much smaller than the stretched backbone length $L = N\ell$ of the polymer, their ratio being of order $N^{-1/2}$. (This result for the typical relative fluctuations of a macroscopic variable should be familiar from statistical mechanics.) Also note that the information about the microscopic structure of the model is lost in the linear-response relation, which only depends on a mesoscopic phenomenological quantity, namely the average coil size $\mathcal{R}$. Only if the total mass of a polymer is known from an independent measurement, the equivalent segment length ℓ, called the Kuhn length, can be inferred from a linear-response measurement.

For many applications, the freely-jointed chain model is too simplistic. It fails to account for the self-interactions of a real polymer chain and is therefore often called a "phantom chain model". Depending on the solvent conditions, there are exactly three cases. Attractive interactions between the monomers collapse the polymer, $\mathcal{R} = \ell N^{1/3}$. The collapse can essentially be understood as the analogue of a spinodal decomposition of unconnected monomers, i.e., it is a phase transition, sometimes called the Flory or $\theta-$transition. In practice, the physics of crystallization often takes over after an initial collapse phase, so that the polymer conformation then becomes highly sensitive to the details of the interactions, as in a folded protein. In contrast, repulsive interactions swell the polymer, so that $\mathcal{R} = \ell N^{\nu}$ with $\nu \approx 0.588$, and its conformation becomes a highly universal fractal known as a self-avoiding random walk. At the so-called $\theta-$point that separates the two cases, the steric self-avoidance is on average balanced by some self-attractions or "screened" in the sense that the second virial coefficient of the monomers vanishes. In this case, the conformation is to a first approximation ideal, so that Eq. (153), or $\nu = 1/2$ holds.

Self-similarity and renormalization

In some respect, the freely-jointed chain model can also be criticized for being too detailed. The nonlinearity of the force-extension relation in Eq. (151) and the microscopic structure only matters if the equilibrium coil is very strongly deformed[32]. But the rod-like segment structure of the model, revealed by such indiscrete treatments, is neither realistic nor technically very simple. So, one could wonder why to represent it in the model, in the first place. Indeed, the standard model of a flexible polymer, which is also a practical starting point for dealing with the mentioned self-interactions and any other perturbative calculations, is the so-called *Gaussian chain* that only has a single parameter and does away with the whole microstructure. The basic idea can be phrased as a

[32]Note from Eq. (151) that the range of validity of the linear response for the phantom chain exceeds by far (by a factor $\simeq \sqrt{N}$) the expected range of validity, namely $|\mathbf{F}| \lesssim k_B T/\mathcal{R}$.

simple renormalization procedure that explains, in a nutshell, how phenomenological models are constructed and where their great universality, exactness and robustness come from, in general. Starting from a model with microstructure and exploiting its scale-invariant[33] linear response, one constructs a model without microstructure by replacing the microstructural elements (e.g. the rigid rod segments) by rescaled images of the whole polymer. Repeating this procedure *ad infinitum*, one ends up with a universal phenomenological polymer model devoid of artificial model details. In practice, one starts with integrating the linear force-extension relation, Eq. (152), to obtain the corresponding harmonic free energy for the end-to-end vector $\mathbf{R}$ of the polymer,

$$A(\mathbf{R}) = \frac{3k_BT}{2}\frac{\mathbf{R}^2}{\ell^2 N} \; . \tag{154}$$

This free energy, which clearly is entirely of entropic origin, is now adapted for the individual segments by setting $\mathbf{R} \equiv \mathbf{r}_N - \mathbf{r}_1 \to \mathbf{r}_{n+1} - \mathbf{r}_n = \mathbf{u}_n$ and $N \to 1$, so that one arrives at the following (discrete) Gaussian chain Hamiltonian for the complete polymer

$$H(\{\mathbf{r}_n\}) = \frac{3k_BT}{2\ell^2}\sum_n (\mathbf{r}_{n+1} - \mathbf{r}_n)^2 \; . \tag{155}$$

This insertion leaves the phenomenology in terms of $\langle \mathbf{R}^2 \rangle = \ell^2 N$ for the total chain, and the corresponding free energy, Eq. (154), invariant, as you can explicitly check in the exercises by integrating out all $\mathbf{r}_n$ except the end points from the Boltzmann factor. For such a chain of entropic springs, the continuum limit is therefore easily taken by simultaneously sending $N \to \infty$ and $\ell \to 0$ at constant $\langle \mathbf{R}^2 \rangle = \ell^2 N$. The resulting Gaussian chain Hamiltonian then reads

$$\beta H[\mathbf{r}_n] = \frac{3}{2\ell^2}\int_0^N \mathrm{d}n\, (\partial_n \mathbf{r}_n)^2 = \frac{3}{2\ell^2 N}\int_0^1 \mathrm{d}\zeta\, (\partial_\zeta \mathbf{r}_\zeta)^2 = \frac{3}{2\mathcal{R}^2}\int_0^1 \mathrm{d}\zeta\, (\partial_\zeta \mathbf{r}_\zeta)^2 \; . \tag{156}$$

The first form, with formally divergent parameters, is found in many textbooks. The second form makes the parametrization invariance hidden in the finite product $\ell^2 N$ of the infinite microscopic (or "bare") parameters more explicit, which the first form conceals. And only the third form fully reveals the fact that the model features only a single phenomenological parameter $\mathcal{R}$ corresponding to the average overall coil size, and no microscopic information, whatsoever. Also note that $\mathbf{r}_n$ and $\mathbf{r}_\zeta$ are now understood to be continuous functions of their arguments, so that the partition sum over the Boltzmann factor $e^{-\beta H}$ turns from a multidimensional Gaussian integral into a functional integral or path integral[34]

$$\int \mathcal{D}[\mathbf{r}_\zeta]\, \exp\Big[-\frac{3}{2\mathcal{R}^2}\int \mathrm{d}\zeta\, (\partial_\zeta \mathbf{r}_\zeta)^2\Big] \; . \tag{157}$$

[33] This is the reason why the renormalization procedure is trivial, here, as are, in return, the emerging macroscopic properties.

[34] In fact, this is the mother of all path integrals, the Wiener integral.

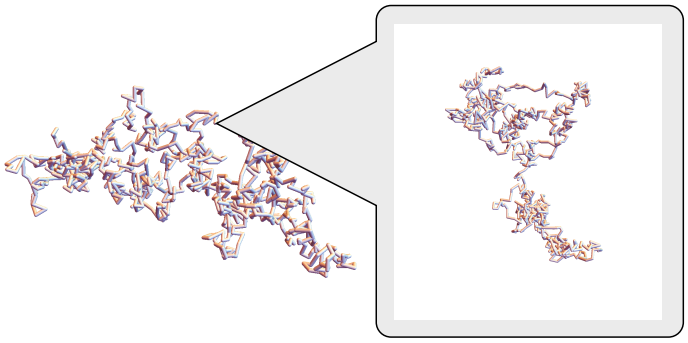

Figure 6: Self-similarity of a long polymer chain.

If you ever need to calculate it, just turn the Hamiltonian back into its above discretized form (or alternatively into a Fourier series), do the Gaussian integrals, and then take the continuum limit of the result. The solution of the Wiener integral for fixed ends $\mathbf{r}_0 = 0$, $\mathbf{r}_N = \mathbf{R}$, is the (unnormalized) distribution

$$P(\mathbf{R}, N) \propto \exp[-3\mathbf{R}^2/(2\mathcal{R}^2)] \,, \qquad \mathcal{R} = \ell\sqrt{N} \tag{158}$$

of the end-to-end-vector $\mathbf{R}$, derived in the exercises. It is propotional to the propagator or conditional probability for a Brownian particle with diffusivity $D = \ell^2/6$ starting at the origin at "time" $n = 0$ to arrive at $\mathbf{R}$ at $n = N$. In other words, the Wiener integral is the solution, at time $n = N$, of the diffusion equation

$$\partial_N P(\mathbf{R}, N) = (\ell^2/6)\nabla^2 P(\mathbf{R}, N) \tag{159}$$

with the initial condition $\delta(\mathbf{R})$ at time $n = 0$.

The parametrization invariance of the Gaussian chain under the simultaneous scale transformation $\ell \to \lambda\ell$ and $N \to \lambda^{-1/\nu}N$, with $\nu = 1/2$, is plainly obvious from the above expressions and analyzed further in the exercises. Physically, it a consequence of the self-similar, fractal structure of the polymer coil with fractal dimension $1/\nu = 2$, illustrated in Fig. 6. It is useful to express this "dilation symmetry" in a slightly more cumbersome way, since this provides a formal basis for practical renormalization group calculations for more difficult models. In fact, the above procedure of taking the continuum limit amounts to a trivial renormalization. As already pointed out above, it owes its simplicity to the plain scale invariance of the Hamiltonian. The whole procedure becomes much more involved for a more complex Hamiltonian, as illustrated by the Edwards Hamiltonian, below, where the formal overhead eventually pays off.

The conventional notation for the parameter renormalization is

$$\ell \to \tilde{\ell} = \lambda\ell \,, \quad N \to \tilde{N} = Z^{-1}(\lambda)N \quad \text{with } Z(\lambda) = \lambda^{1/\nu} \tag{160}$$

the so-called Z factor or Z function that takes a power-law form for a self-similar, fractal structure. It leaves the macroscopic phenomenological observables ("the phenomenology") invariant:

$$\mathcal{R}(\ell, N) = \mathcal{R}(\tilde{\ell}, \tilde{N}) \equiv \mathcal{R}(\lambda\ell, Z^{-1}N) \quad \Rightarrow \quad \partial_\lambda \mathcal{R}|_{\lambda=1} = 0\,, \tag{161}$$

hence

$$\big[\ell\partial_\ell - \partial_\lambda \ln Z|_{\lambda=1}\, N\partial_N\big]\mathcal{R} = \big[\ell\partial_\ell - (N/\nu)\partial_N\big]\mathcal{R} = 0\,. \tag{162}$$

This is the renormalization group equation in the special form it takes at a critical point[35], namely that of a fixed-point equation for the rescaling transformation. It provides a differential formulation of the scale invariance of the phenomenology, namely that the observable $\mathcal{R}$ depends on the parameters ℓ and N only in a special invariant combination. To solve the equation and thereby recover the invariant scaling, one uses the method of characteristics. That is, one interprets ℓ and N as functions of a time-like parameter t, on which $\mathcal{R}(t)$ implicitly depends. Equation (162) is then understood as a conservation equation for $\mathcal{R}(t)$ along a streamline of the renormalization flow, akin to Bernoulli's law, Eq. (121), with the velocity (or rate-of-change) vector $(\ell, -N/\nu)$,

$$(\ell, -N/\nu) \cdot \tbinom{\partial_\ell}{\partial_N}\mathcal{R} = \mathrm{d}\mathcal{R}/\mathrm{d}t = (\dot{\ell}, \dot{N}) \cdot \tbinom{\partial_\ell}{\partial_N}\mathcal{R} = 0. \tag{163}$$

From a comparison of these equations, one reads off

$$\dot{\ell} = \ell\,, \quad \dot{N} = -N/\nu\,, \tag{164}$$

or

$$\nu\frac{\dot{N}}{N} + \frac{\dot{\ell}}{\ell} = 0 \quad \Rightarrow \quad \ln N^\nu \ell = \text{ const.} \tag{165}$$

So the parametrization invariant $\mathcal{R}$ must be a function of ℓ and N in the particular combination $N^\nu\ell$, and since, as a length, it must moreover be linear in ℓ, it follows that (up to a numerical factor)

$$\mathcal{R}(\ell, N) = \mathcal{R}(N^\nu\ell) \simeq \ell N^\nu\,. \tag{166}$$

Edwards' Hamiltonian and Flory argument

As already announced above, the whole procedure appears less inflated if the Hamiltonian contains monomer-monomer interactions, i.e. an additional term

$$\sum_{n<m} \nu(\mathbf{r}_n - \mathbf{r}_m)\,. \tag{167}$$

[35]Indeed, a 1:1 relation between a self-avoiding polymer and a ferromagnet (with a strange 0-dimensional magnetic vector) can be established. It relates the exponent ν to the critical exponents of magnets if N^{-1} is identified with $T - T_c$ and the end-to-end distance with the correlation length. P.-G. de Gennes, Scaling Concepts in Polymer Physics, Cornell 1979.

Since the monomers are supposed to fluctuate quickly compared to the relevant (long-wavelength) polymer degrees of freedom, it is, in the spirit of a DFT, appropriate to coarse-grain the bare monomeric interaction to a "dressed" one, i.e., to the direct correlation function of the monomer solution. Moreover, since the polymer in its swollen state corresponds to a very dilute monomer solution, the situation is similar to that in Onsager's DFT for the nematic transition, and the direct correlation function is represented by the (negative) Mayer function. Finally, to account for the overall effect of the self-interactions, it is sufficient to replace them by a contact interaction, with the effective, dressed interaction strength given by k_BT times the integral over the negative Mayer function, i.e., twice the negative second virial coefficient B. Altogether, the interaction term can thus be written in the form

$$k_BT \sum_{n,m} B(T)\delta(\mathbf{r}_n - \mathbf{r}_m)\,. \tag{168}$$

These interactions clearly do not prevent self-crossings, but they assign an entropic penalty to them. In the continuum formulation, the above leads to the Edwards Hamiltonian (which is actually a free energy, per construction),

$$\beta H_E = \frac{3}{2\ell^2}\int_0^N \mathrm{d}n \left(\partial_n \mathbf{r}_n\right)^2 + B(T)\int_0^N \mathrm{d}n \int_0^N \mathrm{d}n'\ \delta(\mathbf{r}_n - \mathbf{r}_{n'})\ . \tag{169}$$

While it neither faithfully represents the microstructure of the polymer, nor the impossibility of self-crossings and the ensuing complicated topology, it turns out to be a very effective way of mimicking the physics responsible for the phenomenology on the scale of the overall polymer conformation. As it stands, the Edwards Hamiltonian is not yet mathematically very meaningful, though, as it contains divergent parameters. The same problem was encountered above, for the continuous Gaussian chain. But it is now more severe, as becomes more apparent when the second virial coefficient B is explicitly expressed in terms of the monomer diameter ℓ for monomers that are modeled as hard spheres,

$$B = \frac{1}{2}\frac{2\pi^{d/2}}{d\,\Gamma(d/2)}\ell^d \qquad \text{for hard spheres in } d \text{ dimensions.} \tag{170}$$

(Recall that this is the pairwise excluded volume "distributed" among a pair of particles by the leading factor 1/2.) The Edwards Hamiltonian in a $d-$dimensional embedding space then takes the form

$$\beta H_E = \frac{d}{2\mathcal{R}^2}\int_0^1 \mathrm{d}\zeta \left(\partial_\zeta \mathbf{r}_\zeta\right)^2 + g\frac{\mathcal{R}^4}{\ell^{4-d}}\int_0^1 \mathrm{d}\zeta \int_0^1 \mathrm{d}\xi\ \delta(\mathbf{r}_\zeta - \mathbf{r}_\xi)\ , \tag{171}$$

with a dimensionless coupling parameter g that takes the value

$$g \equiv \frac{\pi^{d/2}}{d\,\Gamma(d/2)} \overset{(d=3)}{=} \frac{2\pi}{3} \qquad \text{for hard spheres in } d \text{ dimensions.} \tag{172}$$

It could in principle turn negative if the monomers were endowed with sufficiently strong mutual attractions, but, in any case, it will be some finite number. Note that N has been eliminated in favor of the ideal coil size $\mathcal{R}$, which clearly demonstrates that the Edwards Hamiltonian has actually only two parameters, $\mathcal{R}$ and ℓ. Obviously, the good old trick form above did not help to get rid of diverging bare parameters in the Hamiltonian, this time, though. The interaction term is seen to be manifestly[36] divergent in $d < 4$ dimensions and to vanish in $d > 4$ dimensions, in the continuum limit $\ell \to 0$. Thereby, $d_u = 4$ is identified as the upper critical dimension. In dimensions higher than $d_u = 4$, a random walk practically never intersects itself and can for $N \to \infty$ be described by the Gaussian chain, no matter what the (finite) self-interactions are. In lower dimensions it crosses itself frequently, and the polymer will therefore be swollen compared to the ideal random-walk case for $N \to \infty$, no matter how weak the (finite) self-repulsions are. This implies that, in presence of monomer-monomer interactions, the ideal coil size $\mathcal{R}$ can no longer be considered a good phenomenological parameter, below the upper critical dimension. It now takes the role of a bare parameter itself, since it vanishes compared to the actual phenomenological coil size, i.e. $\mathcal{R}/\langle \mathbf{R}^2 \rangle^{1/2} \to 0$, in the appropriate version of the continuum limit $\ell \to 0$ and $N \to \infty$ that leaves the phenomenological coil size invariant. This implies that actually both terms of the Hamiltonian are divergent. Far from being a peculiarity of the Edwards model, this dilemma is actually characteristic of any strongly interacting microscopic theory, and at the root of any non-trivial emergent phenomenology.

Interestingly, one can still make use of the divergent Hamiltonian, for example by expanding the Boltzmann factor $e^{-\beta H_E}$ into an asymptotic perturbation series in the interaction term, arguing that ℓ is actually not infinitely small for real polymers. Applying resummation tricks to this series, which has a large (for $\ell \to 0$ diverging) expansion parameter that comes with prefactors of oscillating sign that grow exponentially with the order of the expansion, has provided accurate estimates of the value of ν for a self-avoiding polymer. Another common strategy exploits that the divergence is tamed at the upper critical dimension $d_u = 4$. This suggests to extrapolate down from the upper critical dimension, where $\nu = 1/2$. The idea is formalized in the so-called $\varepsilon-$expansion in the "small" parameter $\varepsilon = 4 - d$. It is easy to see that the double perturbation expansion in ε and in the interaction term helps to calm down the divergencies that occur in a naive perturbation expansion of $e^{-\beta H_E}$. Simply rewrite the singular factor $\ell^{-\varepsilon}$ in H_E in the form

$$\ell^{-\varepsilon} = e^{-\varepsilon \ln \ell} = \sum_{n=0}^{\infty} \frac{(-\ln \ell)^n}{n!} \varepsilon^n \; . \tag{173}$$

Now, to each order in ε only logarithmic divergencies remain, which do not affect

[36]Note that the double integral over the $\delta-$function counts the $\mathcal{O}(N^2/R^d)$ intersections per coil volume in Eq. (169), so that it is $\mathcal{O}(R^{-d})$ and independent of ℓ and N, in Eq. (171).

power-law exponents. In practice, since one is interested in $\varepsilon = 1$ (at least), one has to push the expansion to higher orders in ε and afterwards again apply resummation tricks to get useful quantitative results via this otherwise very appealing strategy.

Luckily, a good estimate of ν can be obtained from a much simpler calculation that merely retains the basic idea of extrapolating down from the upper critical dimension. In departing from $d = d_u$ to $d < d_u$ for small but finite ℓ, the interaction term blows up. The excluded volume obliges the polymer to swell so that its typical end-to-end distance $\langle \mathbf{R}^2 \rangle^{1/2}$ increases beyond the ideal value $\mathcal{R}$. In other words, the (now "bare") parameter $\mathcal{R}$ shrinks relative to the relevant (and therefore imagined to be fixed) phenomenological scale $\langle \mathbf{R}^2 \rangle^{1/2}$. To find out how much, one makes a simple dimensional estimate, which should not be too bad for guessing a dimension, after all. It relies on the anticipation of no more than a single characteristic length scale $\langle \mathbf{R}^2 \rangle^{1/2}$, namely the cutoff scale for the otherwise fractal structure with a yet unknown fractal dimension $1/\nu \neq 2$. Indeed, for the ideal Gaussian chain, the dimensional estimate $k_B T (\mathbf{R}/\mathcal{R})^2$ of the Hamiltonian exactly amounts to the identification of the Hamiltonian $H(\{\mathbf{r}_i\})$ for all monomeric degrees of freedom with the free energy $A(\mathbf{R})$ for the overall coil size, or, equivalently, of the Boltzmann factor $e^{-\beta H\{(\mathbf{r}_i\})}$ with the distribution $P(\mathbf{R}) \propto e^{-\beta A(\mathbf{R})}$ of the end-to-end vector, given in Eq. (158). The peak in the corresponding radial distribution $\tilde{P}(R)$ defined by

$$\tilde{P}(R)\mathrm{d}R = P(\mathbf{R})\mathrm{d}\mathbf{R} \propto e^{-\beta A(R)} R^2 \mathrm{d}R \tag{174}$$

is located around $\mathcal{R}$. Similarly, for the more complicated Edwards Hamiltonian, one expects a free energy with a single minimum and a corresponding radial distribution with a single peak, which both have merely been shifted to a much larger value $R_* \simeq \langle \mathbf{R}^2 \rangle^{1/2} \gg \mathcal{R}$. Dropping constant numerical factors, as appropriate for a rough dimensional estimate, one thus writes

$$\beta H_E \simeq \beta A(R) \simeq \frac{R^2}{\mathcal{R}^2} + \frac{\mathcal{R}^4}{R^d \ell^\epsilon} \, . \tag{175}$$

For the optimum coil size R_* that minimizes this free energy, both terms in the Hamiltonian turn out to have similar magnitude, corresponding to a balanced blow-up of both terms in Eq. (171), so that

$$\partial_R A(R)|_{R_*} = 0 \quad \Leftrightarrow \quad \frac{R_*^2}{\mathcal{R}^2} \simeq \frac{\mathcal{R}^4}{R_*^d \ell^\varepsilon} \quad \Rightarrow \quad R_* \simeq \frac{\mathcal{R}^{6/(2+d)}}{\ell^{\varepsilon/(2+d)}} \, . \tag{176}$$

The position R_* of the free-energy minimum and the peak in the radial distribution function $\tilde{P}(R)$ gives the dominant contributions in calculations of moments of $\mathbf{R}$. One hence expects $\langle R^2 \rangle \simeq R_*^2$. The jargon is that the phenomenological observable $\sqrt{\langle R^2 \rangle}$, which has physical units of length and must thus be proportional to the elementary physical length scale ℓ of the model, on dimensional

grounds, has thereupon acquired an *anomalous dimension* $-\varepsilon/(2+d)$. The apparent contradiction is of course immediately resolved by inserting the definition of $\mathcal{R} = \ell\sqrt{N}$, which yields

$$\langle \mathbf{R}^2 \rangle^{1/2} \simeq R_* \simeq \ell N^{\nu_F} \ , \qquad \text{with } \nu_F \equiv 3/(2+d) \tag{177}$$

the so-called Flory-exponent. So, R_* solves the renormalization-group equation (162) for the Edwards Hamiltonian with the value $\nu = \nu_F$. The obtained simple estimate for ν turns out to be exact in 1, 2 and 4 dimensions and to provide an excellent approximation to the numerical value $\nu \approx 0.588$ in 3 dimensions[37]. Assuming the Flory approximation $\nu = \nu_F$ to provide the proper phenomenological coil size, the bare Edwards Hamiltonian is in retrospect seen to diverge as $\beta H_E \propto \ell^{-\varepsilon/(2+d)}$, somewhat less than naively expected from a first glance at Eq. (169), and apparently too weakly to deserve a mention in some polymer-physics textbooks.

Crossover-scaling ("blob arguments")

The knowledge of the scale invariance of the individual polymer chain is the basis for a treatment of many complicated problems, even involving semidilute polymer solutions and nonlinear deformations, by strikingly simple scaling arguments also known as crossover-scaling or "blob arguments"[38]. The basic idea is that the natural scaling is preserved up to a certain length scale, the crossover scale or blob scale, and perturbed by external forces or influences from other interpenetrating polymer chains etc., beyond that scale. Formally, one represents a certain observable by a natural phenomenological parameter combination that fixes its physical dimension and possibly already properly represents its value in the unperturbed limit, multiplied by a dimensionless crossover scaling function of the dimensionless perturbation. The power-law form of scaling function in the unknown limit is then constrained by some additional generic physical argument, such as extensivity. A good example is provided by the force-extension relation. Using the blob argument, the somewhat counter-intuitive prediction in Eq. (151), that the linear response extends up to forces $F \simeq k_B T/\ell$, is found to be modified by the self-interactions. Namely, to recover the linear-response result, Eq. (152), known from the fluctuation-response theorem for weak forces, the general scaling ansatz

$$\langle R \rangle_F = R_* \varphi(F/F_c) \ , \qquad \text{with } \varphi(x \ll 1) \sim x \tag{178}$$

requires the crossover force $F_c \equiv d k_B T/R_*$ rather than $k_B T/\ell$. "Weak forces" are thus indeed smaller than $k_B T/R_*$, as also intuitively expected, while the intermediate force regime $k_B T/R_* \ll F \ll k_B T/\ell$ turns out to be nonlinear

[37] To go beyond the Flory estimate, one might wish to improve the perturbative calculation of $\langle \mathbf{R}^2 \rangle$ by resorting to the differential formulation of the dilation symmetry in Eq. (162).

[38] P.-G. de Gennes, Scaling Concepts in Polymer Physics, Cornell 1979

because of the non-trivial self-interactions. The physical intuition provided by the blob picture suggests that large forces deform the polymer coil into a linear chain of blobs, because the parts of the polymer pulled apart about a distance R_* can no longer collide with each other to contribute to the interaction term in H_E. Therefore, the end-to-end distance of the chain must ultimately, for $F \gg F_c$, scale extensively in the total polymer length L or N. (By connecting two non-interacting chains pulled apart by the same force, in series, the length doubles.) Accordingly, one needs $\varphi(x \gg 1) \sim x^{1/\nu-1}$, so that[39]

$$\langle R\rangle_F = R_*(F/F_c)^{1/\nu-1} \propto R_*^{1/\nu}F^{1/\nu-1} \propto N \qquad (k_BT/R_* \ll F \ll k_BT/\ell) \quad (179)$$

Rewriting $\langle R\rangle_F = \xi M_b$, as appropriate for a necklace of M_b blobs of length ξ, one can deduce the size and scaling of the blobs. Namely, since the blob size ξ must be independent of N, while the number M_b of blobs must be extensive (proportional to N),

$$\xi = R_*F_c/F = k_BT/F \ \text{ and } \ M_b = (F/F_c)^{1/\nu} \quad (180)$$

must hold. The scaling inside the blobs is thus undisturbed by the external force, $\xi \propto (R_*/N^\nu)(N/M_b)^\nu$. Here, the first factor is recognized as the monomer size and the second as the number N_b of monomers per blob. One can summarize the essence of the crossover scaling behavior by saying that the external force pulls the polymer apart into a freely jointed chain of blobs, each of which can be thought of as an essentially undisturbed self-avoiding walk.

Contrary to the natural expectation that nonlinear deformations should reveal information about the specific microstructure, this result is (like the linear-response result) completely universal and phenomenological. Neither of them gives a clue about the microstructure, unless combined with complementary measurements. Only at forces $F \gg k_BT/\ell$ that pull the polymer almost completely straight, so that the role of self-intersections diminishes, the force-extension relation of the freely-jointed-chain, Eq. (151), ultimately obtains, and the microstructure is revealed. Of course, Eq. (151) is not really needed to learn about ℓ if the polymer has already been pulled straight. Then L and R_* are known, and so is $\ell = (R_*/L^\nu)^{1/(1-\nu)}$. But Eq. (151) can be used to decide whether the polymer is microscopically well approximated by the freely-jointed chain model, which does not matter for the rest of the above discussion that equally applies for a long wormlike chain (introduced further below), say.

Another important result that is easily obtained by crossover-scaling arguments, is the pressure equation of state of polymers in a semidilute solution, where the individual coils overlap. Note that this is a horrible many-body problem with very many simultaneously interacting polymers, each made of very many interacting monomers — a strongly interacting many-body problem squared, so

[39]The counter-intuitive giant linear-response regime survives for $d > d_u = 4$, where $\nu = 1/2$.

to say. At infinite dilution, the osmotic pressure $p = n_p k_B T$ (the pressure exerted by the polymer coils on a semipermeable membrane) scales linearly in the polymer concentration $n_p = n/N \ll n$, which is of course much smaller than the monomer concentration n. This is van't Hoff's law, simply saying that, like any molecule, each polymer behaves as a little ball that bumps into the walls with a speed corresponding (on average) to the thermal energy $k_B T$. Nonetheless, the small pressure $n_p k_B T$ after polymerization compared to the monomers' osmotic pressure $n k_B T$ before polymerization was historically called the osmotic pressure anomaly of polymers. Interestingly, the concentration dependence of the osmotic pressure remains somewhat anomalous also at higher concentrations, at least compared to the expectation of a naive liquid state theory or virial expansion. Yet, it is easily deduced from a scaling argument that exploits the scale-free self-similar structure of the individual polymer coils to conclude that the equation of state has to exhibit a crossover from van't Hoff's law to an asymptotically scale-free relation (a power-law) that does not any more depend on the length of the individual polymers, which are then strongly intermingled, but only on the monomer concentration. One anticipates the crossover concentration to be given by concentration $n_p^* = 1/R_*^3$ where the individual polymer coils start to overlap and to merge into a spaghetti soup. The corresponding mass density is conventionally denoted by

$$c_* \propto N/R_*^3 \propto N^{1-3/\nu} \, . \tag{181}$$

A crossover scaling argument constructed along the same lines as above for polymer stretching represents the pressure p by its natural dimensional estimate $k_B T/R_*^3$ times a dimensionless crossover scaling function $\Pi(x)$.

$$p = \frac{k_B T}{R_*^3} \Pi(c/c_*) \, , \qquad \Pi(x \ll 1) = x \, , \quad \Pi(x \gg 1) = x^\delta \, . \tag{182}$$

Notice that the anticipated expression for the crossover scale c_* follows from this scaling ansatz if van't Hoff's law is required to hold for small concentrations. The exponent δ is fixed by the requirement that the pressure at strong polymer overlap, where the polymers interpenetrate and thus "loose their identity", cannot depend on the number of polymers or on their length N but only on the monomer concentration n (or mass density c). This requires $\Pi(c/c_* \gg 1) \propto R_*^3 \propto N^{3\nu}$ to cancel out the N-dependence hidden in the prefactor, i.e.

$$\Pi(c/c_* \gg 1) \propto (c/c_*)^\delta \propto N^{3\nu} \quad \Rightarrow \quad \delta = 3\nu/(3\nu - 1) \approx 9/(7-d) \, . \tag{183}$$

Therefore, one concludes that the osmotic pressure in a semidilute solution scales as

$$p(c \gg c_*) \propto c^\delta \propto c^{3\nu/(3\nu-1)} \overset{\nu=\nu_F}{\approx} c^{9/(7-d)} \overset{d=3}{=} c^{9/4} \tag{184}$$

with the mass concentration c. This non-trivial result can also be rephrased in terms of blobs. The idea is that the correlation length or blob scale ξ, to which

the fractal correlations with dimension $1/\nu$ extend, is given by $\xi = R_* \hat{\xi}(c/c_*)$ with $\hat{\xi}(1) \simeq 1$ and $\hat{\xi}(x \gg 1) \sim x^{\nu/(1-3\nu)}$ so that ξ becomes asymptotically independent of the polymer length. The osmotic pressure can now be written as $k_B T/\xi^3$ (thermal energy divided by the available volume per blob), which looks like an extension of van't Hoff's law to blobs of diameter

$$\xi \propto c^{\nu/(1-3\nu)} \overset{d=3}{\propto} c^{-3/4} . \tag{185}$$

The discussion for the osmotic pressure reveals that blobs are a powerful practical concept to break up a strongly interacting many-body problem into an essentially free (or weakly interacting) theory of some composite effective particles. In this sense, blobs are recognized as a classical counterpart of the quantized quasi-particles used to describe the low-energy excitations of a Bose–Einstein condensate or a degenerate Fermi gas, or of electrons and holes in a semiconductor. In a dense system they take over the role played by individual particles in a dilute system.

9 Semiflexible polymers and elastic singularities

Important biological chain molecules, such as F-actin, microtubules, double-stranded DNA, and some others, are not well represented by the freely-jointed chain or even the Gaussian chain. They look more like slingering snakes, with a substantial scale separation between the microscopic backbone thickness (or monomer size) ℓ and the correlation length ℓ_p of the tangents, the so-called *persistence length*. Instead of the $\delta-$correlations of the FJC in Eq. (153) one has

$$\langle \hat{\mathbf{u}}_s \hat{\mathbf{u}}_{s'} \rangle = \exp(-|s - s'|/\ell_p) , \tag{186}$$

as familiar from ferromagnetic (as opposed to paramagnetic) spin chains. As a consequence, there is interesting physics to be found below the overall coil size, given by the mean-square end-to-end distance (exercises)

$$\langle \mathbf{R}^2 \rangle = 2\ell_p^2 \left(e^{-L/\ell_p} - 1 + L/\ell_p \right) \sim \begin{cases} L^2(1 - L/3\ell_p) & (L \ll \ell_p) \\ 2\ell_p L(1 - \ell_p/L) & (L \gg \ell_p) \end{cases} . \tag{187}$$

The notation $\sim$ stands for "asymptotically equal to". Equation (187) captures the crossover from a flexible phantom chain of "Kuhn[40]" length $2\ell_p$ on large scales to a stiff rod on short scales. This is why one speaks of *semiflexible polymers* if the double scale separation $\ell \ll \ell_p \ll L$ holds. But there is a more interesting structure, besides this crossover, hidden at length scales smaller than ℓ_p, where the typical equilibrium conformation of the polymer is only weakly bent. In this so-called stiff-polymer or weakly-bending-rod (WBR) intermediate asymptotic

[40] The equivalent FJC segment length

regime, $\ell \ll |s - s'| \ll \ell_p$, the polymer contour is not entirely smooth but still displays many tiny thermally induced wrinkles. Closer inspection shows that they exhibit an asymptotic "affine" (i.e. anisotropic) self-similarity that plays an analogous role as the fractal structure for flexible polymers (i.e. it is the source of a zoo of scaling exponents governing all kinds of static and dynamic observables).

To see this, it is useful to introduce the small transverse and longitudinal components $\hat{\mathbf{u}}_\perp$ and $\hat{u}_\parallel$ of the tangent vector $\hat{\mathbf{u}} = \partial_s \mathbf{r}_s = (\hat{\mathbf{u}}_\perp, 1 - \hat{u}_\parallel)$, for which one has

$$\hat{\mathbf{u}}^2 \equiv 1 \qquad \Rightarrow \qquad \hat{u}_\parallel = 1 - \sqrt{1 - \hat{\mathbf{u}}_\perp^2} = \hat{\mathbf{u}}_\perp^2/2 + \mathcal{O}(\hat{\mathbf{u}}_\perp^4) \; . \tag{188}$$

and corresponding notation for the longitudinal and transverse components of the end-to-end vector $\mathbf{R} = (\mathbf{R}_\perp, R_\parallel)$ of a stiff polymer with $\ell \ll L \ll \ell_p$. Here

$$R_\parallel \equiv L - r_\parallel \quad \text{with} \quad r_\parallel \equiv \int_0^L \mathrm{d}s \, \hat{u}_\parallel \; . \tag{189}$$

At the clamped end $\hat{\mathbf{u}}_0 = (\mathbf{0}, 1)$ of a stiff grafted polymer, $\langle \hat{\mathbf{u}}_s \hat{\mathbf{u}}_0 \rangle = 1 - \langle \hat{u}_{\parallel s} \rangle = 1 - s/\ell_p$, according to Eq. (186). Therefore, for a grafted stiff polymer,

$$\langle r_\parallel \rangle = L^2/(2\ell_p) \; , \qquad \langle \mathbf{R}_\perp^2 \rangle = 2L^3/3\ell_p \equiv 2\mathcal{R}_\perp^2/3 \; , \tag{190}$$

where the second result follows from Eq. (187) via $\mathbf{R}^2 = \mathbf{R}_\perp^2 + L^2 - 2r_\parallel L + \mathcal{O}(r_\parallel^2)$. The relation $\mathcal{R}_\perp \propto L^\zeta$ with the *roughness exponent* $\zeta = 3/2$ plays a similar role for stiff polymers as the relation $\mathcal{R} \propto L^\nu$ plays for flexible polymers. It implies that the contour fluctuations are self-similar under a spatial rescaling, which, in contrast to the case of the Gaussian chain, has to be anisotropic, though. Due to the intrinsic stiffness, self-interactions are of minor importance for stiff polymers and certainly do not renormalize ζ.

To get a more thorough grip onto the statistical mechanics of semiflexible polymers, it is useful to turn to a Hamiltonian description. The minimal model from which the above results are easily deduced is the *wormlike chain* (WLC) model. It can be understood as the continuum limit of a ferromagnetic Heisenberg spin chain or, alternatively, of a "not so freely jointed" chain, in which neighboring segments are subject to a nearest neighbor interaction that tries to keep them aligned:

$$H = -K \sum_i^N \hat{\mathbf{u}}_i \hat{\mathbf{u}}_{i+1} = K \sum_i^N (\hat{\mathbf{u}}_i - \hat{\mathbf{u}}_{i+1})^2 - \text{const.} \to \frac{K\ell}{2} \int_0^L \mathrm{d}s \, (\partial_s \hat{\mathbf{u}}_s)^2 \; . \tag{191}$$

The segment length $\ell \equiv L/N$, which plays the role of a discretization scale, has to vanish in the continuum limit $N \to \infty$, $\ell \to 0$, meaning that the bare coupling K has to diverge such as to keep both the so-called bending rigidity $\kappa \equiv K\ell$ and the backbone length L finite. Note that, in contrast to the continuum limit

taken for the Gaussian chain, L is now not a diverging "microscopic" or "bare" parameter but a phenomenological observable.

In the continuum limit, the ferromagnetic spin energy becomes the integral over the squared first derivative of the unit tangent $\hat{\mathbf{u}}_s$ (or second derivative of the contour $\mathbf{r}_s$) with respect to the arc length s, i.e., the integral over the squared curvature of the contour. It thus represents the elastic energy cost of the bending undulations of an elastic rod. The ground states of the Hamiltonian are therefore the equilibrium conformations of elastic rods, so-called Kirchhoff elastica (a straight line for free ends, a circle of smoothly connected ends, etc.). A comparison with the Gaussian-chain-Hamiltonian moreover reveals Eq. (191) as the Hamiltonian for diffusion on the unit sphere. The conformations of the Kirchoff elastica as a function of the arclength s can therefore also be identified with the (deterministic) dynamic trajectories of a spinning top as a function of time.

The Boltzmann factor of the WLC Hamiltonian then gives the statistical weight for the thermal excitations over such ground states, corresponding to the conformations of semiflexible polymers. And the computation of the path integral representing the canonical partition sum for the WLC Hamiltonian amounts to solving the angular part of the three-dimensional diffusion (or Schrödinger) equation. While this is a feasible task for the explicit calculation of static correlation functions such as the tangent correlations in Eq. (186) and even of some more ambitious (partial) free energies, a formulation in terms of the tangent vectors becomes cumbersome, as soon as one wants to formulate a dynamical problem. At least at this point, one would prefer to switch to a formulation in terms of the spatial contour coordinates $\mathbf{r}_s$, i.e., to the following standard form of the WLC Hamiltoanian

$$H_{\mathrm{WLC}} = \frac{\kappa}{2} \int_0^L \mathrm{d}s \, (\partial_s^2 \mathbf{r}_s)^2 \, , \qquad |\partial_s \mathbf{r}_s| = 1 \, . \tag{192}$$

This seemingly innocent rewriting entails the unpleasant task of taking care of the (infinite dimensional) rigid constraint maintaining the unit tangent length, since otherwise s is not guaranteed to be the arc-length, so that $\partial_s^2 \mathbf{r}_s$ is not guaranteed to be the curvature, and the Hamiltonian is not guaranteed to be the bending energy of the space curve $\mathbf{r}_s$, as it should be. A possible way to do this is via the Lagrange multiplier function f_s, which has the physical interpretation of a backbone tension that builds up in order to the make the contour $\mathbf{r}_s$ satisfy the inextensibility constraint:

$$H_{\mathrm{WLC}} = \frac{\kappa}{2} \int_0^L \mathrm{d}s \, (\partial_s^2 \mathbf{r}_s)^2 + \frac{1}{2} \int_0^L \mathrm{d}s \, f_s (\partial_s \mathbf{r}_s)^2 \tag{193}$$

The implicit dependence of the tension f_s on the contour $\mathbf{r}_s$ via the arc-length constraint makes this seemingly quadratic Hamiltonian actually highly nonlinear and difficult to use. It is of similar complexity as the Edwards Hamiltonian, with

one important difference. Namely, in contrast to the Edwards Hamiltonian, which describes a non-trivial fractal with a irrational fractal dimension $1/\nu$, the wormlike chain Hamiltonian describes not a fractal but a crossover structure from the (simple) self-affine structure identified in Eq. (189) to the (simple) fractal structure of the Gaussian chain, Eq. (153). As a consequence, the WLC Hamiltonian is not divergent in the continuum limit, indicating that it can, in contrast to the Gaussian chain or the Edwards Hamiltonian, be interpreted as a viable — albeit simplistic — microscopic model of a polymer.

A formidable simplification occurs in the intermediate asymptotic limit of a stiff polymer ($\ell \ll L \ll \ell_p$), where Eq. (192) reduces to the weakly-bending-rod (WBR) or stiff-polymer Hamiltonian for the small transverse coordinates, alone,

$$\beta H_{\mathrm{WBR}} = \frac{\kappa}{2k_BT}\int_0^L \mathrm{d}s\,(\partial_s^2 \mathbf{r}_{\perp s})^2 = \frac{1}{2\mathcal{R}_\perp^2}\int_0^1 \mathrm{d}\zeta\,(\partial_\zeta^2 \mathbf{r}_{\perp\zeta})^2 \tag{194}$$

In the second formulation $\kappa = \ell_p k_B T$ was used, as appropriate for a free polymer in $d = 3$ dimensions[41]. Now, the rigid constraint is gone, as it can always *a posteriori* be fulfilled to leading order by choosing $\hat{u}_\parallel$ and $r_\parallel$ appropriately (if needed), as apparent from Eq. (188). As a consequence, the WBR-Hamiltonian is indeed harmonic and only depends on a single relevant parameter $\mathcal{R}_\perp$, as familiar from the Gaussian chain. The corresponding Boltzmann factor is Gaussian, so that everything can be calculated explicitly in a straightforward way. One can thus say that taking the stiff limit $L/\ell_p \to 0$ restores the ultimate simplicity enjoyed by the Gaussian chain, on a level of higher spatial resolution, so to say (and encoding a self-affine rather than fractal scaling). Whenever it does not suffice for a given practical purpose, one has to deal with the much more complicated, effectively nonlinear wormlike-chain Hamiltonian, Eq. (192).

As a concrete application of the above, consider the polymer exposed to a static force of magnitude F that pulls its ends apart. The backbone tension f_s in Eq. (193) is then constant and equal to the external force, i.e. $f_s = F =$ constant. Therefore, the Lagrange term in the Hamiltonian becomes — in the weak-bending limit, using Eq. (188) — identical to the negative of the mechanical work

$$\mathbf{F}\cdot\mathbf{R} = FR_\parallel = F(L - r_{\parallel L}) = FL - F\int_0^L \mathrm{d}s\,\hat{u}_\parallel = -\frac{F}{2}\int_0^L \mathrm{d}s\,\hat{\mathbf{u}}_\perp^2 + \text{ const.} \tag{195}$$

done by the external force. In other words, the WBR-Hamiltonian for a polymer

[41] By calculating the tangent correlations in Eq. (186) from Eq. (194), one finds $(d-1)k_BT\ell_p = 2\kappa$, which shows that, for finite κ, the persistence length ℓ_p diverges in a one-dimensional embedding space and diminishes in high dimensional spaces, as it must be.

that has its ends pulled apart by a force of magnitude F is

$$\begin{aligned}\beta H_F &= \frac{\kappa}{2k_BT}\int_0^L \mathrm{d}s\,\left(\partial_s^2\mathbf{r}_{\perp s}\right)^2 + \frac{F}{2k_BT}\int_0^L \mathrm{d}s\,\left(\partial_s\mathbf{r}_{\perp s}\right)^2 \\ &= \frac{1}{2\mathcal{R}_\perp^2}\int_0^1 \mathrm{d}\zeta\,\left(\partial_\zeta^2\mathbf{r}_{\perp\zeta}\right)^2 + \frac{1}{2\mathcal{R}_{\perp F}^2}\int_0^1 \mathrm{d}\zeta\,\left(\partial_\zeta\mathbf{r}_{\perp\zeta}\right)^2 \\ &= \frac{1}{2\mathcal{R}_\perp^2}\int_0^1 \mathrm{d}\zeta\,\left[\left(\partial_\zeta^2\mathbf{r}_{\perp\zeta}\right)^2 + M_b^2\left(\partial_\zeta\mathbf{r}_{\perp\zeta}\right)^2\right]\end{aligned} \tag{196}$$

The simplified description in terms of the weak-bending parametrization is now also applicable for not so stiff polymers with $L \gg \ell_p$, as long as the force guarantees a (more or less) stretched conformation, i.e., $\mathcal{R}_{\perp F}^2 \equiv k_BTL/F \ll L^2$. Power counting in the first line of Eq. (196) suggests that the second term dominates over the first for $F > F_c \equiv \kappa/L^2$. This is, from the second line, seen to be the case when $\mathcal{R}_{\perp F} < \mathcal{R}_\perp$, i.e., when the force limits the transverse excursions of the contour more strongly than the bending rigidity alone would do. Due to the different orders of the derivatives in both terms in the Hamiltonian, one can also say that the first term will dominate over short distances whereas the second term will dominate over long distances. In Fourier space, the first term will be proportional to q^4 and thus dominate, for large wave vectors q, over the second term, which is proportional to q^2. This observation can be illustrated in a real-space representation by the blob picture, which emerges in a natural way from any Hamiltonian with a crossover structure. The dimensionless quantity M_b in Eq. (196) is extensive in L and can therefore be identified as the number L/ℓ_F of blobs, namely,

$$M_b \equiv L/\ell_F = \mathcal{R}_\perp/\mathcal{R}_{\perp F} = \sqrt{F/F_c} \quad \text{with} \quad F_c \equiv \kappa/L^2\,, \quad \ell_F = L\sqrt{F_c/F} \tag{197}$$

being the Euler buckling force and the blob length, respectively. (The Euler buckling force is the compressive end-to-end force needed to buckle a rod with bending rigidity κ.) These notions help to make the competition of the two terms in the Hamiltonian more explicit: for forces smaller than the Euler force, the conformation is hardly perturbed by the external force and governed by the first term in the Hamiltonian, whereas, for larger forces, the bending term has little to say and tension (the second term in the Hamiltonian) rules. Or, formulated in terms of length scales: on length scales $L \ll \ell_F$, corresponding to the case $M_b \ll 1$, the first term rules; for $L \gg \ell_F$, corresponding to $M_b \gg 1$, the second. Inside the blob, the conformation is then that of a free, unperturbed stiff polymer, while beyond ℓ_F it is that of a taut linear chain of blobs.

Per construction, the length of the linear chain of blobs is extensive in M_b and L (for large M_b). Since, in this limit, the transverse excursions of the blob chain are governed by the second term in the Hamiltonian, which is a diffusion Hamiltonian, they scale diffusively in M_b and L. Therefore, not only the average

contraction $\langle r_\parallel \rangle$ of the end-to-end vector $\mathbf{R}$ of the polymer along the force direction but also its mean-square excursions $\langle \mathbf{R}_\perp^2 \rangle$ transverse to it scales linearly in M_b. In other words, they both follow from the corresponding quantities of an individual blob via multiplication with M_b. Up to numerical factors that depend on the precise boundary conditions, the equilibrium longitudinal contraction of an individual blob is ℓ_F^2/ℓ_p and its mean-square transverse excursion is ℓ_F^3/ℓ_p, according to Eq. (190), i.e. the semiflexible blobs are, just as the weakly bending polymer itself, anisotropic objects. Altogether, this suggests for the total longitudinal and transverse extension of the polymer:

$$\begin{aligned} \langle R_\parallel \rangle_F &\simeq L - (\ell_F^2/\ell_p) M_b \simeq L - k_B T/(F_c F)^{1/2} \, , \\ \langle \mathbf{R}_\perp^2 \rangle_F &\simeq (\ell_F^3/\ell_p) M_b \simeq k_B T L/F \simeq \mathcal{R}_{\perp F}^2 \, . \end{aligned} \tag{198}$$

Alternatively, one could have followed the formal route, starting from Eq. (190), and multiplying it by a scaling function of the force, namely

$$\langle \delta R_\parallel \rangle_F \simeq (L^2/\ell_p) \phi(F/F_c) \;\; \text{with} \;\; \phi(x \to 0) \sim x \;\; \text{and} \;\; \phi(x \to \infty) \sim x^{-1/2} \, . \tag{199}$$

As usual, the first limit fixes the crossover scale $F_c = \kappa/L^2$ by comparison with the longitudinal linear response, as obtained from the fluctuation-response relation

$$\langle \delta R_\parallel \rangle_F \simeq \frac{\langle \delta R_\parallel^2 \rangle}{k_B T} F \propto \frac{\langle \delta R_\parallel \rangle^2}{k_B T} F \propto \frac{L^4}{\ell_p \kappa} F \, , \tag{200}$$

and the second limit is imposed by the extensivity requirement.

Note from Eq. (198) that the longitudinal contraction is manifestly affected by the semiflexible structure, since it depends on κ (e.g. via F_c), whereas the transverse excursion is independent of it. The former is apparently sensitive to the physics inside the blobs, while the latter is completely dominated by the thermal fluctuations of the end-to-end vector of a taut string (no matter what its constituents are). It would therefore have the same form for a stiff rod or a FJC of length L (composed of different blobs). Indeed, up to a factor, even the first line in Eq. (198) can be obtained by inserting the blob scales from Eq. (197) into the FJC force-extension relation, Eq. (151). This corroborates that a polymer that is pulled taut may always be thought of as a FJC of blobs, no matter whether it is a FJC, SAW, or WLC.

The limiting results for strongly stretched semiflexible polymers given in Eq. (198) (including the non-universal numerical prefactors) can also be reproduced by a direct calculation from the Hamiltonian given in Eq. (196) (exercises), which additionally yields the full crossover scaling function from the linear to the limiting nonlinear response. An interesting aspect revealed by the explicit calculation is the instability of the stiff polymer against buckling upon force reversal ($F \to -F$). This so-called Euler instability is well known from the mechanics of stiff rods and affects each eigenmode of the polymer at its own characteristic

force. The blob result for $\langle R_\parallel \rangle_F$ still catches an accumulated echo of this instability in the non-analytical behavior of the square-root upon reversal of the force and in the apparence of the characteristic force scale $F_c = \kappa/L^2$ (the Euler force of the lowest bending mode).

While a linear beam exhibits a nonlinear force-extension relation for longitudinal forces (directed along its axis), it is interesting to note that, conversely, an ordinary spring or rubber band, which deforms linearly in response to longitudinal forces, exhibits a nonlinear response to transverse forces. Namely, as elementary geometric arguments reveal, the restoring force is cubic in the transverse extension, unless the spring is set under tension, which then acts as a linear modulus to transverse deformations, as known to anybody who plays a string instrument. For a semiflexible polymer, the transverse and longitudinal elastic singularities conspire with longitudinal and transverse friction to create a rich dynamic response to transverse point forces[42] or even for its free relaxation[43] that would probably not have been anticipated by everybody who plays a string instrument.

Polymer dynamics

To go from the statistical characterization of stationary properties of polymers to their dynamics, one has to explicitly model their friction with the solvent and their thermal fluctuations. This is most intuitively accomplished by Langevin equations that express the force balance between the systematic forces $-\delta H/\delta \mathbf{r}_s$ derived from the Hamiltonian (or a free energy) to the Stokes friction and a thermal random force. For dilute and semidilute polymer solutions, a major simplification is due to the very low volume fraction occupied by the polymer. The solvent hydrodynamics can therefore usually be represented on the level of hydrodynamic interactions mediated between the monomers by the Oseen tensor, or sometimes be neglected altogether. In the latter case, one simply assumes that the solvent exerts Stokes friction on all moving parts ("free-draining" approximation). At short times, the Hamiltonian forces are balanced by both the viscous friction and the thermal agitation, at late times $t \to \infty$ only by the latter, which has to lead back to the results calculated from equilibrium statistical mechanics. Accordingly, the strength of the random forces acting on the monomers that represent the thermal agitation by the fluctuating solvent is dictated by the fluctuation-dissipation theorem and can (in thermal equilibrium) be written down without resorting to an explicit calculation from the fluctuating solvent hydrodynamics.

[42] B. Obermayer, O. Hallatschek, *Coupling of Transverse and Longitudinal Response in Stiff Polymers*, Phys. Rev. Lett. **99** (2007) 098302

[43] B. Obermayer *et al.*, *Freely relaxing polymers remember how they were straightened*, Phys. Rev. E **79** (2009) 021804; O. Otto *et al.*, *Rapid internal contraction boosts DNA friction*, Nat. Comm. **4** (2013) 1780

If one turns the above words into mathematical equations, one obtains the dynamic standard models of polymer physics. The model for flexible polymers is the so-called *Rouse model*, which is essentially an entropic spring with the dynamic conformation $\mathbf{r}_\nu(t)$ and some effective (not to say fictitious) Stokes friction coefficient ζ,

$$\zeta \partial_t \mathbf{r}_\nu = k\, \mathbf{r}''_\nu + \xi_\nu \tag{201}$$

where $\mathbf{r}''_\nu$ is a shorthand notation for $\partial_\nu^2 \mathbf{r}_\nu$, the spring constant is $k = 3k_BT/\mathcal{R}^2$ and ν is a parameter running from 0 to 1. The thermal noise is modeled as a Gaussian stochastic variable with vanishing mean and a covariance given by the fluctuation-dissipation relation:

$$\langle \xi_\nu(t) \rangle = 0 \;, \qquad \langle \xi^i_\nu(t) \xi^j_{\nu'}(t') \rangle = 2\zeta k_B T \delta_{i,j} \delta(\nu - \nu') \delta(t - t') \tag{202}$$

On the level of a dimensional analysis, it is immediately clear that the fractal structure of the model gives rise to "fractal dynamics" i.e. dynamic correlation functions that are self-similar in time. For example, the mean-square displacement is given by

$$\langle \mathbf{R}(t)^2 \rangle \simeq \frac{k_BT}{\mathcal{R}^2} \frac{t}{\zeta} \;. \tag{203}$$

This result can clearly only hold for intermediate times and has to cross over to the constant $\mathcal{R}^2$ for times $t \gtrsim \tau_R$ longer than the longest relaxation time or Rouse time, $\tau_R \simeq \zeta \mathcal{R}^2/k_BT$. It is difficult to modify the somewhat schematic Rouse model in a systematic way to account for the self-avoidance of the polymer, its internal hydrodynamic interactions, or its locally semiflexible structure. A common strategy to include self-avoidance is to do analytical calculations with the Rouse model and then fudge in the corresponding corrections by scaling arguments, *a posteriori* (e.g. by replacing $\mathcal{R}$ by R_*). Further, the inverse friction coefficient ζ^{-1} can formally be replaced by the Oseen mobility matrix $\mathbf{H}(\mathbf{r}_\nu - \mathbf{r}_{\nu'})$ or, for practical calculations, rather by its "pre-averaged" version $h_{\nu,\nu'}\mathbf{1} = \langle \mathbf{H}(\mathbf{r}_\nu - \mathbf{r}_{\nu'}) \rangle$ in what is called the *Zimm model*:

$$\partial_t \mathbf{r}_\nu = \int \mathrm{d}\nu'\, \mathbf{H}(\mathbf{r}_\nu - \mathbf{r}_{\nu'}) \cdot (k\, \mathbf{r}''_{\nu'} + \xi_{\nu'}) \approx \int \mathrm{d}\nu'\, h_{\nu,\nu'} (k\, \mathbf{r}''_{\nu'} + \xi_{\nu'}) \tag{204}$$

On a similar level, one can write down the dynamic wormlike chain model for semiflexible polymers. In view of their relatively stretched conformations and rare self-encounters, one can usually safely employ the free-draining approximation

$$[\zeta_\perp (\mathbf{1} - \mathbf{r}_s \mathbf{r}_s) + \zeta_\parallel \mathbf{r}_s \mathbf{r}_s] \cdot \partial_t \mathbf{r}_s = -\kappa\, \mathbf{r}''''_s + (\mathbf{r}'_s f_s)' + \xi_s \;. \tag{205}$$

Here $f_s(t)$ is the backbone tension that builds up in order to maintain the rigid constraint of unit tangent length, and the friction matrix elements for transverse and parallel motion are (exercises)

$$\zeta_\perp = 2\zeta_\parallel \approx 4\pi\eta / \ln(L/a) \;. \tag{206}$$

Here, the backbone diameter a of the polymer enters, as a reminder of the singularity of the Oseen matrix at short distances (which actually ought to be cut off by neglected near-field contributions). For explicit calculations one usually has to resort to the weakly-bending approximation. To leading order in the small parameter L/ℓ_p, one obtains the simple (Rouse-type) linear Langevin equation

$$\zeta_\perp \partial_t \mathbf{r}_\perp = -\kappa \mathbf{r}_s'''' + \xi_\perp \; . \tag{207}$$

A dimensional analysis completely analogous as performed above for the Rouse model suggests a characteristic subdiffusively growing dynamic correlation length $\ell_t \propto L(\zeta t/\kappa)^{1/4}$, which plays the role of an "elasto-hydrodynamic penetration depth", measured along the backbone. Pushing the expansion of Eq. (205) to higher order is somewhat subtle, since the limits $t \to 0$ and $L/\ell_p \to 0$ do not interchange, and a multiple-scale perturbation method is required. Together with the mentioned elastic singularities of thin elastic rods, this explains the zoo of dynamic intermediate asymptotic scaling regimes that show up in the dynamics of semiflexible polymers.